

12-1-2000

# Synthesis and characterization of functionalized zirconium pendent polyamic acids and polyimides based on 3,4'-ODA and ODPA

Wei Wang

Follow this and additional works at: <http://scholarworks.rit.edu/theses>

---

## Recommended Citation

Wang, Wei, "Synthesis and characterization of functionalized zirconium pendent polyamic acids and polyimides based on 3,4'-ODA and ODPA" (2000). Thesis. Rochester Institute of Technology. Accessed from

This Thesis is brought to you for free and open access by the Thesis/Dissertation Collections at RIT Scholar Works. It has been accepted for inclusion in Theses by an authorized administrator of RIT Scholar Works. For more information, please contact [ritscholarworks@rit.edu](mailto:ritscholarworks@rit.edu).

SYNTHESIS AND CHARACTERIZATION OF  
FUNCTIONALIZED ZIRCONIUM PENDENT  
POLYAMIC ACIDS AND POLYIMIDES BASED ON  
3,4'-ODA AND ODPA

**WEI WANG**

THESIS

SUBMITTED IN PARTIAL FULFILLMENT OF THE REQUIREMENTS  
FOR THE DEGREE OF MASTER OF SCIENCE  
**DEPARTMENT OF CHEMISTRY**  
**ROCHESTER INSTITUTE OF TECHNOLOGY**  
**ROCHESTER, NEW YORK**

December, 2000

SYNTHESIS AND CHARACTERIZATION OF FUNCTIONALIZED ZIRCONIUM  
PENDENT POLYAMIC ACIDS AND POLYIMIDES BASED ON  
3,4'-ODA AND ODPA

Approved:

Marvin Lee Illingsworth

---

Thesis Advisor

Terence C. Morill

---

Department Head

## COPYRIGHT STATEMENT

Title of thesis SYNTHESIS AND CHARACTERIZATION OF FUNCTIONALIZED  
ZIRCONIUM PENDENT POLYAMIC ACIDS AND POLYIMIDES  
BASED ON 3,4'-ODA AND ODPA

I, Wei Wang, hereby grant permission to the Wallace Memorial Library, of Rochester Institute of Technology, to reproduce my thesis in whole or in part. Any reproduction will not be for commercial use or profit.

December, 2000

## ACKNOWLEDGEMENTS

The work would not have been fulfilled without the guidance and support from my advisor, Dr. Marvin L. Illingsworth. His guidance, knowledge and kind assistance are greatly appreciated.

I would like to thank my committee members and chemistry department for their great support.

I would like to thank NASA Langley Center for the GPC measurements and supply of LARC-IA, Dr. Kotlarchyk of Physics Department, RIT, for the light scattering measurement, Dr. Fuller of Microelectronic Engineering Department, RIT, for the use of the SEM instrument, Mr. Andrew Jensen of Astra, USA, for the Elemental Analysis, and Mr. Dilip Chatterjee of Eastman Kodak Co. for melt pressing LARC-IA for contact angle measurement.

I would also like to thank the chemical stockroom personnel for their support.

# Table of Contents

## ABSTRACT

INTRODUCTION .....	1
EXPERIMENTAL.....	7
2.1 CHEMICALS .....	7
2.2 SYNTHESIS OF SUBSTITUTED N,N'-DISALICYLIDENE-1,2-PHENYLENEDIAMINE (H <sub>2</sub> RDSP) .....	7
2.2.1 N,N'-Disalicylidene-1,2-phenylenediamine, H <sub>2</sub> dsp .....	7
2.2.2 4-Nitro-N,N'-disalicylidene-1,2-phenylenediamine, H <sub>2</sub> ndsp .....	8
2.2.3 4-Cyano-N,N'-disalicylidene-1,2-phenylenediamine, H <sub>2</sub> cdsp .....	8
2.3 SYNTHESIS OF SUBSTITUTED (N,N'-DISALICYLIDENE-1,2-PHENYLENEDIAMINATO)(4-AMINO N,N'-DISALICYLIDENE-1,2-PHENYLENEDIAMINATO)ZIRCONIUM(IV), ZR(RDSP)(ADSP).....	9
2.3.1 (4-Amino-N,N'-disalicylidene-1,2-phenylenediaminato)(4-cyano-N,N'-disalicylidene-1,2-phenylenediaminato)zirconium(IV), Zr(adsp)(cdsp) .....	9
2.3.2 (4-Amino-N,N'-disalicylidene-1,2-phenylenediaminato)(4-methyl-N,N'-disalicylidene-1,2-phenylenediaminato)zirconium(IV), Zr(adsp)(mdsp).....	9
2.3.3 (4-Amino-N,N'-disalicylidene-1,2-phenylenediaminato)(N,N'-disalicylidene-1,2-phenylenediaminato)zirconium(IV), Zr(adsp)(dsp); (4-Amino-N,N'-disalicylidene-1,2-phenylenediaminato)(N,N'-di-3-methoxysalicylidene-1,2-phenylenediaminato)-zirconium(IV), Zr(adsp)(3-OCH <sub>3</sub> dsp); (4-Amino-N,N'-disalicylidene-1,2-phenylenediaminato)(N,N'-di-5-methoxysalicylidene-1,2-phenylenediaminato)zirconium(IV), Zr(adsp)(5-OCH <sub>3</sub> dsp) .....	10
2.4 MELLITIC DIANHYDRIDE, MADA.....	10
2.5 POLY(4,4'-OXYDIPHTHALIC ANHYDRIDE/3,4'-OXYDIANILINE/10 MOL% MELLITIC DIANHYDRIDE), PAA(ODPA/3,4'-ODA/ 10 MADA) .....	11
2.6 SYNTHESIS OF ZR(ADSP)(RDSP) PENDENT POLY(4,4'-OXYDIPHTHALIC ANHYDRIDE/3,4'-OXYDIANILINE/10 MOL% MELLITIC DIANHYDRIDE), PAA(ODPA/3,4'-ODA/ 10 MADA/10 ZR) .....	12
2.7 SYNTHESIS OF ZR(ADSP)(RDSP) PENDENT POLY(4,4'-OXYDIPHTHALIC ANHYDRIDE/3,4'-OXYDIANILINE/10 MOL% MELLITIC DIANHYDRIDE)IMIDE, PI(ODPA/3,4'-ODA/ 10 MADA/10 ZR), AND FILM PREPARATION .....	14
2.8 INSTRUMENTS AND EXPERIMENTAL METHODS.....	14
2.8.1 Fourier Transform Infrared Spectroscopy (FTIR) .....	14
2.8.2 Proton Nuclear Magnetic Resonance Spectroscopy ( <sup>1</sup> H NMR).....	15
2.8.3 Thermogravimetric Analysis (TGA) .....	15
2.8.4 Differential Scanning Calorimetry (DSC) .....	16
2.8.5 Gel Permeation Chromatography (GPC).....	16
2.8.6 Film Flexibility and Solvent Resistance.....	17
2.8.7 Light Scattering.....	17
2.8.8 Contact Angle.....	17
2.8.9 Oxygen Plasma Etching.....	18
2.8.10 Scanning Electron Micrograms (SEM) .....	18

<b>RESULTS .....</b>	<b>19</b>
3.1 SYNTHESIS OF Zr(ADSP)(MDSP) AND THE OTHER Zr(ADSP)(RDSP) .....	19
3.2 SYNTHESIS OF MELLITIC DIANHYDRIDE (MADA) .....	20
3.3 SYNTHESIS OF POLYMER .....	20
3.3.1 <i>Synthesis of Polyamic Acid</i> .....	20
3.3.2 <i>Synthesis of Zirconium Pendent Polyamic Acid</i> .....	20
(a) <i>Before, and (b) After Reaction with DCC</i> .....	23
3.3.3 <i>Imidization of Parent Polyamic Acid and Zirconium Pendent Polyamic Acid films</i> .....	23
3.4 CHARACTERIZATION OF POLYAMIC ACIDS AND POLYIMIDES .....	24
3.4.1 <i>Infrared Spectrometry (IR)</i> .....	24
3.4.2 <i>Proton Nuclear Magnetic Resonance (<sup>1</sup>H NMR)</i> .....	24
3.4.4 <i>Differential Scanning Calorimetry (DSC)</i> .....	53
3.4.5 <i>Scanning Electron Microscopy (SEM)</i> .....	60
3.4.6 <i>Gel Permeation Chromatography (GPC)</i> .....	60
3.4.7 <i>Light Scattering Tests</i> .....	70
3.4.8 <i>Contact Angle</i> .....	71
3.4.9 <i>Film Flexibility and Solvent Resistance Test</i> .....	71
<b>DISCUSSION .....</b>	<b>73</b>
4.1 SYNTHESIS .....	73
4.1.1 <i>Zirconium Complexes</i> .....	73
4.1.2 <i>Mellitic Dianhydride (MADA)</i> .....	73
4.1.3 <i>Parent Polyamic Acid</i> .....	74
4.1.4 <i>Zirconium Pendent Polyamic Acids</i> .....	75
4.1.5 <i>Zirconium Pendent Polyimides</i> .....	76
4.2 POLYMER CHARACTERIZATION .....	76
4.2.1 <i>Thin Layer Chromatography (TLC)</i> .....	76
4.2.2 <i>Infrared Spectrometry (IR)</i> .....	76
4.2.3 <i>Nuclear Magnetic Resonance (NMR)</i> .....	77
4.2.4 <i>Thermogravimetric Analysis (TGA)</i> .....	77
4.2.5 <i>Differential Scanning Calorimetry (DSC)</i> .....	77
4.2.6 <i>Scanning Electron Microscopy (SEM) and Atomic Oxygen Durability Characterization</i> .....	78
4.2.7 <i>Gel Permeation Chromatography (GPC)</i> .....	78
4.2.8 <i>Light Scattering Tests</i> .....	79
4.2.9 <i>Solvent Resistance</i> .....	79
4.2.10 <i>Contact Angle Measurement</i> .....	80
<b>SUGGESTION FOR FUTURE WORK .....</b>	<b>81</b>
<b>CONCLUSIONS .....</b>	<b>82</b>
<b>REFERENCES .....</b>	<b>83</b>
<b>APPENDIX .....</b>	<b>85</b>

## List of Abbreviations

AO	atomic oxygen
ISS	International Space Station
LEO	low earth orbit
H <sub>2</sub> dsp	N,N'-disalicylidene-1,2-phenylenediamine
H <sub>2</sub> ndsp	4-nitro-N,N'-disalicylidene-1,2-phenylenediamine
MA	mellitic acid
MADA	mellitic acid dianhydride
NMP	1-methyl-2-pyrrolidone
DCC	dicyclohexylcarbodiimide
ODPA	4,4'-oxydiphthalic anhydride
3,4'-ODA	3,4'-oxydianiline
PAA	polyamic acid
PI	polyimide
Zr(dsp)(ndsp)	(4-nitro-N,N'-disalicylidene-1,2-phenylenediaminato)(N,N'-disalicylidene-1,2-phenylenediaminato)zirconium(IV)
Zr(H) or Zr(adsp)(dsp)	(4-amino-N,N'-disalicylidene-1,2-phenylenediaminato)(N,N'-disalicylidene-1,2-phenylenediaminato)zirconium(IV)
Zr(c) or Zr(adsp)(cdsp)	(4-amino-N,N'-disalicylidene-1,2-phenylenediaminato)(4-cyano-N,N'-disalicylidene-1,2-phenylenediaminato)-zirconium(IV)
Zr(m) or Zr(adsp)(mdsp)	(4-amino-N,N'-disalicylidene-1,2-phenylenediaminato)(4-methyl-N,N'-disalicylidene-1,2-phenylenediaminato)-zirconium(IV)
Zr(3-OCH <sub>3</sub> ) or Zr(adsp)(3-OCH <sub>3</sub> dsp)	(4-amino-N,N'-disalicylidene-1,2-phenylenediaminato)(N,N'-di-3-methoxysalicylidene-1,2-phenylenediaminato)-zirconium(IV)
Zr(5-OCH <sub>3</sub> ) or Zr(adsp)(5-OCH <sub>3</sub> dsp)	(4-amino-N,N'-disalicylidene-1,2-phenylenediaminato)-(N,N'-di-5-methoxysalicylidene-1,2-phenylenediaminato)-zirconium(IV)



## List of Figures

Figure 1.1 Structure of Polyimide Kapton™	1
Figure 1.2 Structure of Zr(dsp) <sub>2</sub>	2
Figure 1.3 Structure of Zr(adsp)(dsp)	3
Figure 1.4 Structure of Zr(adsp)(dsp) Pendent Kapton-like Terpolymer	4
Figure 1.5 Structure of LARC-IA	4
Figure 1.6 Structure of Zr(adsp)(Rdsp) to be used in this study	5
Figure 1.7 Synthesis of Zr(adsp)(dsp) Pendent Polyimide	6
Figure 2.1 Synthesis of MADA	10
Figure 2.2 Dianhydride Converts to Trianhydride in TGA	11
Figure 2.3 Synthesis of Copolyamic Acid	11
Figure 2.4 Synthesis of Zirconium Pendent Copolyamic Acid	12
Figure 2.5 Imidization of Copolyamic Acid	14
Figure 2.6 Synthesis of Zr(adsp)(Rdsp) Pendent Copolyimide	15
Figure 3.1 Hydrogenation of 4-Amino-3-nitrobenzonitrile	19
Figure 3.2 Synthetic Scheme of Substituted Schiff Base-H <sub>2</sub> Rdsp	19
Figure 3.3 TGA Graph of MADA	21
Figure 3.4 Synthesis of Zr(adsp)(Rdsp) Pendent Copolyimide	22
Figure 3.5 TLC Indicating Attaching Zirconium Complex to Parent Polyamic Acid	23
Figure 3.6 IR Spectrum of Zr(adsp)(dsp)	27
Figure 3.7 IR Spectrum of PAA and PAA/Zr(R)	28
Figure 3.8 IR Spectrum of Parent Polyimide	29
Figure 3.9 IR Spectrum of Zr(adsp)(dsp) Pendent Polyimide	30
Figure 3.10 IR Spectrum of Zr(adsp)(mdsp) Pendent Polyimide	31
Figure 3.11 IR Spectrum of Zr(adsp)(cdsp) Pendent Polyimide	32
Figure 3.12 IR Spectrum of Zr(adsp)(3-OCH <sub>3</sub> dsp) Pendent Polyimide	33
Figure 3.13 IR Spectrum of Zr(adsp)(5-OCH <sub>3</sub> dsp) Pendent Polyimide	34
Figure 3.14 <sup>1</sup> HNMR Spectrum of Parent Polyamic Acid	35
Figure 3.15 <sup>1</sup> HNMR Spectrum of Zr(adsp)(dsp)	36
Figure 3.16 <sup>1</sup> HNMR Spectrum of Zr(adsp)(dsp) Pendent Polyamic Acid	37
Figure 3.17 <sup>1</sup> HNMR Spectrum of Zr(adsp)(mdsp)	38

Figure 3.18 $^1\text{H}$ NMR Spectrum of Zr(adsp)(mdsp) Pendent Polyamic Acid	39
Figure 3.19 $^1\text{H}$ NMR Spectrum of Zr(adsp)(cdsp)	40
Figure 3.20 $^1\text{H}$ NMR Spectrum of Zr(adsp)(cdsp) Pendent Polyamic Acid	41
Figure 3.21 $^1\text{H}$ NMR Spectrum of Zr(adsp)(3-OCH <sub>3</sub> dsp)	42
Figure 3.22 $^1\text{H}$ NMR Spectrum of Zr(adsp)(3-OCH <sub>3</sub> dsp) Pendent Polyamic Acid	43
Figure 3.23 $^1\text{H}$ NMR Spectrum of Zr(adsp)(5-OCH <sub>3</sub> dsp)	44
Figure 3.24 $^1\text{H}$ NMR Spectrum of Zr(adsp)(5-OCH <sub>3</sub> dsp) Pendent Polyamic Acid	45
Figure 3.25 TGA Graph of Parent Polyamic Acid	47
Figure 3.26 TGA Graph of Zr(adsp)(dsp) Pendent Polyamic Acid	48
Figure 3.27 TGA Graph of Zr(adsp)(mdsp) Pendent Polyamic Acid	49
Figure 3.28 TGA Graph of Zr(adsp)(cdsp) Pendent Polyamic Acid	50
Figure 3.29 TGA Graph of Zr(adsp)(3-OCH <sub>3</sub> dsp) Pendent Polyamic Acid	51
Figure 3.30 TGA Graph of Zr(adsp)(5-OCH <sub>3</sub> dsp) Pendent Polyamic Acid	52
Figure 3.31 DSC Graph of Parent Polyamic Acid	54
Figure 3.32 DSC Graph of Zr(adsp)(dsp) Pendent Polyamic Acid	55
Figure 3.33 DSC Graph of Zr(adsp)(mdsp) Pendent Polyamic Acid	56
Figure 3.34 DSC Graph of Zr(adsp)(cdsp) Pendent Polyamic Acid	57
Figure 3.35 DSC Graph of Zr(adsp)(3-OCH <sub>3</sub> dsp) Pendent Polyamic Acid	58
Figure 3.36 DSC Graph of Zr(adsp)(5-OCH <sub>3</sub> dsp) Pendent Polyamic Acid	59
Figure 3.37 SEM Pictures Before Atomic Oxygen Etching	61
Figure 3.38 SEM Pictures After Atomic Oxygen Etching at 2,500 Magnification	62
Figure 3.39 SEM Pictures After Atomic Oxygen Etching at 10,000 Magnification	63
Figure 3.40 GPC Graph of Parent Polyamic Acid	64
Figure 3.41 GPC Graph of Zr(adsp)(dsp) Pendent Polyamic Acid	65
Figure 3.42 GPC Graph of Zr(adsp)(mdsp) Pendent Polyamic Acid	66
Figure 3.43 GPC Graph of Zr(adsp)(cdsp) Pendent Polyamic Acid	67
Figure 3.44 GPC Graph of Zr(adsp)(3-OCH <sub>3</sub> dsp) Pendent Polyamic Acid	68
Figure 3.45 GPC Graph of Zr(adsp)(5-OCH <sub>3</sub> dsp) Pendent Polyamic Acid	69
Figure 4.1 MADA and Byproducts	74

## List of Tables

Table 2.1 Solvents Used in Column Chromatography-----	10
Table 2.2 Eluting System Used in TLC Measurement-----	13
Table 2.3 Samples for GPC Analysis-----	17
Table 3.1 Elemental Analysis Result-----	20
Table 3.2 Bands from IR Spectra -----	25
Table 3.3 Peaks from NMR-----	25
Table 3.4 Integral Ratio of Imino Proton to Aromatic Proton-----	26
Table 3.5 TGA Results for Parent Polyamic Acid and Zirconium Pendent Polyamic Acids -----	46
Table 3.6 ZrO <sub>2</sub> Residue after Thermal Decomposition Step in TGA-----	53
Table 3.7 Glass Transition Temperature from DSC Result for Polyimide Films-----	53
Table 3.8 GPC Results for Polyamic acid and Zirconium Pendent Polyamic Acids-----	70
Table 3.9 Light Scattering Test Results-----	70
Table 3.10 Result of Contact Angle Measurement -----	71
Table 3.11 Solvent Resistance Test-----	72

## ABSTRACT

The objective of this thesis is to synthesize functionalized zirconium complex pendent polyamic acids and polyimides, then compare their characteristics, e.g. thermal properties, atomic oxygen resistance, and film properties (adhesion, flexibility, and solvent resistance). Towards this end, five different zirconium complexes were attached to the polyamic acid, which is based on 3,4'-oxydianiline (3,4'-ODA), 4,4'-oxydipthalic anhydride (ODPA), and mellitic dianhydride (MADA), in the presence of dicyclohexylcarbodiimide (DCC). The resulting zirconium complex pendent polyamic acids and the parent polyamic acid were cast onto glass substrates, then thermally imidized by heating at 100°C, 200°C, and 300°C for one hour each.

The synthesized zirconium complex pendent polyamic acids and polyimides were characterized by Thin Layer Chromatography (TLC), Fourier Transform Infrared (FT-IR), Proton Nuclear Magnetic Resonance ( $^1\text{H}$  NMR), Gel Permeation Chromatography (GPC), Light Scattering test (LS), Thermogravimetric Analysis (TGA), Differential Scanning Calorimetry (DSC), Scanning Electronic Microscopy (SEM), Refractive index, and Contact Angle Measurement to investigate their adhesive properties. TLC results indicate that no free zirconium complexes remain in the polymer solutions. Spectroscopic results support the conclusion that the structures obtained are consistent with the proposed ones. Both the GPC results and LS results indicate that a moderate degree of polymerization occurred (average degree of polymerization ca. 100), and the weight average molecular weight of the pendent polymers is higher than the parent polymer. Decomposition temperatures of pendent polyimides are slightly lower than that of the parent polyimide, but all are above 500°C, which means that they possess very high thermal stability. The SEM results and visual observation indicate that the atomic oxygen erosion of the zirconium pendent polyimide films leaves a white surface residue, which is due primarily to the formation of zirconium dioxide. The generation of a uniform zirconium dioxide layer protects the original material from atomic oxygen erosion. The zirconium pendent polyimides have higher glass transition temperatures,  $T_g$ , than the parent polyimide.

All of the imidized films passed the solvent resistance test, by remaining flexible following immersion in acetone, methyl ethyl ketone, toluene, dimethylacetamide, and chloroform for 30 minutes followed by a fingernail crease. Two-layer thick films cracked upon imidization.

## INTRODUCTION

The existence of Atomic Oxygen (AO) in the Low Earth Orbit (LEO) has been known for many years. Single, neutral oxygen atoms in the ground state are the most predominant species in LEO between the altitudes of 180 and 650 km.<sup>1</sup> As spacecraft pass through the atmosphere at these altitudes, they collide with the oxygen atoms with an equivalent energy ranging from 3.3 to 5.5 eV.<sup>2</sup> These collisions are energetic enough to break many chemical bonds and allow the highly reactive AO to oxidize many organic and some metallic materials.<sup>3</sup>

A DuPont polyimide, Kapton<sup>TM</sup>, has been used in a variety of applications in LEO and its erosion in LEO has been more extensively studied than any other material. Its outstanding properties, e.g. light weight, flexibility, strength and IR transparency properties, enable it to survive atomic oxygen and other environmental hazards including ultraviolet radiation, thermal cycling, and impact from micrometeoroids and debris, make it suitable for use aboard spacecraft. (See Figure 1.1) However, its oxidation rate in LEO atomic oxygen environment is high.

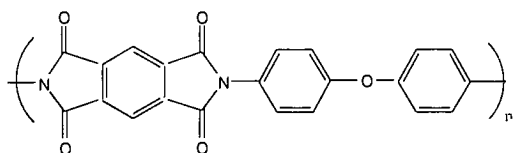


Figure 1.1 Structure of Polyimide Kapton<sup>TM</sup>

The volume of organic material oxidized per incident AO atom, called the erosion yield, was found to be  $3.0 \times 10^{-24}$  cm<sup>3</sup>/atom for polyimide Kapton. When AO reacts with polymers it forms gaseous oxidation products (primarily CO) which results in material loss that can hinder system performance.<sup>4</sup> The International Space Station (ISS) solar array is designed for a 15 years operating life in LEO. However, the oxidation rate of Kapton is great enough that structural failure of the blanket would occur in much less than 15 years. If an ISS photovoltaic array blanket was made of polyimide Kapton alone, it would be oxidized in six months, in spite of its 15-year durability requirement.<sup>5</sup>

Protective films containing a high fraction of metal oxides, such as  $\text{SiO}_2$ , and  $\text{Al}_2\text{O}_3$  films, have been demonstrated in both ground and space tests to be effective in protecting Kapton from being oxidized by LEO AO.<sup>5-7</sup> However, although such coatings are themselves AO durable, defects in these coatings do allow AO attack of the underlying Kapton. Because AO can penetrate through defect areas on protective oxide coating, gradual undercutting occurs. Undercutting oxidation at defect sites, which typically results from processing and/or debris impacts in space, can ultimately lead to complete oxidation of the underlying Kapton if sufficiently high AO exposure occurs.<sup>5</sup>

A modified Kapton, designated as AOR (Atomic Oxygen Resistant) Kapton, has been proposed as a back up material for the ISS solar array design. The ground-based plasma etching tests performed at The National Aeronautics and Space Administration (NASA) showed that AOR Kapton represents a significant improvement in AO resistance over pure Kapton. However, this silicon containing material produced a volatile substance that was deposited on nearby surfaces when tested on the Long-Duration Exposure Facility, which was 69 months in LEO.<sup>8,9</sup>

In 1993, Dr. M. L. Illingsworth found that a zirconium complex produced no volatile intermediates upon ground-based AO exposure. A sapphire disk located adjacent to a glassy film of the zirconium material bis(N, N'-disalicylidene-1, 2-phenylenediaminato)zirconium(IV),  $\text{Zr}(\text{dsp})_2$ , did not show any zirconium upon examination by x-ray photoelectron spectrometry(XPS).<sup>10</sup> (See Figure 1.2)

In addition, zirconium complexes were thought to have all other properties required

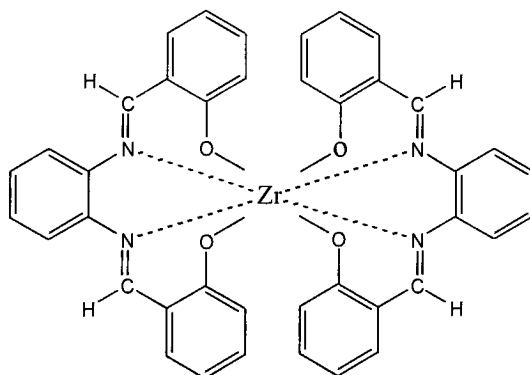


Figure 1.2 Structure of  $\text{Zr}(\text{dsp})_2$

for AOR materials: (a)  $\text{ZrO}_2$  has a standard free energy of formation, which is  $-1042.8 \text{ KJ/mol}^{11}$  and therefore is one of the most stable metal oxides; (b) organically wrapped Zr should blend better, and thus distribute better, than  $\text{ZrO}_2$  in the polyamic acid (re: “like dissolves like”); (c) a  $\text{ZrO}_2$  protective layer should form if the initial protective layer is compromised, i.e., a “self-healing” property similar to that of Si containing AOR film should be exhibited; (d) Zr is relatively abundant and is not expensive; Zr ranks 18<sup>th</sup> in terms of abundance in the earth’s crust.<sup>12</sup>

However, using  $\text{Zr}(\text{dsp})_2$  as a polymer additive, a concentration of only 4 mol% caused polyamic acid of Kapton films to crack upon imidization. The 4 mol% concentration of Zr complex was not enough to form a protective layer when plasma etched.<sup>13</sup>

Preparation of a Zr-MA(maleic acid)/PI blend gave improvement of Zr concentration up to 8 mol% before film cracking was observed.<sup>14, 15</sup>

Currently, efforts are being made to synthesize Zr pendent polyimide, other than via blending with Kapton polyimide, to increase the upper limit of inorganic component concentration to obtain materials possessing higher AO durability.

A zirconium complex pendent polyimide, which contained up to 40 mol% of mixed

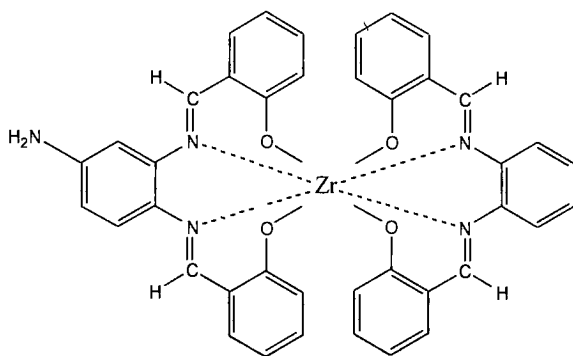


Figure 1.3 Structure of  $\text{Zr}(\text{adsp})(\text{dsp})$

ligand zirconium complex,  $\text{Zr}(\text{dsp})(\text{adsp})$ , was obtained by directly bonding the complex with the soluble polyamic acid precursor of the desired Kapton-like ter-polyimide. (See Figure 1.3 & Figure 1.4) The polyimide film, which was made by casting the polyamic acid solution onto a glass slide followed by heated at 100, 200, 300 °C each for one hour, was transparent and flexible, and no phase separation was observed during the



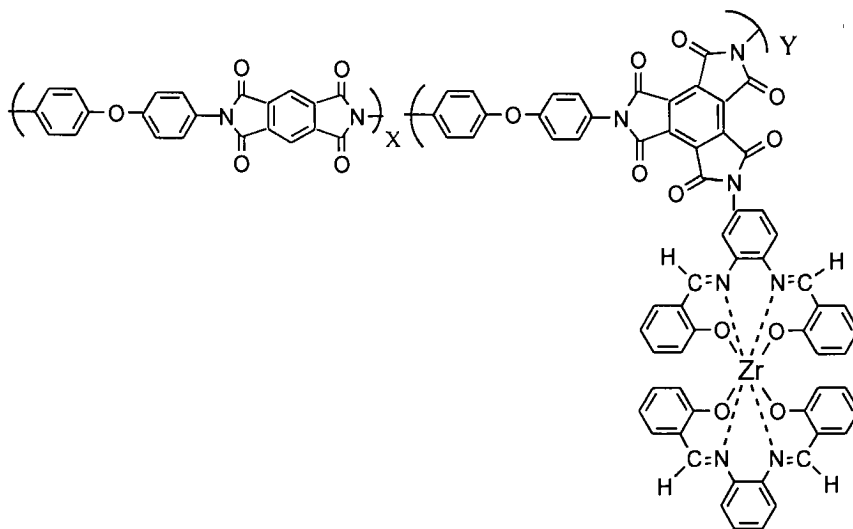


Figure. 1.4 Structure of Zr(adsp)(dsp) Pendent Kapton-like Terpolymer

drying and curing steps. However, only two-layer films could be made before films cracked upon imidization.<sup>16</sup>

Therefore, new approaches intended to produce more flexible Zr pendent polyimides are being investigated.

A new polyimide, designated as LARC-IA (Langley Research Center-Improved Adhesion) which was prepared from 3, 4'-oxydianiline (ODA) and oxydiphthalic anhydride (ODPA) in N-methylpyrrolidone (NMP) as a 30% w/w solid solution, has been synthesized and evaluated. (See Figure 1.5) The molecular weight was controlled by use of mono-functional phthalic anhydride (PA). Excellent adhesive properties and thermo-oxidative stability were obtained with this polymer.<sup>17</sup> Also, it is synthesized from noncarcinogenic nontoxic chemicals, and it is relatively inexpensive. The adhesive properties of LARC-IA

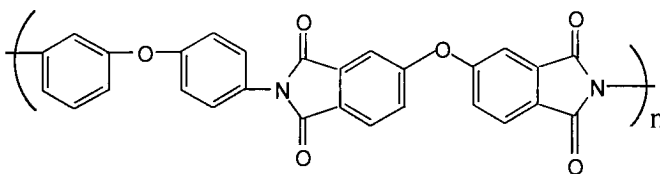


Figure. 1.5 Structure of LARC-IA

have been attributed to the high degree of flexibility in the polymer backbone afforded by the oxygen-bridged dianhydride and the meta-linked diamine.<sup>18</sup>

It has just been shown that the LARC-IA structure could be adapted to accommodate Zr pendent groups.<sup>19</sup> (See Figure 1.6)

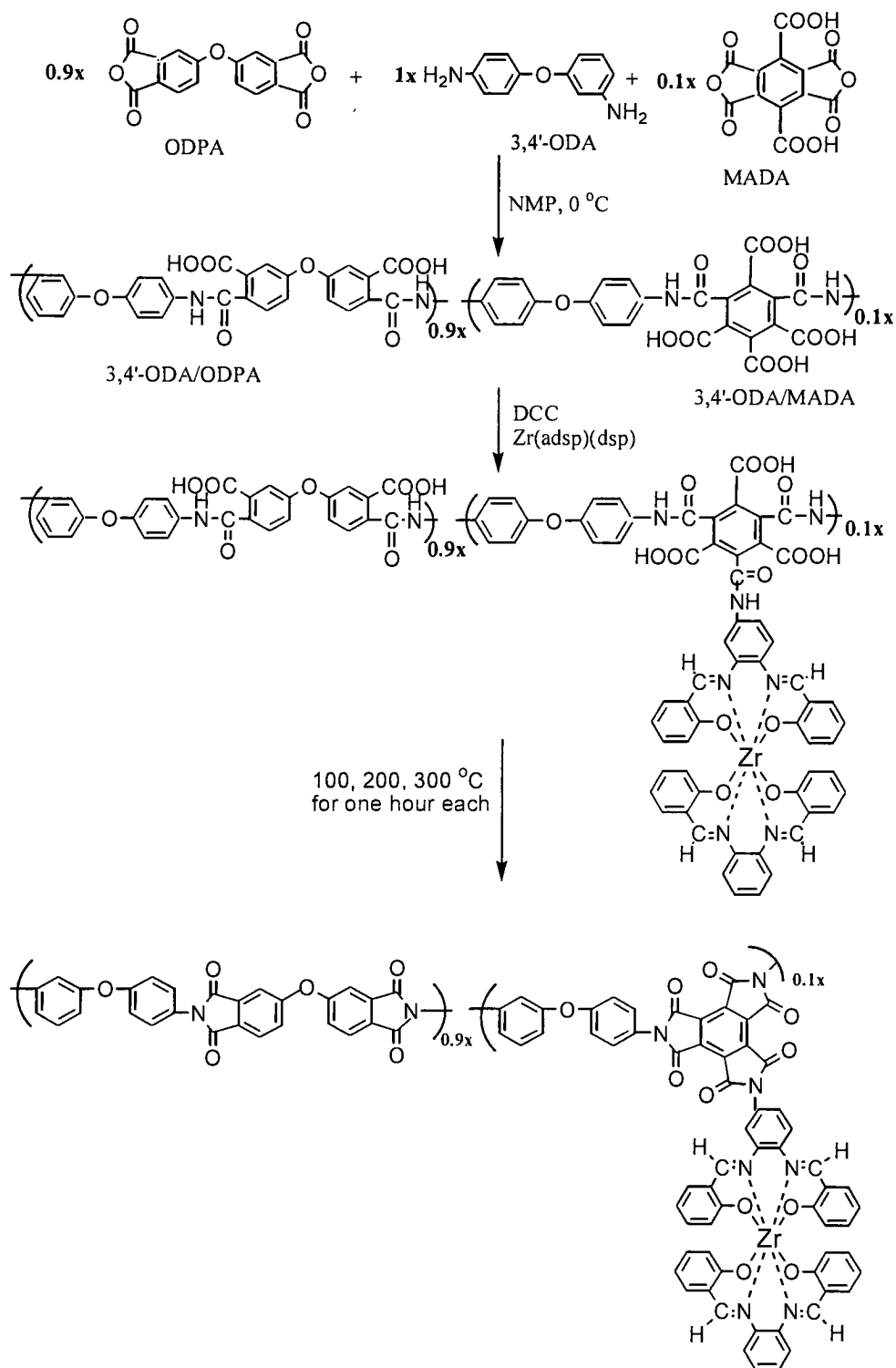
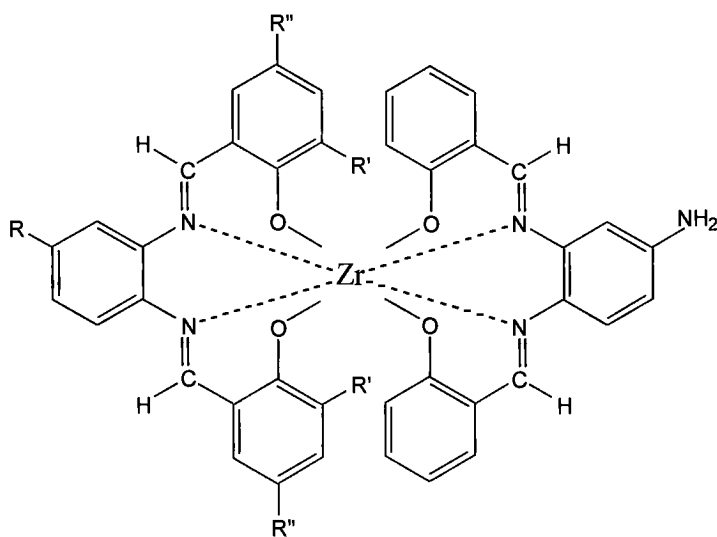


Figure 1.6 Synthesis of Zr(adsp)(dsp) pendent co-polyimide

My research project is also based on modifying the structure of LARC-IA. By introducing a multi-functional monomer into the polymer backbone, and then attaching the zirconium complex to the polymer, a pendent polymer will form. There are five different zirconium complexes that were previous made for attaching to the polymer backbone (See Figure 1.7).



1.  $\text{Zr}(\text{adsp})(5\text{-OCH}_3\text{dsp})$ ---  $\text{R}=\text{H}$ ,  $\text{R}'=\text{H}$ ,  $\text{R}''=\text{OCH}_3$
2.  $\text{Zr}(\text{adsp})(3\text{-OCH}_3\text{dsp})$ ---  $\text{R}=\text{H}$ ,  $\text{R}'=\text{OCH}_3$ ,  $\text{R}''=\text{H}$
3.  $\text{Zr}(\text{adsp})(\text{CNdsp})$ -----  $\text{R}=\text{CN}$ ,  $\text{R}'=\text{H}$ ,  $\text{R}''=\text{H}$
4.  $\text{Zr}(\text{adsp})(\text{CH}_3\text{dsp})$ -----  $\text{R}=\text{CH}_3$ ,  $\text{R}'=\text{H}$ ,  $\text{R}''=\text{H}$
5.  $\text{Zr}(\text{adsp})(\text{dsp})$ -----  $\text{R}=\text{H}$ ,  $\text{R}'=\text{H}$ ,  $\text{R}''=\text{H}$

Figure. 1.7 Structures of  $\text{Zr}(\text{adsp})(\text{Rdsp})$  to be used in this study.

## EXPERIMENTAL

### 2.1 Chemicals

1,2-Phenylenediamine, salicylaldehyde, N,N-dimethylacetamide, 4-nitro 1,2-phenylenediamine, zirconium(IV) n-butoxide [ $\text{Zr}(\text{O-n-Bu})_4$ ] (80 wt% solution in 1-butanol), palladium on activated carbon (Pd 10%),  $\text{P}_2\text{O}_5$ , and dicyclohexylcarbodiimide (DCC) were obtained from Aldrich. Methylene chloride, silica gel Celite 545, chloroform, methyl ethyl ketone, ethyl acetate, tetrahydrofuran were obtained from J. T. Baker. Acetone was obtained from Fisher ChemAlert<sup>®</sup> Guide. 4-Amino-3-nitrobenzonitrile was obtained from Fluka. Benzenhexacarboxylic acid (mellitic acid) was obtained from TLC, Tokyo KASEI. All of these chemicals were used as received.

4,4'-Oxydiphthalic anhydride (ODPA) (Chriskev Company, Inc.) and 3,4'-oxydianiline (3,4'-ODA) (TCI, Tokyo KASEI) were purified by subliming three times at 200 and 80 °C respectively, and stored in a desiccator containing  $\text{P}_2\text{O}_5$  to prevent the absorption of moisture. The 1-methyl-2-pyrrolidinone, NMP, used for polymerization and DCC reactions, obtained from Aldrich, was dried by distillation over  $\text{CaH}_2$  under a flow of nitrogen gas.

All thin layer chromatograms were obtained on silica (Kodak).

### 2.2 Synthesis of Substituted N,N'-Disalicylidene-1,2-phenylenediamine ( $\text{H}_2\text{Rdsp}$ )

#### 2.2.1 N,N'-Disalicylidene-1,2-phenylenediamine, $\text{H}_2\text{dsp}$

To a stirring solution of 8.0 g (0.075 mol) of 1,2-phenylenediamine in 80 mL of absolute ethanol, 17.0 mL (0.150 mol) of salicylaldehyde was added. The mixture was heated and kept at reflux for 1 h, then allowed to cool to room temperature, and suction filtered. The product was thoroughly washed with absolute ethanol three times. After air drying, 24.0 g of reddish orange crystal was obtained; 80% yield.<sup>20</sup>

The purity of the product was confirmed by spotting a dilute methylene chloride solution onto a silica gel TLC plate and eluting with a methylene chloride-hexane solution (7:3). Only one spot was observed in the resultant chromatogram.

### 2.2.2 4-Nitro-N,N'-disalicylidene-1,2-phenylenediamine, H<sub>2</sub>ndsp

To a stirring solution of 8.0 g (0.052 mol) of 4-nitro-1,2-phenylenediamine in 480 mL of absolute ethanol, 12.0 mL (0.122 mol) of salicylaldehyde was added. The mixture was heated and kept at reflux for 8 h, then allowed to cool to room temperature, and suction filtered. The product was thoroughly washed with absolute ethanol three times. After air drying, 8.5 g of fluffy yellow product was obtained; 45% yield.<sup>21</sup>

The purity of the product was confirmed by TLC as described above. Only one spot was observed.

### 2.2.3 4-Cyano-N,N'-disalicylidene-1,2-phenylenediamine, H<sub>2</sub>cdsp

#### 2.2.3.1 Hydrogenation of 4-Amino-3-nitrobenzonitrile

In a Parr bottle 5.0 g of 4-Amino-3-nitrobenzonitrile was completely dissolved in 70 mL of THF, then 0.68 g of activated carbon (Pd 10%) was added. The mixture was then subjected to a hydrogen gas atmosphere of 60 lb/in<sup>2</sup> gauge pressure, with agitation, for 24 hours using a Parr pressure reaction apparatus. Completion of the hydrogenation was confirmed by TLC separation of the reaction solution using methylene chloride- acetonitrile (9:1) as eluting solution; only one spot was observed. When hydrogenation was completed, the catalyst was removed by suction filtration through Celite 545<sup>TM</sup> gel and washed with a fresh portion of solvent. The solution was then rotary evaporated in a 55 °C water bath. The yield of the yellow product is 4.60 g (100%).

#### 2.2.3.2 Synthesis of 4-Cyano-N,N'-disalicylidene-1,2-phenylenediamine, H<sub>2</sub>cdsp

To a stirring solution of 4.6 g (0.031 mol) of 4-cyano-1,2-phenylenediamine in 200 mL of absolute ethanol, 7.0 mL (0.062mol) of salicylaldehyde was added. The mixture was heated and kept at reflux for 20 h, then allowed to cool to room temperature and then kept in refrigerator over night. After that, the solution was rotary evaporated to reduce the volume from 200 mL to 60 mL, kept in refrigerator over night, and suction filtered. The product, 5.3 g of yellow powder, was obtained; yield 63%.

The purity of the product was confirmed by performing TLC with methylene chloride- acetonitrile (9:1) as eluting solution, only one spot was observed in the resultant chromatogram.

## **2.3 Synthesis of Substituted (N,N'-Disalicylidene-1,2-phenylenediaminato)(4-amino N,N'-disalicylidene-1,2-phenylenediaminato)zirconium(IV), Zr(Rdsp)(adsp)**

### **2.3.1 (4-Amino-N,N'-disalicylidene-1,2-phenylenediaminato)(4-cyano-N,N'-disalicylidene-1,2-phenylenediaminato)zirconium(IV), Zr(adsp)(cdsp)**

H<sub>2</sub>cdsp (2.72 g, 8.00 mmol) and H<sub>2</sub>ndsp (2.88 g, 8.00 mmol) were dissolved in the solvent containing 100 mL of acetonitrile and 200 mL of methylene chloride with stirring and heating. After dissolution, the solution was allowed to cool to room temperature, and 3.64 mL (8.00 mmol) of zirconium tetra-n-butoxide, Zr(O-n-BuOH)<sub>4</sub>, were added under a nitrogen atmosphere (glove bag). Then, the flask containing the mixture was stoppered, removed from the glove bag, and heated at reflux for three hours with stirring. Solvent was removed by rotary evaporation. The solid was then dissolved with THF in a Parr bottle, and the same hydrogenation procedure described above was performed.

Completion of the hydrogenation was confirmed by TLC separation of the solution with chloroform-ethyl acetate (9:1) as eluting solution. Three spots were observed in the resultant chromatogram. From highest to lowest R<sub>f</sub> spot, they were 1.00, 0.75, and 0.00, respectively.

The hydrogenation products was then separated on a silica gel column using chloroform-ethyl acetate (8:1) as eluting solution, producing three bands in the column. The second band was collected and concentrated by rotary evaporation to dryness.

The purity of the product was confirmed by spotting a dilute chloroform solution onto a silica gel TLC plate and eluting with a chloroform-ethyl acetate solution (8:1). Only one spot was observed. An orange powder was obtained. The yield is 1.00 g (16.5%).

### **2.3.2 (4-Amino-N,N'-disalicylidene-1,2-phenylenediaminato)(4-methyl-N,N'-disalicylidene-1,2-phenylenediaminato)zirconium(IV), Zr(adsp)(mdsp)**

Equimolar amounts of H<sub>2</sub>ndsp and H<sub>2</sub>mdsp were mixed together and dissolved in THF. Upon cooling to room temperature, the stoichiometric amount of Zr(O-n-Bu)<sub>4</sub> was added into the Schiff base solution and stirred 1 hour. The product was then filtered and dissolved in THF followed by hydrogenation with 10% Pd on activated carbon resulting the mixture of Zr(adsp)<sub>2</sub>, Zr(adsp)(mdsp), and Zr(mdsp)<sub>2</sub>. The mixture was then eluted through

a silica gel column with methylene chloride-ethyl acetate (88:12) as eluting solution, the second band was collected and rotary evaporated to dryness to obtain the solid product, which is yellow powder.

**2.3.3 (4-Amino-N,N'-disalicylidene-1,2-phenylenediaminato)(N,N'-disalicylidene-1,2-phenylenediaminato)zirconium(IV), Zr(adsp)(dsp); (4-Amino-N,N'-disalicylidene-1,2-phenylenediaminato)(N,N'-di-3-methoxysalicylidene-1,2-phenylenediaminato)-zirconium(IV), Zr(adsp)(3-OCH<sub>3</sub>dsp); (4-Amino-N,N'-disalicylidene-1,2-phenylenediaminato)(N,N'-di-5-methoxysalicylidene-1,2-phenylenediaminato)zirconium(IV), Zr(adsp)(5-OCH<sub>3</sub>dsp)**

All the above complexes were synthesized by the same method, except that different elution systems were used.

Table 2.1. Solvents Used in Column Chromatography

Sample	Zr(adsp) (dsp)	Zr(adsp) (mdsp)	Zr(adsp) (cdsp)	Zr(adsp) (3-OCH <sub>3</sub> dsp)	Zr(adsp) (5-OCH <sub>3</sub> dsp)
CH <sub>2</sub> Cl <sub>2</sub> (V%)	90	88	80 (CHCl <sub>3</sub> )	85	80
Ethyl acetate (V%)	10	12	20	15	20
Color of Product	orange	yellow	orange	yellow	orange

## 2.4 Mellitic Dianhydride, MADA

Well ground mellitic acid (benzenehexacarboxylic acid), 2.0 g, was placed on the inner surface of a 20 mL test tube and laid horizontally in a drying pistol equipped with a thermometer, nitrogen inlet and outlet. Mellitic acid was heated under 20 mL/min flow rate

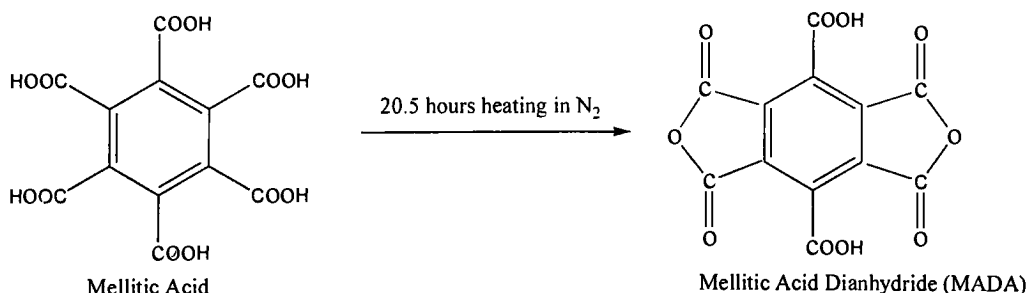


Figure 2.1 Synthesis of MADA

of nitrogen at 190-195°C by using ethylene glycol at reflux for 20.5 hours. Beige powder was obtained.

The purity of the product was confirmed by its thermogravimetric analysis (TGA). There was only one step weight lost shown on its TGA curve with a 5.8% mass loss, which was the result of 1 mole of water removed from MADA upon further heating.

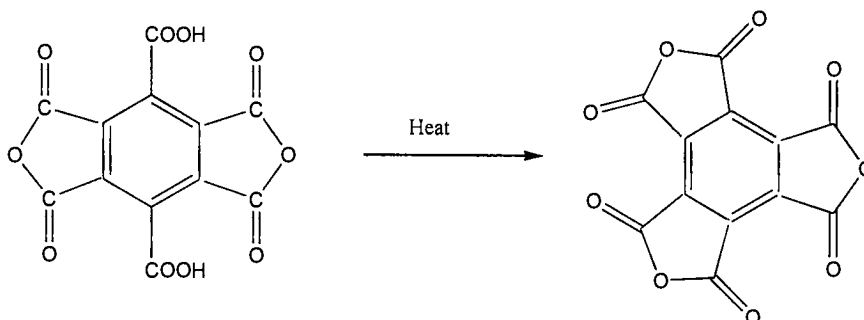


Figure 2.2 Dianhydride Converts to Trianhydride in TGA

## 2.5 Poly(4,4'-oxydiphthalic anhydride/3,4'-oxydianiline/10 mol% mellitic dianhydride), PAA(ODPA/3,4'-ODA/ 10 MADA)

To a mixture of 10.0505 g (32.4000 mmol) of purified ODPA and 1.102 g (3.600 mmol) of MADA in a 250 mL round bottom flask, 56.5 mL (80.6 g) of dried NMP was added. The reaction flask was capped with a rubbery septum with nitrogen flow and stirred for half an hour, the reaction temperature was maintained at 0°C by an ice-water bath. A solution of 7.2072 g (36.000 mmol) of 3,4'-ODA dissolved in 16.5 mL of dried NMP was

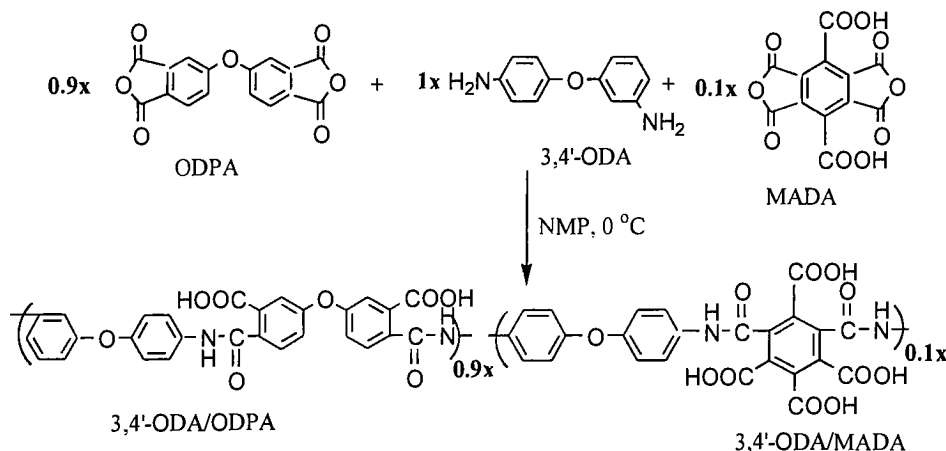


Figure 2.3 Synthesis of Copolyamic Acid



added into the flask dropwise via a 10 mL syringe. An additional 2 X 2.5 mL of NMP was used to rinse the container of the solution and the syringe twice and added to the reaction flask to keep the mole ratio of the reactants 3,4'-ODA:ODPA:MADA equal to 1:0.9:0.1 and the percent solid 15% by weight. With the addition of 3,4'-ODA, the suspended solid ODPA and MADA dissolved gradually. Finally it was completely dissolved after all of the 3,4'-ODA solution was added to the flask and a viscous, light brown, homogenous solution was obtained. It took about 5 hours to finish the process. After that, the polymer solution was moved to a refrigerator room where the temperature was maintained at 4°C and stirring was continued overnight.

## 2.6 Synthesis of Zr(adsp)(Rdsp) Pendent Poly(4,4'-oxydiphthalic anhydride/3,4'-oxydianiline/10 mol% mellitic dianhydride), PAA(ODPA/3,4'-ODA/ 10 MADA/10 Zr)

The polyamic acid solution was separated into six 100 mL round bottom flasks, each portion containing the same amount of polyamic acid solution, which was 6 mmol of 3,4'-ODA, 5.4 mmol of ODPA, and 0.6 mmol of MADA. In order to have a 1:1 mole ratio of Zr(adsp)(Rdsp) to MADA, 0.6 mmol batches of different Zr(adsp)(Rdsp) were dissolved in

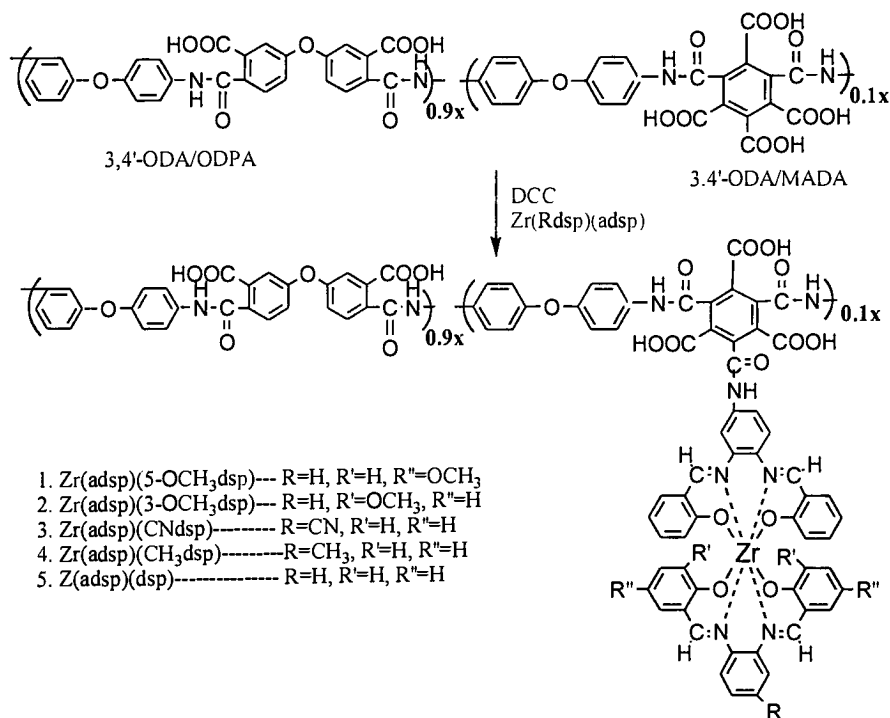


Figure 2.4 Synthesis of Zirconium Pendent Copolyamic Acid

dried NMP for reaction with the fresh prepared PAA (ODPA/3,4'-ODA/10 MADA) polymer.

Each of the five batches of Zr(adsp)(Rdsp) was well mixed with its own portion of polyamic acid solution, leaving one portion of PAA (ODPA/3,4'-ODA/10MADA) for future use. Then, a stoichiometric amount of DCC/NMP solution was added dropwise to each complex-polymer solution via 2 mL syringes. The completion of the reaction was monitored by spotting the solution onto a silica gel TLC plate, and eluting with an eluting system (see Table 2.1). The corresponding zirconium complex and nonpendent polyamic acid were used as references on each TLC plate, which, upon completion, was viewed under UV light. After all of the DCC/NMP solution was added to the reaction flask, a spot due to free zirconium complex was still observed on the TLC plate, which meant that the zirconium complex was not completely attached to polymer. Therefore, 10 mol% of additional DCC/NMP solution was prepared and added. The same TLC test was performed and this time no free zirconium complex spot was observed.

One mL portions of each PAA (ODPA/3,4'-ODA/10 MADA/10 Zr) solution and the polyamic acid solution were separately added into a blender with stirring anhydrous ether. After filtering and washing with anhydrous ether, solid polymer powder was obtained. The six different polymers were then dried in vacuum desiccator at room temperature for at least two days until the constant weight was reached.

Table 2.2 Eluting System Used in TLC Measurement

	CH <sub>2</sub> Cl <sub>2</sub> (V %)	Ethyl acetate (V %)
Zr(adsp)(dsp)	90	10
Zr(adsp)(mdsp)	80 (CHCl <sub>3</sub> )	20
Zr(adsp) (cdsp)	88	12
Zr(adsp)(3-OCH <sub>3</sub> dsp)	85	15
Zr(adsp)(5-OCH <sub>3</sub> dsp)	80	20

## 2.7 Synthesis of Zr(adsp)(Rdsp) Pendent Poly(4,4'-oxydiphthalic anhydride/3,4'-oxydianiline/10 mol% mellitic dianhydride)imide, PI(ODPA/3,4'-ODA/ 10 MADA/10 Zr), and Film Preparation

The polyamic acid solutions, both with and without zirconium pendent groups, were cast onto glass slides, followed by heating consecutively at 100, 200, and 300°C for one hour each. After cooling to room temperature, the glass slides with the polymer films were allowed to soak in water to obtain free standing polymer films, which would later be used for infrared spectrometric measurements and solvent resistance measurements.

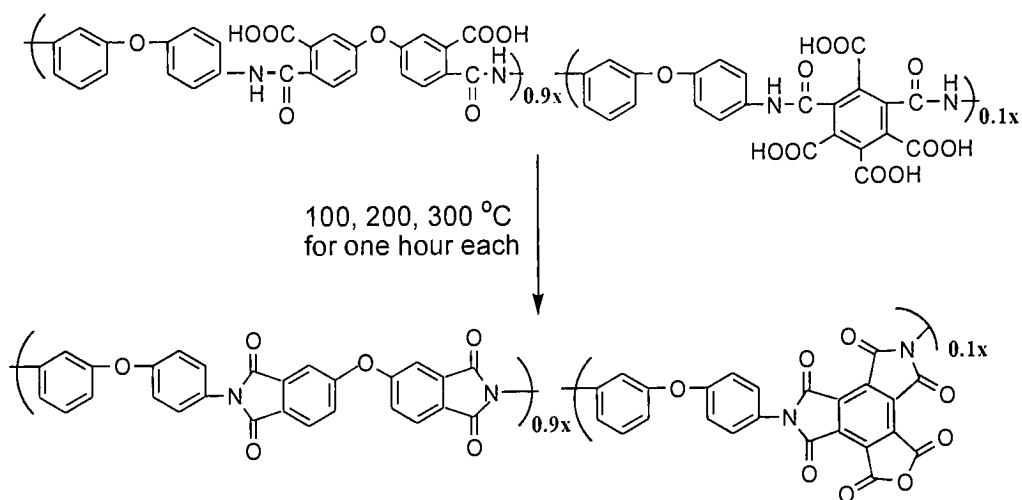


Figure 2.5 Imidization of Copolyamic acids

## 2.8 Instruments and Experimental Methods

### 2.8.1 Fourier Transform Infrared Spectroscopy (FTIR)

Fourier Transform Infrared spectra were recorded on a BIO-RAD Excalibur Series FTS 3000. Free standing Polyimide films obtained above were used for FTIR measurement. The IR spectra were obtained from 400  $\text{cm}^{-1}$  to 4000  $\text{cm}^{-1}$ .

## 2.8.2 Proton Nuclear Magnetic Resonance Spectroscopy ( $^1\text{H}$ NMR)

$\text{Zr}(\text{adsp})(\text{Rdsp})$ , precipitated polyamic acid, and  $\text{Zr}(\text{adsp})(\text{Rdsp})$  pendent polyamic acid powders were separately dissolved in deuterated dimethylsulfoxide ( $\text{DMSO-d}_6$ ), TMS is used as internal standard. The one-dimension  $^1\text{H}$  NMR spectra were recorded on a 300 MHz Bruker NMR Spectrometer by using Bruker's ICON-NMR 1.1 software at room temperature.

## 2.8.3 Thermogravimetric Analysis (TGA)

TGA were performed on a Seiko TG/DTA 220 system (Seiko Instruments Inc.). The

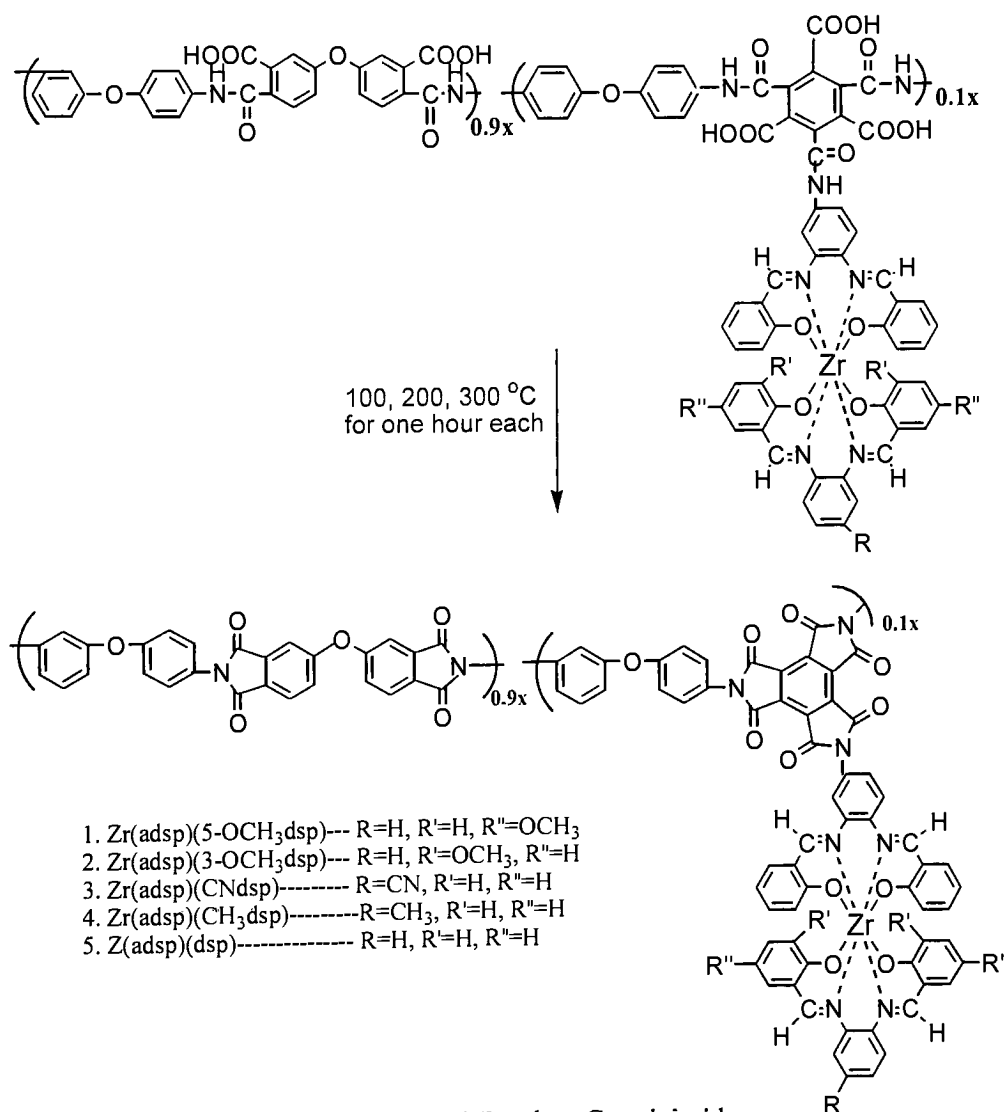


Figure2.6 Synthesis of  $\text{Zr}(\text{adsp})(\text{Rdsp})$  Pendent Copolyimide

amount of sample used in each measurement was 6-10 mg. The results were plotted as percentage of weight loss versus temperature.

MADA was measured under nitrogen atmosphere with a flow rate of 250 mL/min. The sample was heated from 20 to 150°C with a heating rate of 10°C/min, then from 150 to 500°C with a heating rate of 1°C/min. Aluminum pans were used in the MADA measurements.

Polyamic acid and all Zr pendent polyamic acids were measured under air atmosphere with a flow rate of 250 mL/min. Each sample was heated from 20 to 750°C with a heating rate of 10°C/min and held at 750°C for 5min. Ceramic pans were for these analyses.

#### **2.8.4 Differential Scanning Calorimetry (DSC)**

DSC measurements were performed on TA Instruments DSC 2010 (TA Instruments, Inc). Between 5 to 10 mg of sample was used in the DSC measurement with a nitrogen flow rate of 100 mL/min. For polyamic acid and Zr(adsp)(Rdsp) pendent polyamic acid samples, the operating program caused the temperature to be raised from 20 to 150°C at a heating rate of 10°C/min. The operating program for the corresponding polyimide and Zr(adsp)(Rdsp) pendent polyimide samples caused the temperature to be raised from 25 to 450°C at a heating rate of 10°C/min. The polyimide samples were prepared by heating precipitated polyamic acid powder at 100, 200 and 300°C for one hour each. The results were plotted as heat flow (W/g) versus temperature (°C).

#### **2.8.5 Gel Permeation Chromatography (GPC)**

This experiment was performed at NASA Langley Research Center. The PAA solutions were prepared a few minutes before injection into the chromatograph. Solutions were filtered through a 0.2  $\mu\text{m}$  teflon filter prior to injection. (see Table 2.3)

Chromatography was done in filtered and degassed, freshly distilled NMP/0.02 M LiBr, on a three column bank consisting of a linear Waters Styragel HT 6E column, which covers a molecular weight range from  $10^3$  to  $10^7$  g/mol, in series with a Styragel HT 3 column, which covers the range from  $5 \times 10^2$  to  $3 \times 10^4$  g/mol and a Styragel HT 2 column, which covers the range from  $10^2$  to  $10^4$  g/mol. The Waters 150C Gel Permeation Chromatograph

was equipped with a model 150R differential viscosity detector and a differential refractive index detector. The universal calibration curve used was generated with Polymer Laboratories narrow molecular weight distribution Polystyrene standards having molecular weight ranging from 472 to 2,890,000 g/mole.

Table 2.3 Samples for GPC Analysis

Sample name	Description (wt.%)
MADA	18% 3,4'-ODA/ODPA/MADA PAA in 0.02M LiBr/NMP
ZRHA	14.5% 3,4'-ODA/ODPA/MADA/Zr(H) PAA in 0.02M LiBr/NMP
ZRMEA	14.5% 3,4'-ODA/ODPA/MADA/Zr(m) PAA in 0.02M LiBr/NMP
ZR3OME	14.5% 3,4'-ODA/ODPA/MADA/Zr(3-OCH <sub>3</sub> ) PAA in 0.02M LiBr/NMP
ZR5OME	14.5% 3,4'-ODA/ODPA/MADA/Zr(5-OCH <sub>3</sub> ) PAA in 0.02M LiBr/NMP
ZRCNA	14.5% 3,4'-ODA/ODPA/MADA/Zr(c) PAA in 0.02M LiBr/NMP

### 2.8.6 Film Flexibility and Solvent Resistance

Free standing polyimide and Zr(adsp)(Rdsp) pendent polyimide films were bent. If no crack was observed after bending, they would pass the film flexibility test.

The same film samples were immersed in acetone, chloroform, dimethylacetamide (DMAc), methyl ethyl ketone, and toluene for 30 min followed by a fingernail crease. The samples would pass the solvent resistance test if there were no cracks observed after this process.

### 2.8.7 Light Scattering

This work was performed by Dr.Kotlarchyk, Department of Physics, RIT. Measurement of the refractive index of pendent polyamic acid solutions, which would be used in light scattering measurements, were carried out on Spectronic Instrument 334610.

### 2.8.8 Contact Angle

This experiment was carried out on the surface of free standing polyimide and Zr(adsp)(Rdsp) pendent polyimide films. The LARC-IA films were prepared by scientists working at Kodak. This experiment was performed on Rame-Hart 100-00 115.

### **2.8.9 Oxygen Plasma Etching**

Oxygen plasma etching of polyimide and Zr(adsp)(Rdsp) pendent polyimide films was performed using a SPI Plasma Prep II, which employed a 13.56 MHz RF discharge to create a plasma of oxygen ions and atoms in various energy states at 80-100 mTorr. The thin film samples cast onto glass slides were placed near the center of the quartz sample chamber for three hours.

### **2.8.10 Scanning Electron Micrograms (SEM)**

Free standing polyimide and Zr(adsp)(Rdsp) pendent polyimide films, before and after plasma etching, were cut into small pieces to make the stub, and then coated with approximately 100 angstroms of gold. SEM pictures were taken by using a PHILIPS 501 SCANNING ELECTRON MICROSCOPE. The conditions were 30kv, spot size 500, number of lines 250, filament 40x100 $\mu$ A, and magnification 2500K and 10000K. Pictures were taken at tilt angle 55°.

## RESULTS

### 3.1 Synthesis of Zr(adsp)(mdsp) and the Other Zr(adsp)(Rdsp)

The synthetic route to the Schiff base compounds in this study is shown:

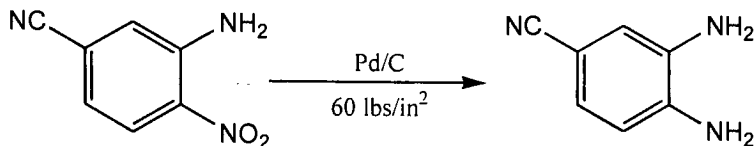


Figure 3.1 Hydrogenation of 4-amino-3-nitrobenzonitrile

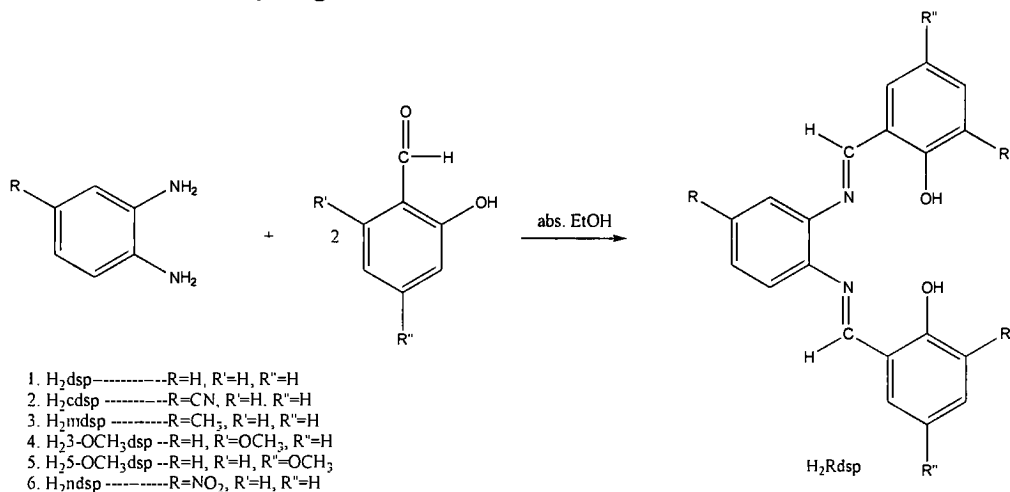
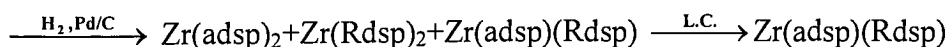
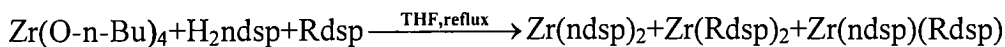


Figure 3.2 Synthetic Scheme of Substituted Schiff Base-H<sub>2</sub>Rdsp

The synthesis route to the zirconium complexes is as shown:



L.C. = liquid chromatography

R = H, CN, CH<sub>3</sub>, 3-OCH<sub>3</sub>, or 5-OCH<sub>3</sub>, respectively

The purity of the column-separated Zr(adsp)(mdsp) product was confirmed by TLC, only one spot was observed. Then, since Zr(adsp)(mdsp) is a new compound, this product was placed in a drying pistol for three days under vacuum. Elemental analysis was performed on this sample at Astra, USA. As shown in Table 3.1 the elemental analysis results for Zr(adsp)(mdsp), a new compound, are in agreement with the calculated (theoretical) values.



Table 3.1 Elemental Analysis Result

	C (H%)	H (%)	N (%)
Calculated	65.75	4.17	9.35
Found	66.06	4.13	9.36
Difference	0.31	0.04	0.01
Error (%)	0.47	0.95	0.11

### 3.2 Synthesis of Mellitic Dianhydride (MADA)

There is one mole (18 g) of water loss per mole of MADA during the TGA measurement, when MADA is converted to trianhydride. Theoretically, 100% pure of MADA is expected to have one step weight loss that is 5.8% in TGA progress. The TGA result is shown in Figure 3.3. The one step weight loss on its TGA curve is in agreement with this theoretical value.

### 3.3 Synthesis of Polymer

#### 3.3.1 Synthesis of Polyamic Acid

With the addition of adding 3,4'-ODA/NMP solution, the viscosity of the reaction mixture increased noticeably. The reaction mixture turned to a light brown solution at the end of adding 3,4'-ODA/NMP solution. (See Figure 3.4, top.)

#### 3.3.2 Synthesis of Zirconium Pendent Polyamic Acid

The zirconium complex pendent polyamic acids were prepared by attaching zirconium complexes  $Zr(adsp)(Rdsp)$  to the polyamic acid backbone (See Figure 3.4).

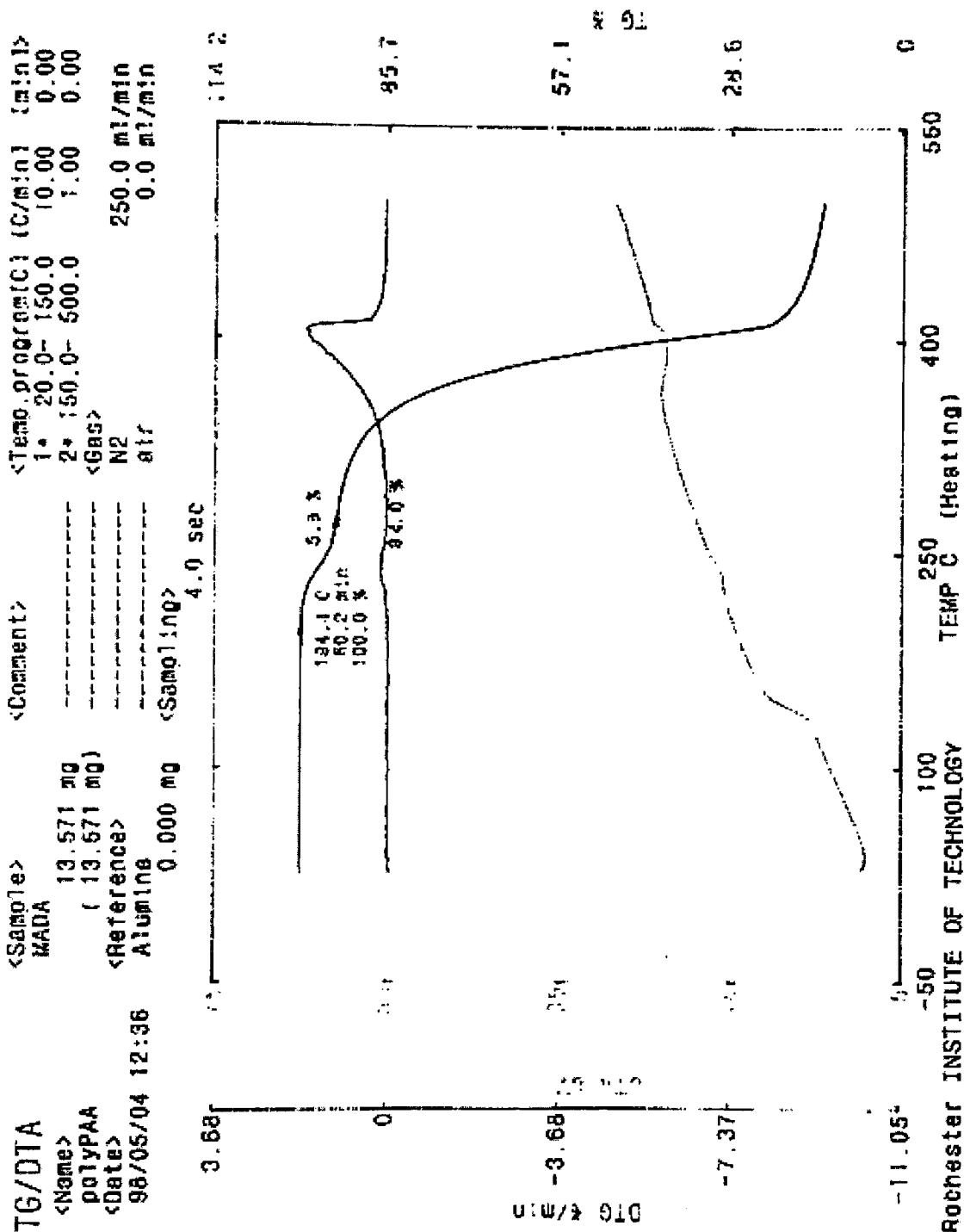


Figure 3.3 TGA Graph of MADA

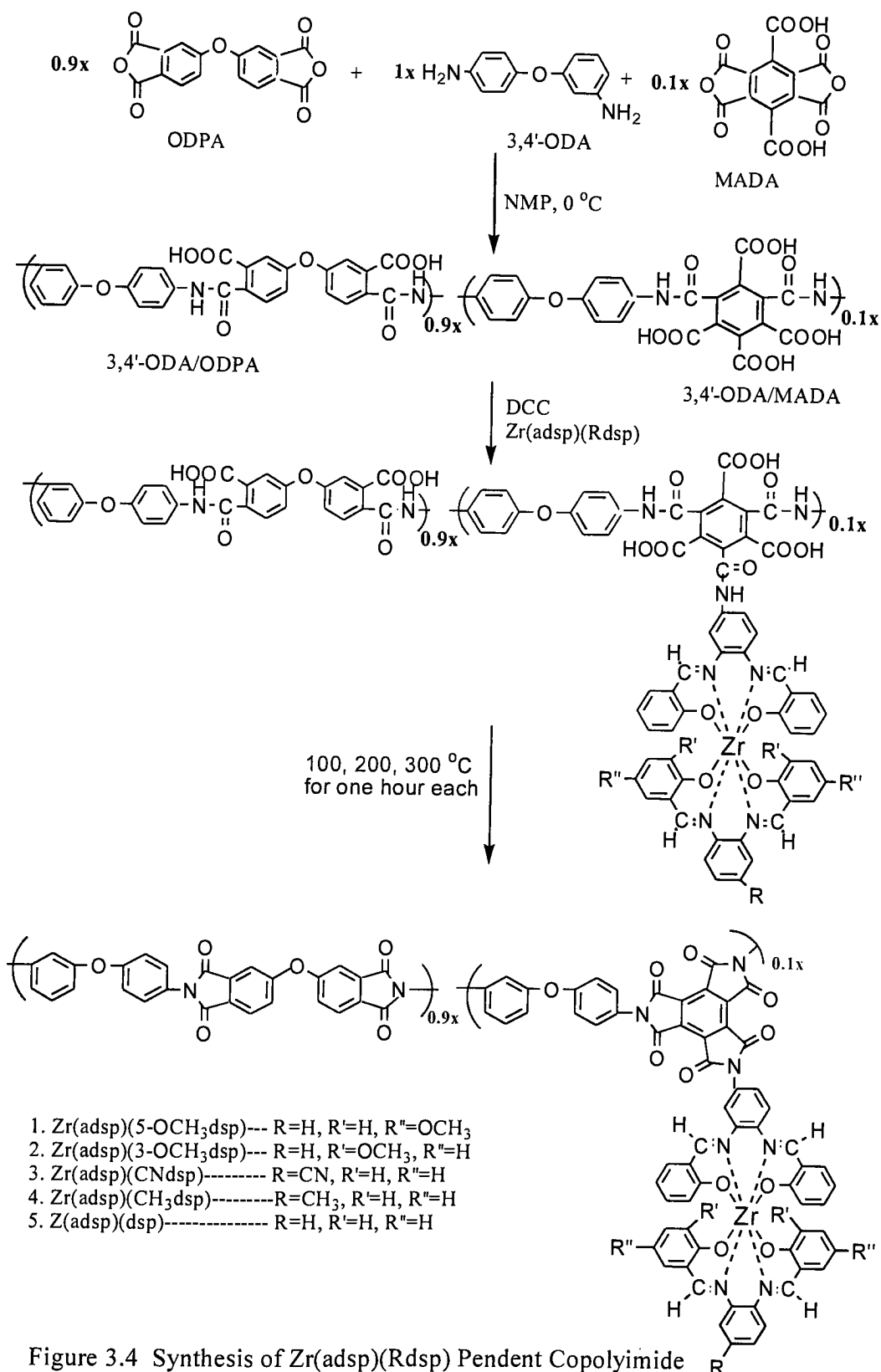
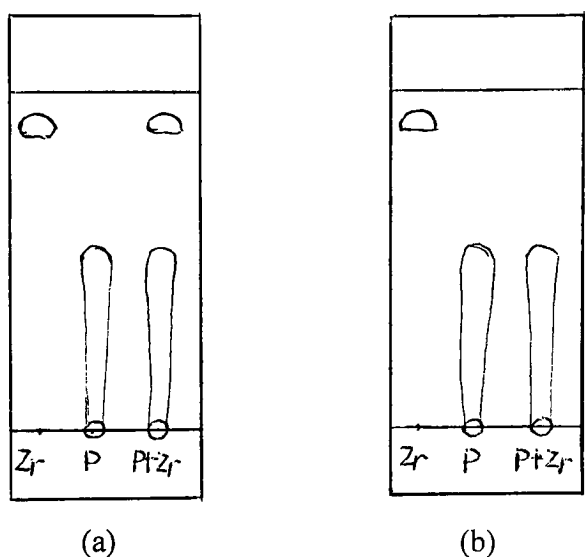


Figure 3.4 Synthesis of Zr(adsp)(Rdsp) Pendent Copolyimide

The color of the zirconium pendent polymers varied from yellow to orange depending the color of the zirconium complex. TLC was performed to confirm the addition of zirconium complex. Before the addition of DCC, the TLC showed two spots, which represented polymer and free zirconium complex respectively. At the end of addition of DCC, the TLC showed just one spot, which meant that the zirconium complex was attached to the polymer backbone completely. See Figure 3.5.



P: Polymer

Zr: Zirconium Complex

P + Zr: Polymer + Zirconium Complex

Figure 3.5 TLCs Indicating Attaching Zirconium Complex to Parent Polyamic Acid  
(a) Before, and (b) After Reaction with DCC

### 3.3.3 Imidization of Parent Polyamic Acid and Zirconium Pendent Polyamic Acid films

After casting two layers of zirconium pendent polyamic acids on glass slides, cracks were observed following imidization.

### 3.4 Characterization of Polyamic Acids and Polyimides

#### 3.4.1 Infrared Spectrometry (IR)

The FT-IR spectrum of Zr(adsp)(dsp) is shown in Figure 3.6. The major characteristic bands are 2924, 1616, 1543, 1309, 740  $\text{cm}^{-1}$ , which are due to C-H (imino), C=N, C=C, C-O, and C-H (aromatic, out of plane bending), respectively.<sup>15</sup>

Figure 3.7 shows the IR spectra of parent PAA and zirconium pendent PAAs. Because the huge bands of solvent and water, we can't get any information from them.

Figure 3.8 shows the spectrum of imidized parent polymer backbone. The major absorption bands are 3073, 1851, 1779, 1720, 1606, 1376, 1276, and 774  $\text{cm}^{-1}$ , which are assigned to C-H (aromatic), C=O (anhydride, symmetric and asymmetric), C=O (imide ring), C=C (aromatic), C-N, C-O (aromatic ether), and C-H (aromatic out of plane bending), respectively.<sup>19</sup>

Figures 3.9 to 3.13 show the spectra of zirconium pendent polyimides. The specific bands for the zirconium pendent polyimides and the difference between the parent polyimide and the zirconium pendent polyimides are summarized in Table 3.2.

From Table 3.2 we see that in the parent polyimide there is an anhydride band at 1851, but this band is no longer exist in the pendent polyimides. Additional information obtained from the IR spectra is the presence of bands at 2930 and 2860  $\text{cm}^{-1}$ , the latter only observed in the spectra of zirconium pendent polyimides, and are assigned to the imino and amido C-H vibrations, respectively. A band at 2227  $\text{cm}^{-1}$  was observe from the spectrum of Zr(adsp)(cdsp) pendent polyimide (Figure 3.11), which is due to the cyano group in the zirconium complex.

#### 3.4.2 Proton Nuclear Magnetic Resonance ( $^1\text{H}$ NMR)

Due to the limited solubility of these polymers, even in  $d^6$ -DMSO the peaks attributed to zirconium complex pendent groups are too small to make precise assignments. The content of zirconium complexes in the pendent polymer can only be roughly estimated based on peak integration.

Figure 3.14 is the  $^1\text{H}$  NMR spectrum of the parent polyamic acid (3,4'-ODA/ODPA/MADA). The peaks from 6.6 ppm to 8.2 ppm are signed to the aromatic

Table 3.2 Bands from IR Spectra (cm<sup>-1</sup>)

Type of Vibration	C-H (aromatic)	C-H (imine)	C≡N	C=O anhydride	C=O imide ring	C=C aromatic	C=C	C-N	C-O aromatic ether	C-H out of plane bending
Wave number (cm <sup>-1</sup> )										
PI	3073			1851	1779 1720	1606		1376	1276	744
PI/Zr(H)	3071	2932 2857			1778 1723	1607	1542	1376	1248	748
PI/Zr(m)	3071	2935 2858			1780 1725	1607	1542	1376	1246	748
PI/Zr(c)	3072	2932 2858	2227		1778 1724	1607	1544	1376	1246	748
PI/Zr(3-OCH <sub>3</sub> )	3072	2931 2860			1780 1724	1607	1544	1375	1247	746
PI/Zr(5-OCH <sub>3</sub> )	3072	2933 2856			1778 1724	1607	1543	1375	1247	747

Table 3.3 Peaks from NMR (ppm, d<sup>6</sup>-DMSO)

Sample	Aromatic and Amino (complex)	Aromatic (complex and polymer)	imine	amide
PAA		6.27-8.19 (95.01)		10.87-10.86 (13.14)
Zr(H)	5.25-6.01 (13.92)	6.29-7.84 (48.23)	8.37-8.95 (10.15)	
PAA/Zr(H)	5.45-6.02 (0.78)	6.16-8.23 (29.40)	8.33-8.92 (0.6465)	10.12-11.00 (3.66)
Zr(m)	5.3-5.8 (13.41)	6.3-7.4 (34.85)	8.3-8.7 (7.95)	
PAA/Zr(m)	5.44-6.01 (0.78)	6.15-8.24 (30.54)	8.31-8.92 (0.66)	10.30-10.90 (3.96)
Zr(c)	5.09-6.02 (16.32)	6.07-8.20 (50.26)	8.22-8.93 (10.65)	
PAA/Zr(c)	5.60-6.00 (0.41)	6.27-8.18 (30.73)	8.46-8.96 (0.53)	10.15-10.94 (3.97)
Zr(3-OCH <sub>3</sub> )	4.98-7.89 (50.16)		8.2-8.9 (8.33)	
PAA/Zr(3-OCH <sub>3</sub> )		6.19-8.17 (33.23)	8.48-8.84 (0.38)	10.18-10.88 (4.01)
Zr(5-OCH <sub>3</sub> )	5.37-6.07 (8.59)	6.36-7.85 (24.66)	8.43-8.95 (5.73)	
PAA/Zr(5-OCH <sub>3</sub> )	5.59-5.93 (0.39)	6.45-8.37 (28.76)	8.37-8.88 (0.62)	10.22-10.98 (3.90)

protons, the peak at 10.3-10.5 is assigned to the amide proton. The carboxylic acid protons normally appear at ca. 13 ppm.

Figure 3.15 is the  $^1\text{H}$  NMR spectrum of  $\text{Zr}(\text{adsp})(\text{dsp})$ . The three peaks at 8.5-8.8 ppm are due to the four imino-protons, two of which are equivalent protons for the dsp ligand. The multiple peaks at 5.7-7.7 ppm are due to the aromatic protons.<sup>15</sup>

Figure 3.16 is the  $^1\text{H}$  NMR spectrum of  $\text{Zr}(\text{adsp})(\text{dsp})$  pendent polyamic acid. The peaks at 8.5-8.8 ppm are due to the imino protons from zirconium complex. The peaks at 5.7-8.2 ppm are due to the aromatic protons. According to the integral ratio of imino proton to aromatic proton, we can estimate the amount of zirconium complex attached to the polymer backbone.<sup>19</sup>

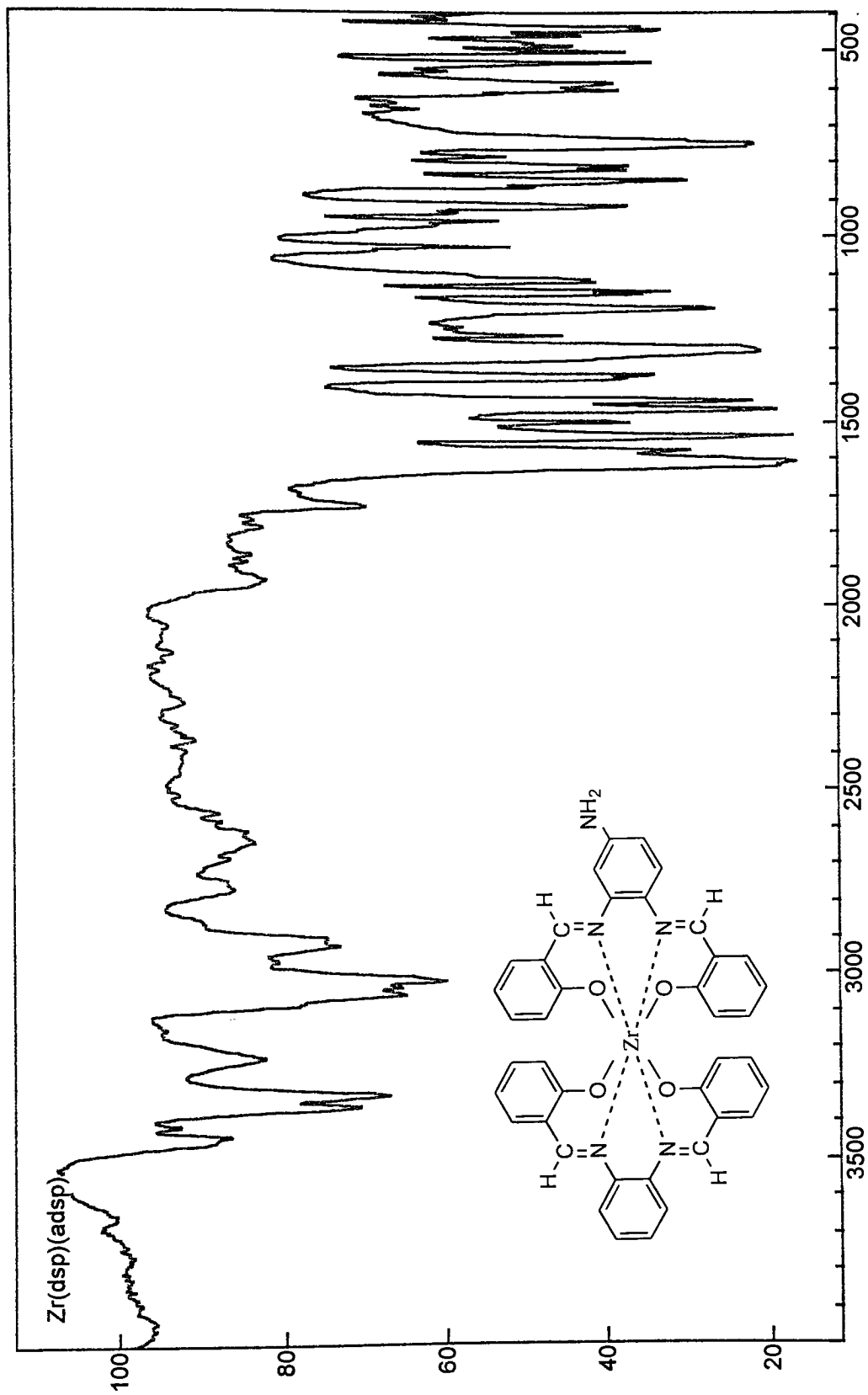
Figure 3.17 shows the  $^1\text{H}$  NMR spectrum of  $\text{Zr}(\text{adsp})(\text{mdsp})$ . In this spectrum, four peaks are assigned to imino proton peaks rather than three, which indicates that none of the imino protons are equivalent. The same observation can be made for the  $^1\text{H}$  NMR spectrum of  $\text{Zr}(\text{adsp})(\text{cdsp})$  (Figure 3.19), four imino proton peaks were observed because there are no equivalent imino protons. However, in  $^1\text{H}$  NMR spectra of  $\text{Zr}(\text{adsp})(3\text{-OCH}_3\text{dsp})$  and  $\text{Zr}(\text{adsp})(5\text{-OCH}_3\text{dsp})$ , Figures 3.21 and 3.23, the two imino protons from 3-OCH<sub>3</sub>dsp or 5-OCH<sub>3</sub>dsp are equal to other, respectively. Figures 3.18, 3.20, 3.22 and 3.24 show the spectra of corresponding zirconium pendent polymers, respectively.

Table 3.4 shows the theoretical and experimental result of the ratio of imino proton and aromatic proton.

Table 3.4 Integral Ratio of Imino Proton to Aromatic Proton

Sample	Theoretical	Experimental	Error(%)
PAA/ $\text{Zr}(\text{adsp})(\text{dsp})$	0.0255	0.0204	25.0
PAA/ $\text{Zr}(\text{adsp})(\text{mdsp})$	0.0256	0.0215	19.0
PAA/ $\text{Zr}(\text{adsp})(\text{cdsp})$	0.0256	0.0173	48.1
PAA/ $\text{Zr}(\text{adsp})(3\text{-OCH}_3\text{dsp})$	0.0258	0.0115	125.1
PAA/ $\text{Zr}(\text{adsp})(5\text{-OCH}_3\text{dsp})$	0.0258	0.0182	42.0

$$\text{Theoretical ratio} = \frac{\text{imino protons from zirconium complex}}{\text{aromatic protons from both polymer and zirconium complex}}$$



Wavenumber

Figure 3.6 IR Spectrum of  $\text{Zr}(\text{dsp})(\text{dsp})$



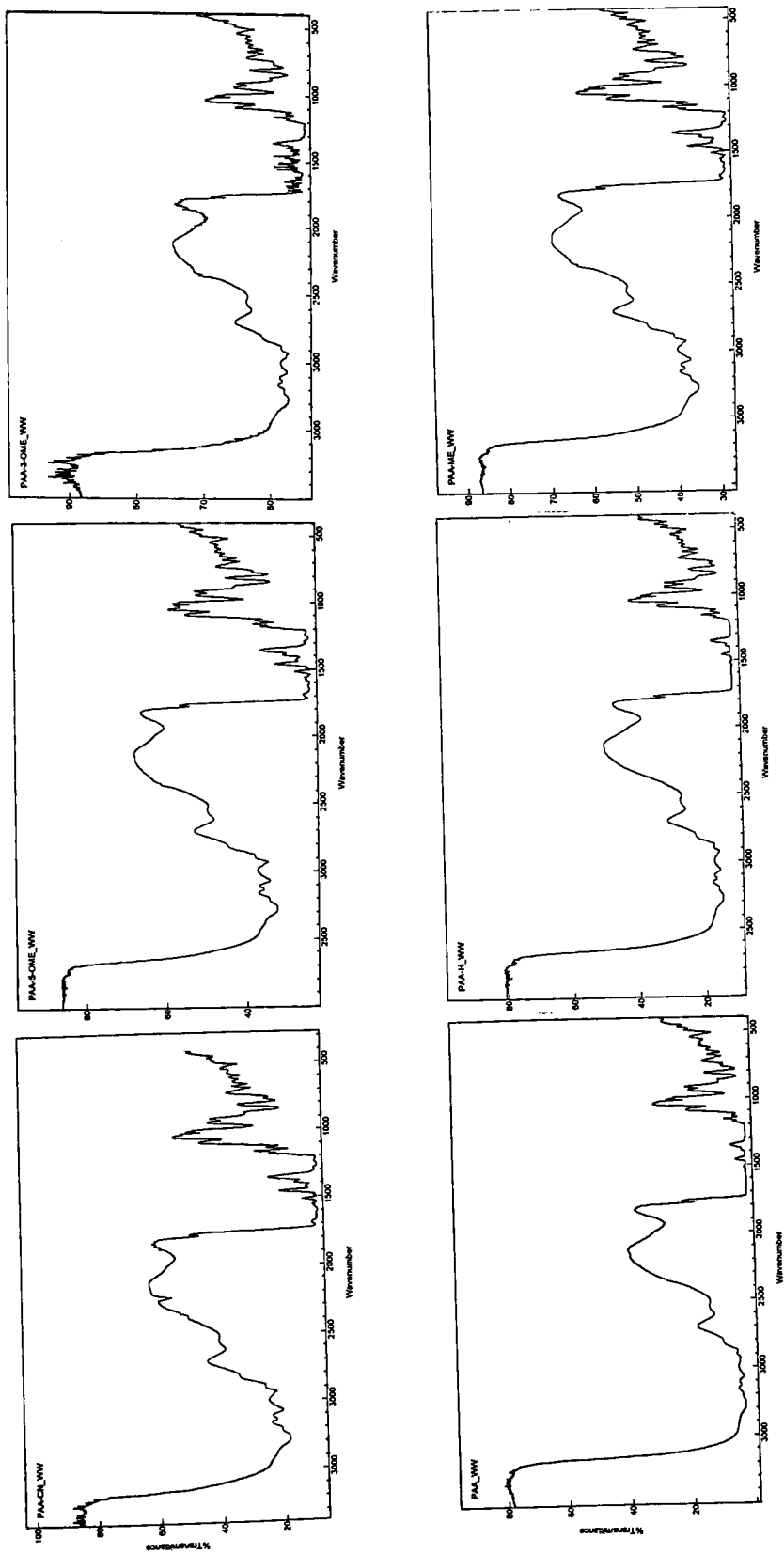


Figure 3.7 IR Spectrum of PAA and PAA/Zr(R)

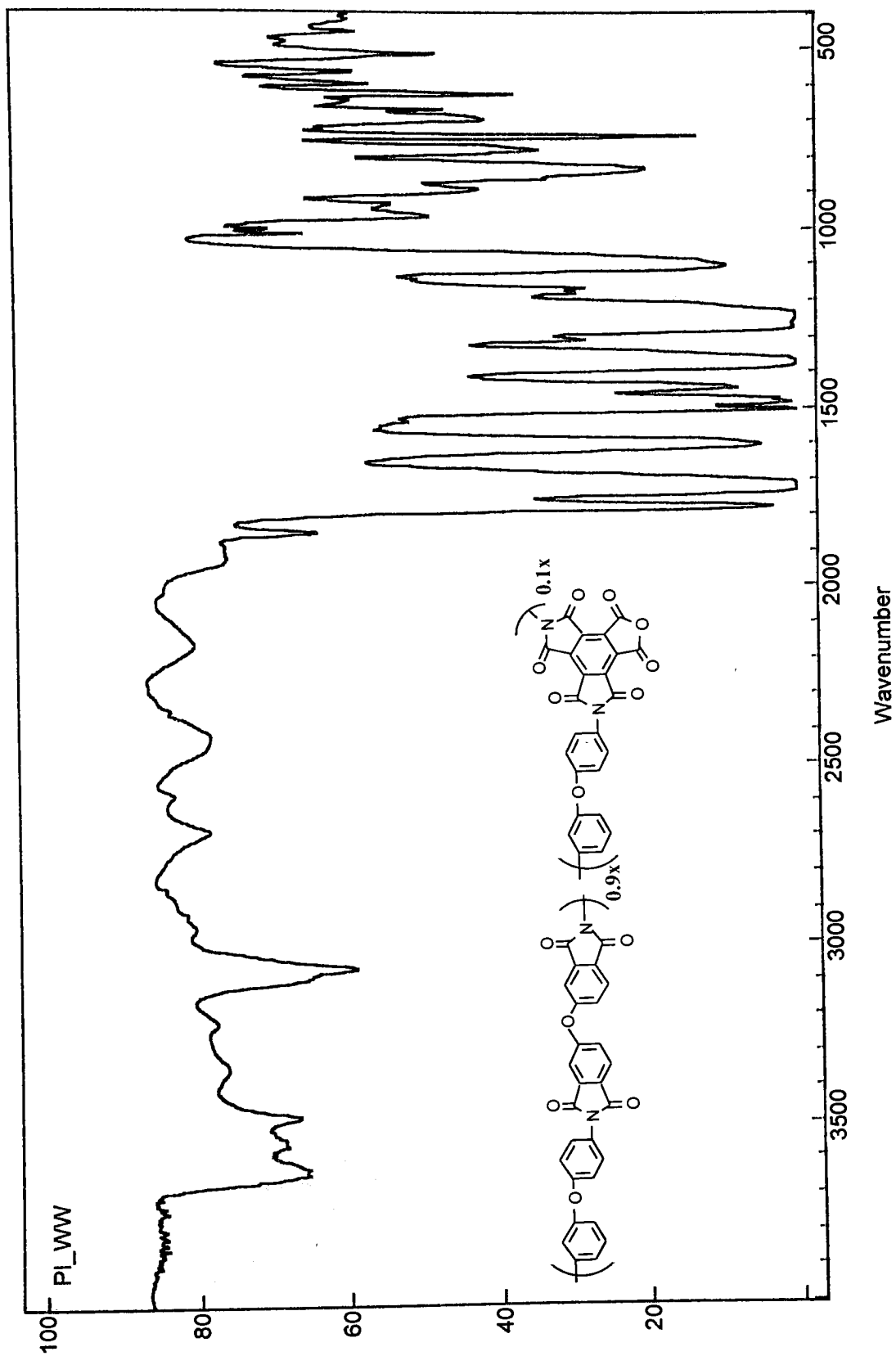


Figure 3.8 IR Spectrum of Parent Polyimide

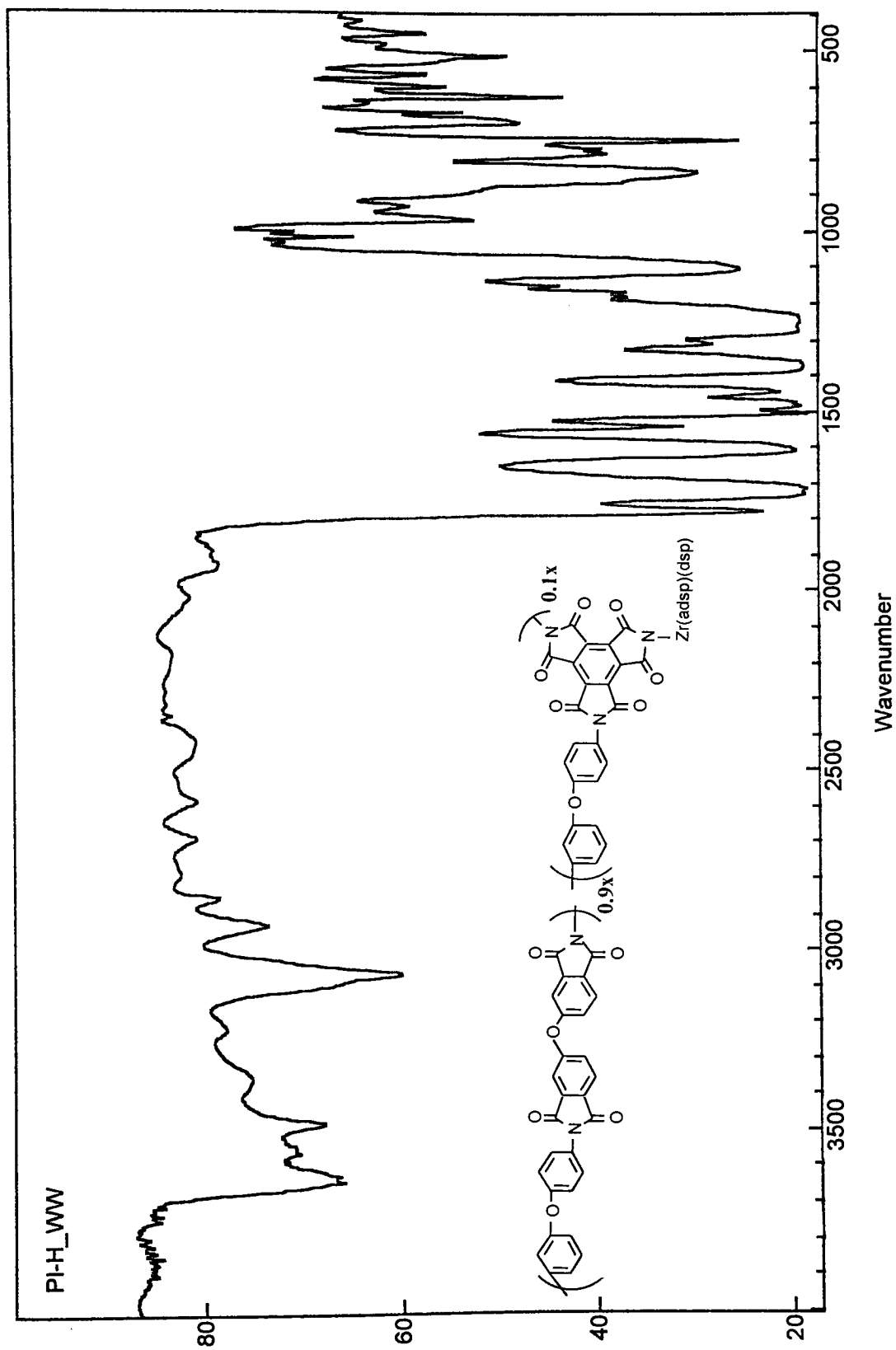


Figure 3.9 IR Spectrum of  $Zr(adsp)(dsp)$  Pendent Polyimide

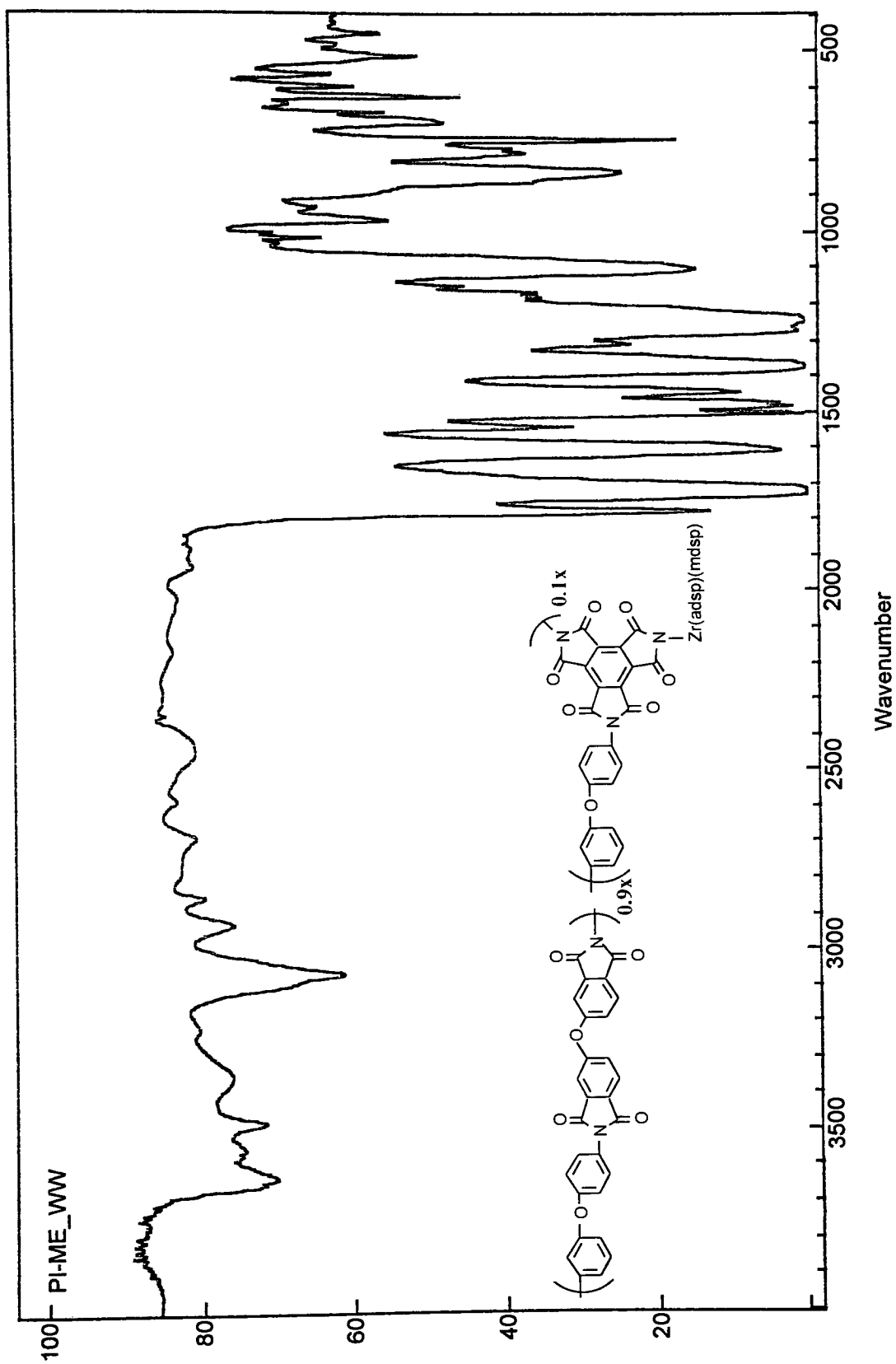


Figure 3.10 IR Spectrum of Zr(adsp)(mdsp) Pendent Polyimide

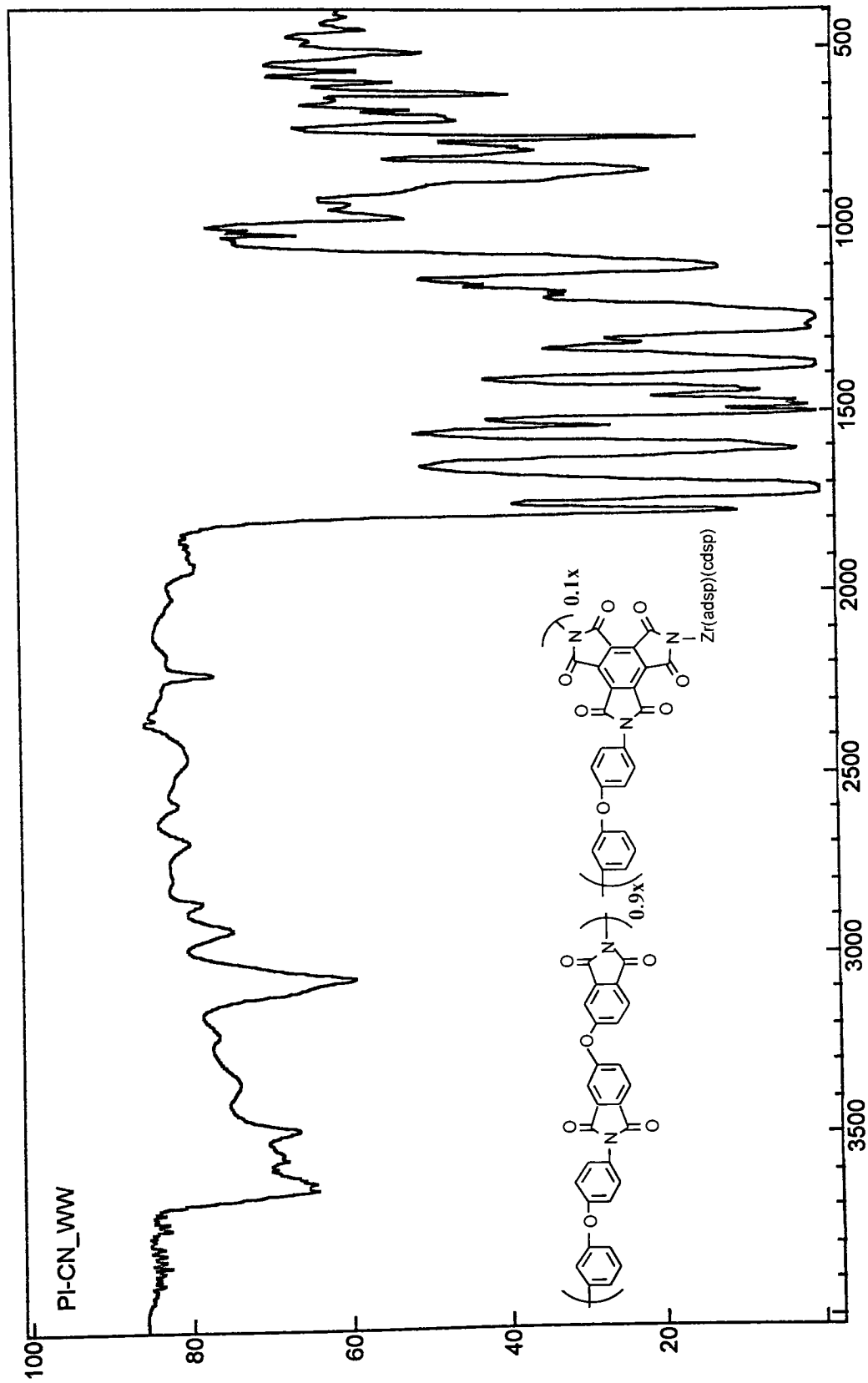
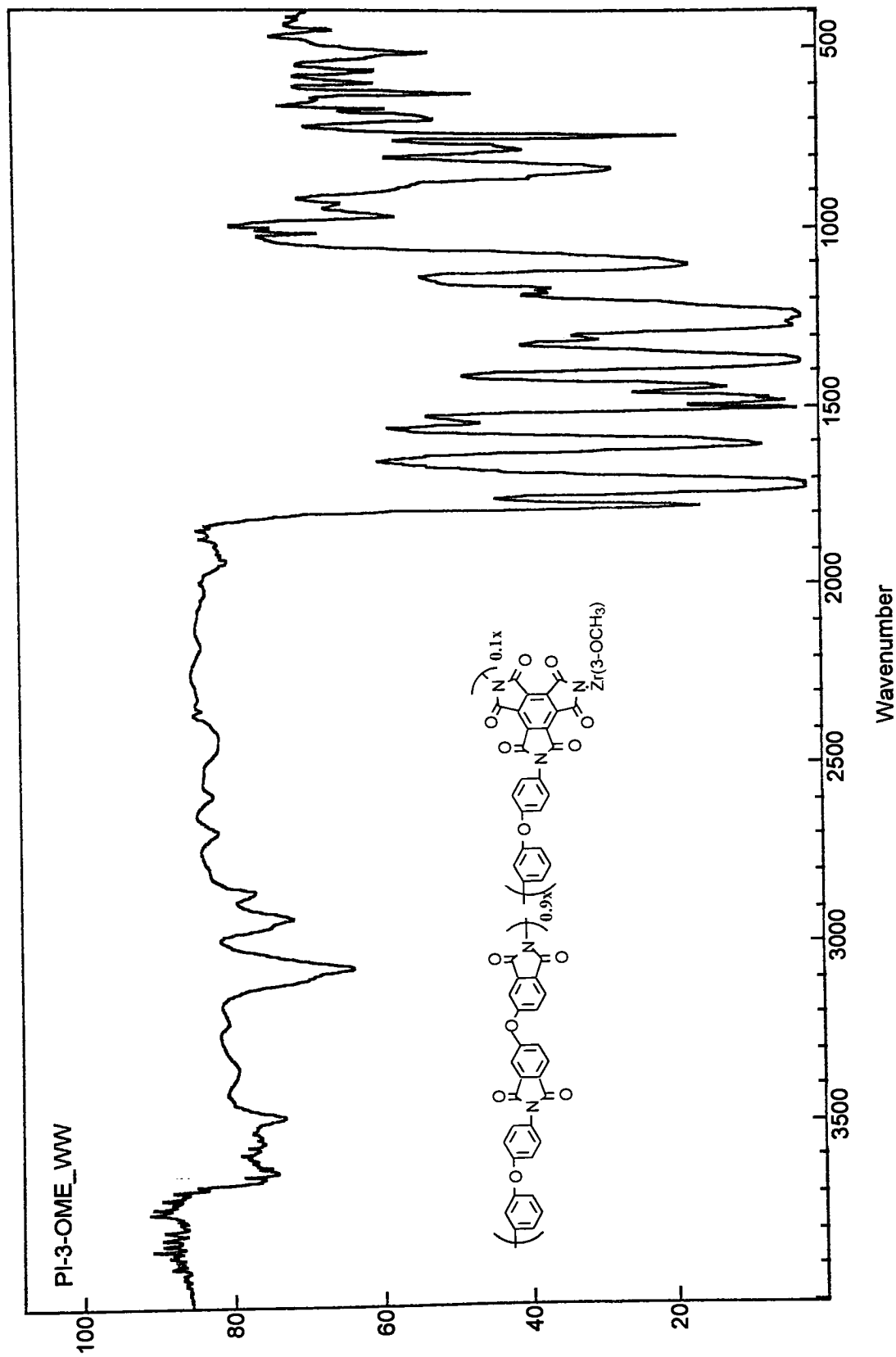
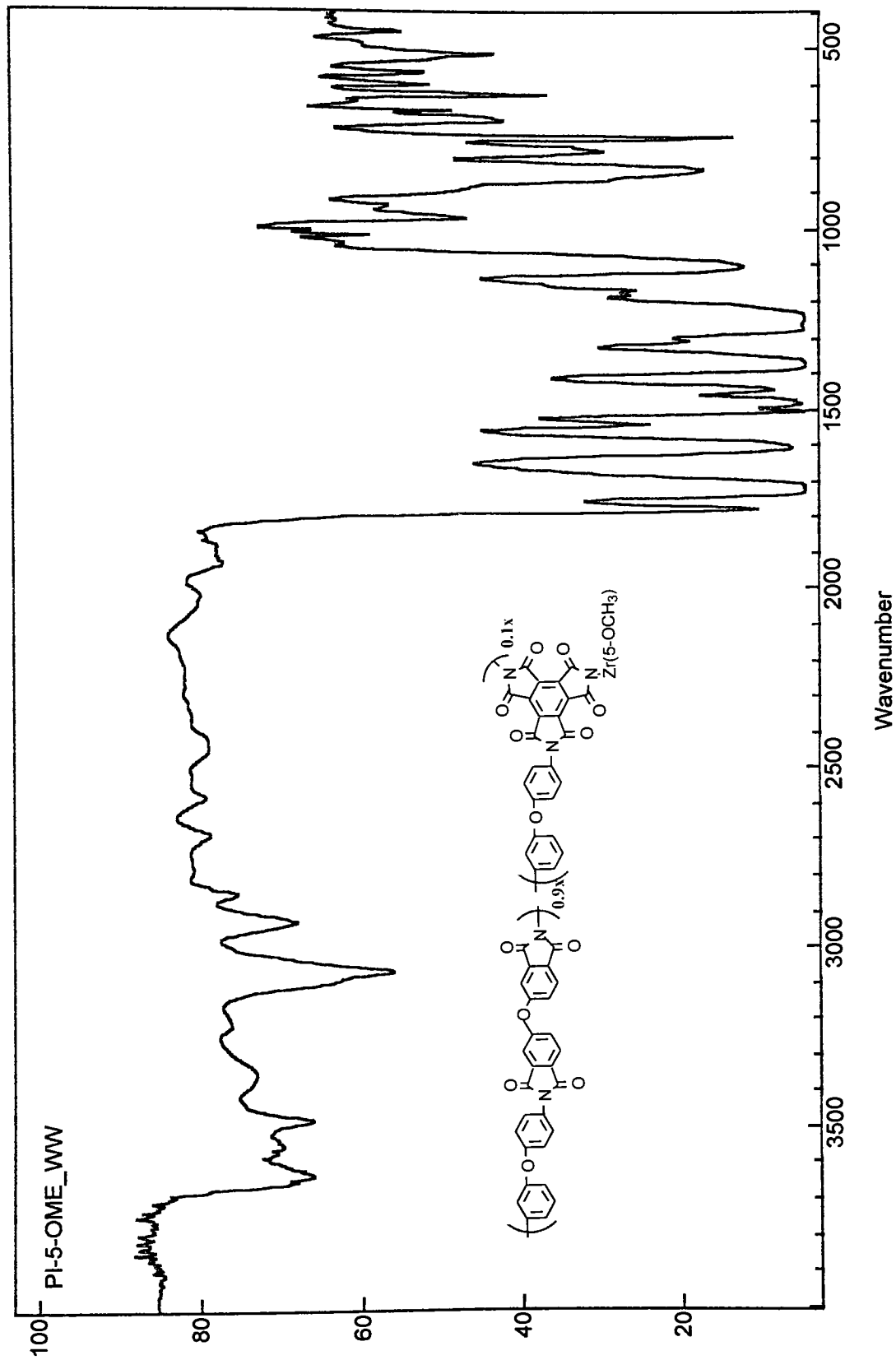


Figure 3.11 IR Spectrum of Zr(adsp)(cdsp) Pendent Polyimide





Current Data Parameters  
NAME PAA\_WW\_1  
EXPNO 1  
PROCNO 1

F2 - Acquisition Parameters

Date\_ 990728  
Time 13.37  
INSTRUM spect  
PROBHD 5 mm QNP 1H  
PULPROG zg  
TO 32768  
SOLVENT DMSO  
NS 228  
DS 2  
SWH 4496.403 Hz  
FIDRES 0.137219 Hz  
AQ 3.6438515 sec  
RG 71.8  
OW 111.200 usec  
QE 6.00 usec  
TE 300.0 K  
O1 2.00000000 sec  
P1 9.00 usec  
QE 6.00 usec  
SF01 300.1318534 MHz  
NUC1 1H  
PL1 -5.00 dB

F2 - Processing parameters

SI 16384  
SF 300.1300000 MHz  
WOW EM  
SSB 0  
LB 0.30 Hz  
GB 0  
PC 1.00

10 NMR plot parameters

CX 20.00 cm  
F1P 11.000 ppm  
F1 3301.43 Hz  
F2P -1.000 ppm  
F2 -300.13 Hz  
PPMCM 0.60000 ppm/cm  
HZCM 180.07800 Hz/cm

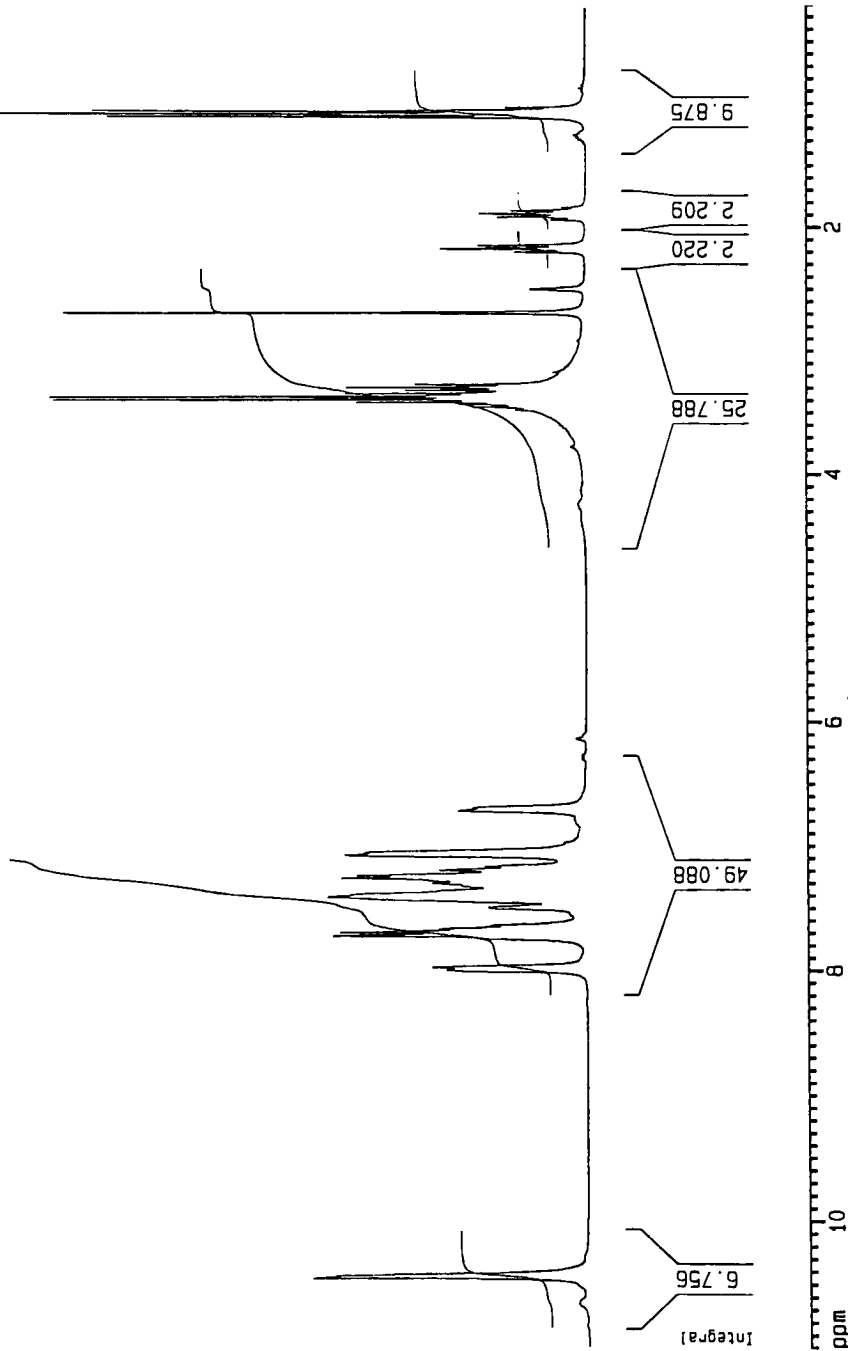
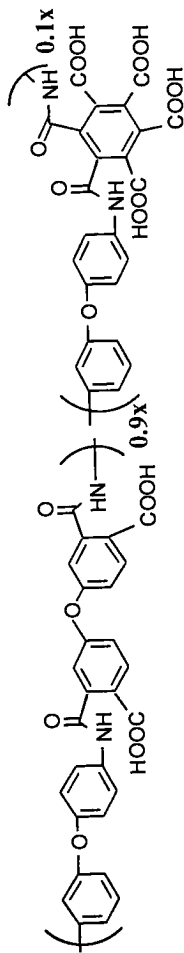
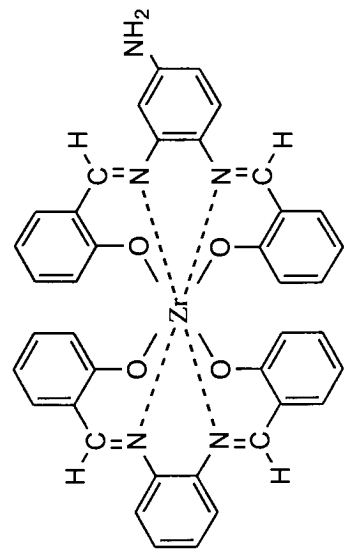


Figure 3.14 <sup>1</sup>H NMR Spectrum of Parent Polyamic Acid





Current Data Parameters  
 NAME Zr-H\_HM\_1  
 EXPNO 1  
 PROCNO 1

# F2 - Acquisition Parameters

Date\_ 990728  
 Time 14.53  
 INSTRUM spect  
 PROBHD 5 mm QNP 1H  
 PULPROG zg30  
 TD 32768  
 SOLVENT DMSO  
 NS 16  
 DS 2  
 SWH 6172.839 Hz  
 FIDRES 0.188380 Hz  
 AQ 2.6542580 sec  
 RG 574.7  
 DM 81.000 usec  
 DE 6.00 usec  
 TE 300.0 K  
 D1 1.00000000 sec  
 P1 9.00 usec  
 DE 6.00 usec  
 SFO1 300.1318534 MHz  
 NUC1 1H  
 PL1 -5.00 dB

# F2 - Processing parameters

SI 16384  
 SF 300.1299810 MHz  
 WDW EM  
 SSB 0  
 LB 0.30 Hz  
 GB 0  
 PC 1.00

# 1D NMR plot parameters

CX 20.00 cm  
 F1P 11.000 ppm  
 F1 3301.43 Hz  
 F2P -1.000 ppm  
 F2 -300.13 Hz  
 PPMCM 0.60000 ppm/cm  
 HZCM 180.07799 Hz/cm

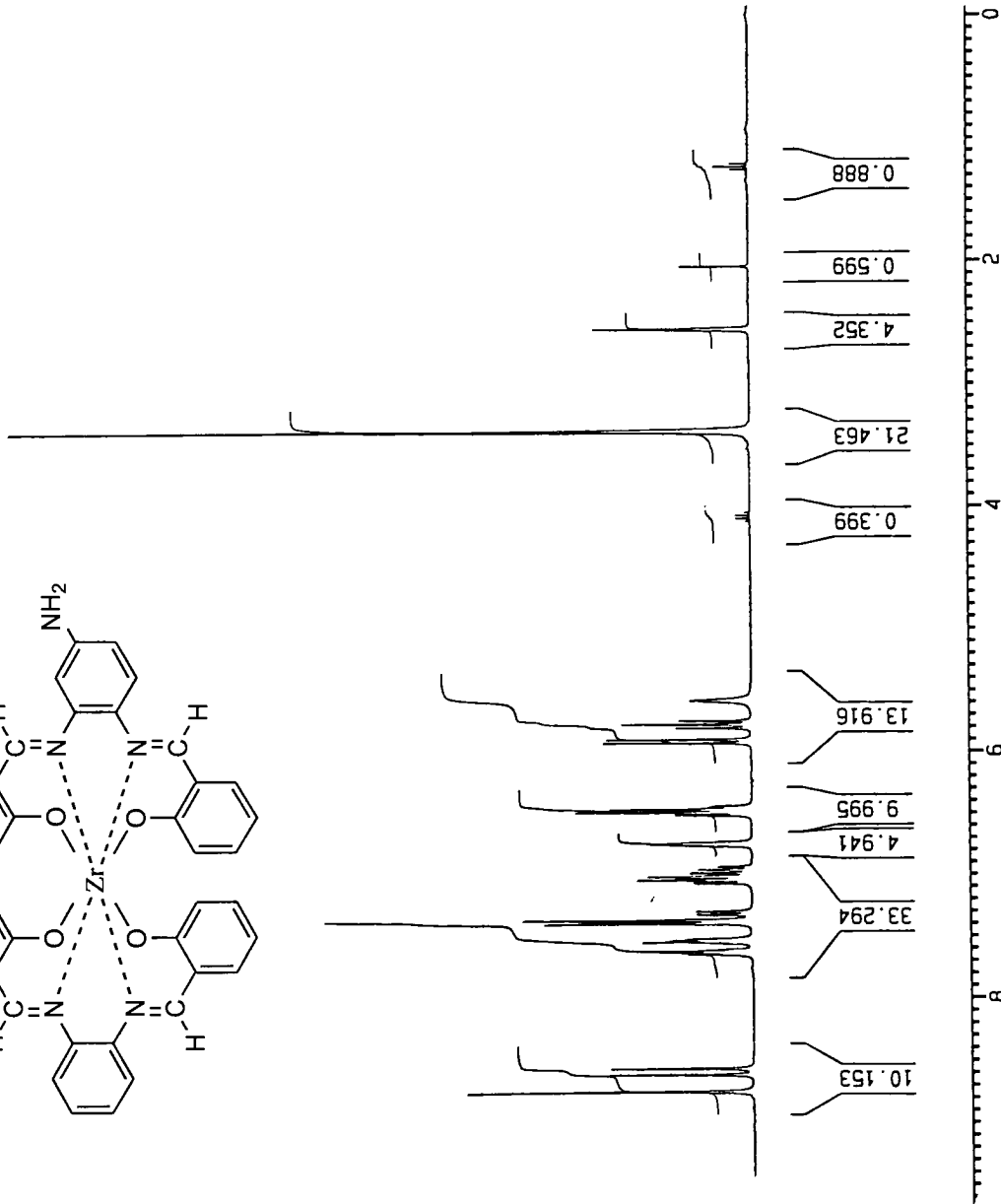


Figure 3.15 <sup>1</sup>H NMR Spectrum of Zr(adsp)(dsp)

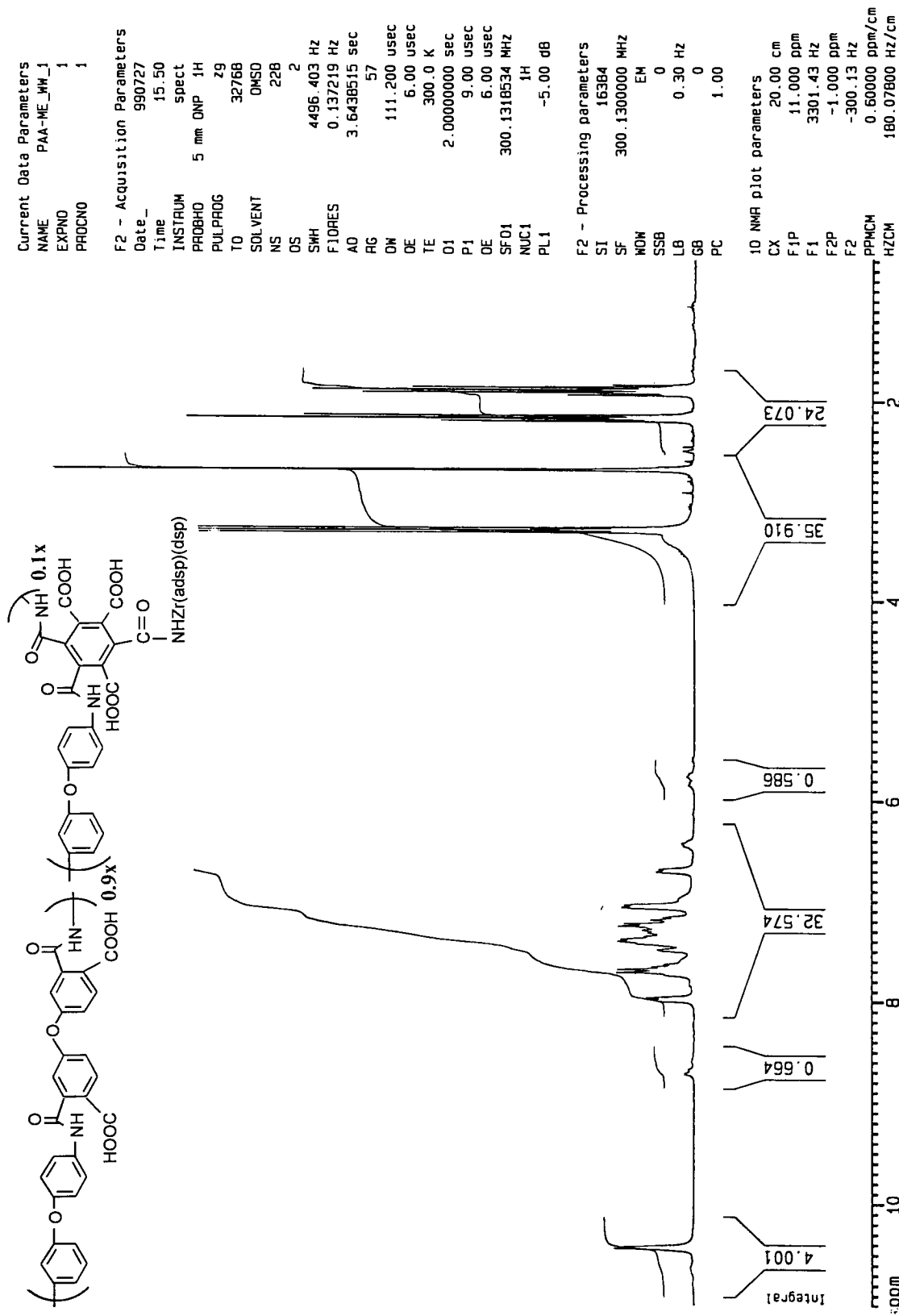


Figure 3.16 <sup>1</sup>HNMR Spectrum of Zr(adsp)(dsp) Pendent Polyamic Acid

Current Data Parameters  
 NAME Zr--ME\_WW\_1  
 EXPNO 1  
 PROCNO 1

F2 - Acquisition Parameters  
 Date\_ 990728  
 Time 14.17  
 INSTRUM spect  
 PROBHD 5 mm QNP 1H  
 PULPROG zg30  
 TO 32768  
 SOLVENT DMSO  
 NS 16  
 OS 2  
 SWH 6172.839 Hz  
 FIDRES 0.188380 Hz  
 AQ 2.6542580 sec  
 RG 456.1  
 OW 81.000 usec  
 OE 6.00 usec  
 TE 300.0 K  
 O1 1.00000000 sec  
 P1 9.00 usec  
 OE 6.00 usec  
 SF01 300.1318534 MHz  
 NUC1 1H  
 PL1 -5.00 dB

F2 - Processing parameters  
 SI 16384  
 SF 300.1300279 MHz  
 WDW EM  
 SSB 0  
 LB 0.30 Hz  
 GB 0  
 PC 1.00

10 NMR plot parameters  
 CX 20.00 cm  
 F1P 10.000 ppm  
 F1 3001.30 Hz  
 F2P 0.000 ppm  
 F2 0.00 Hz  
 PPMCM 0 50000 ppm/cm  
 HZCM 150 06502 Hz/cm

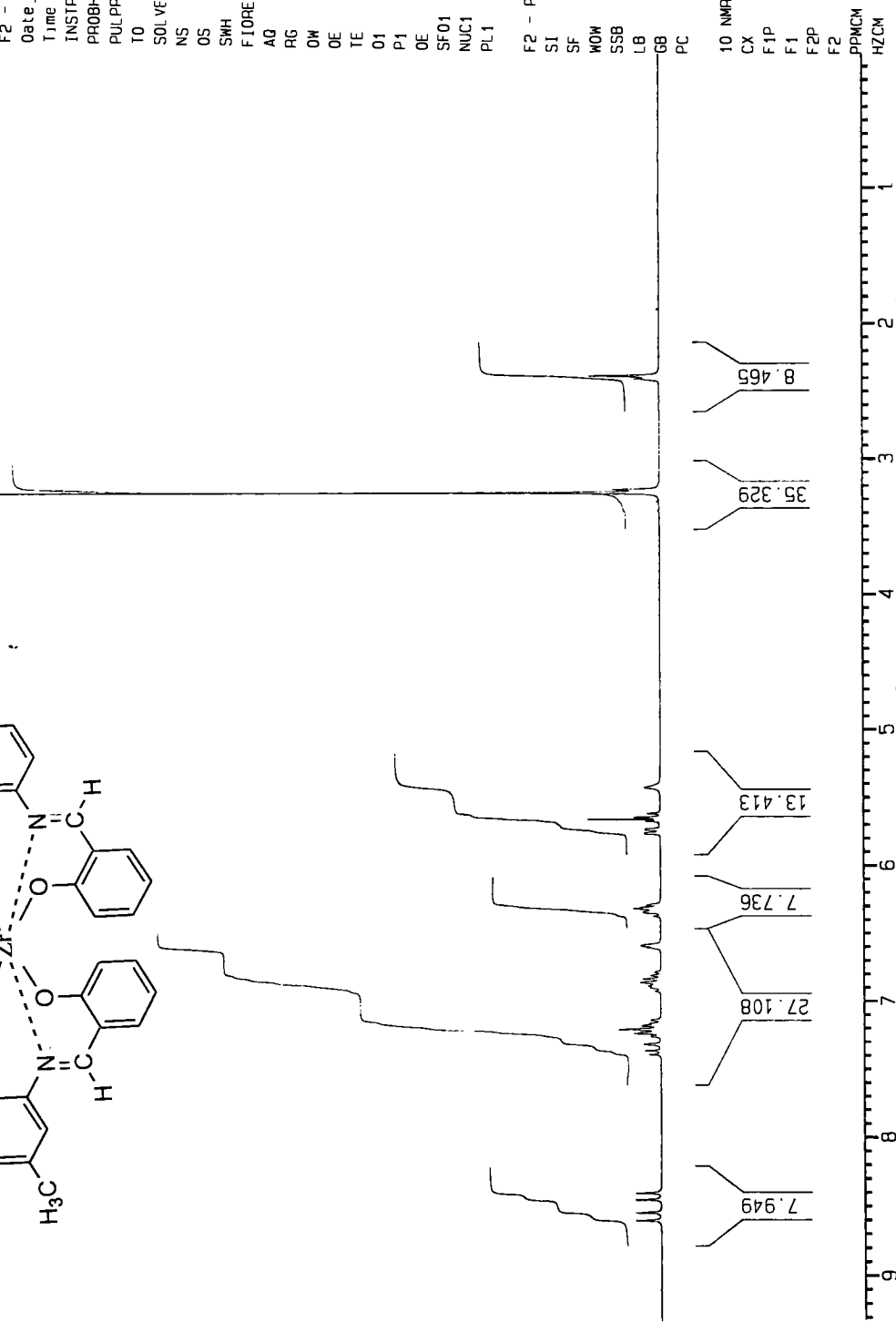
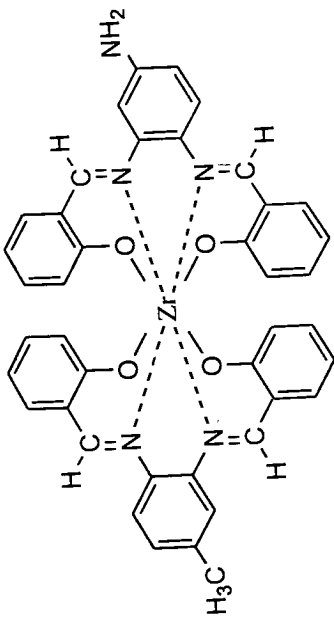


Figure 3.17 <sup>1</sup>H NMR Spectrum of Zr(adsp)(mdsp)



Current Data Parameters  
NAME Zr-CN\_WW\_1  
EXPNO 1  
PROCNO 1

F2 - Acquisition Parameters  
Date\_ 990728  
Time 14.34  
INSTRUM spect  
PROBHD 5 mm QNP 1H  
PULPROG zg30  
TD 32768  
SOLVENT DMSO  
NS 16  
DS 2  
SWH 6172.839 Hz  
FIDRES 0.188380 Hz  
AQ 2.6542580 sec  
RG 362  
DM 81.000 usec  
DE 6.00 usec  
TE 300.0 K  
D1 1.00000000 sec  
P1 9.00 usec  
DE 6.00 usec  
SF01 300.1318534 MHz  
NUC1 1H  
PL1 -5.00 dB

F2 - Processing parameters  
SI 16384  
SF 300.1300332 MHz  
WDW EM  
SSB 0  
LB 0.30 Hz  
GB 0  
PC 1.00

10 NMR plot parameters  
CX 20.00 cm  
F1P 11.000 ppm  
F1 3301.43 Hz  
F2P -1.000 ppm  
F2 -300.13 Hz  
PPMCM 0.60000 ppm/cm  
HZCM 180.07802 Hz/cm

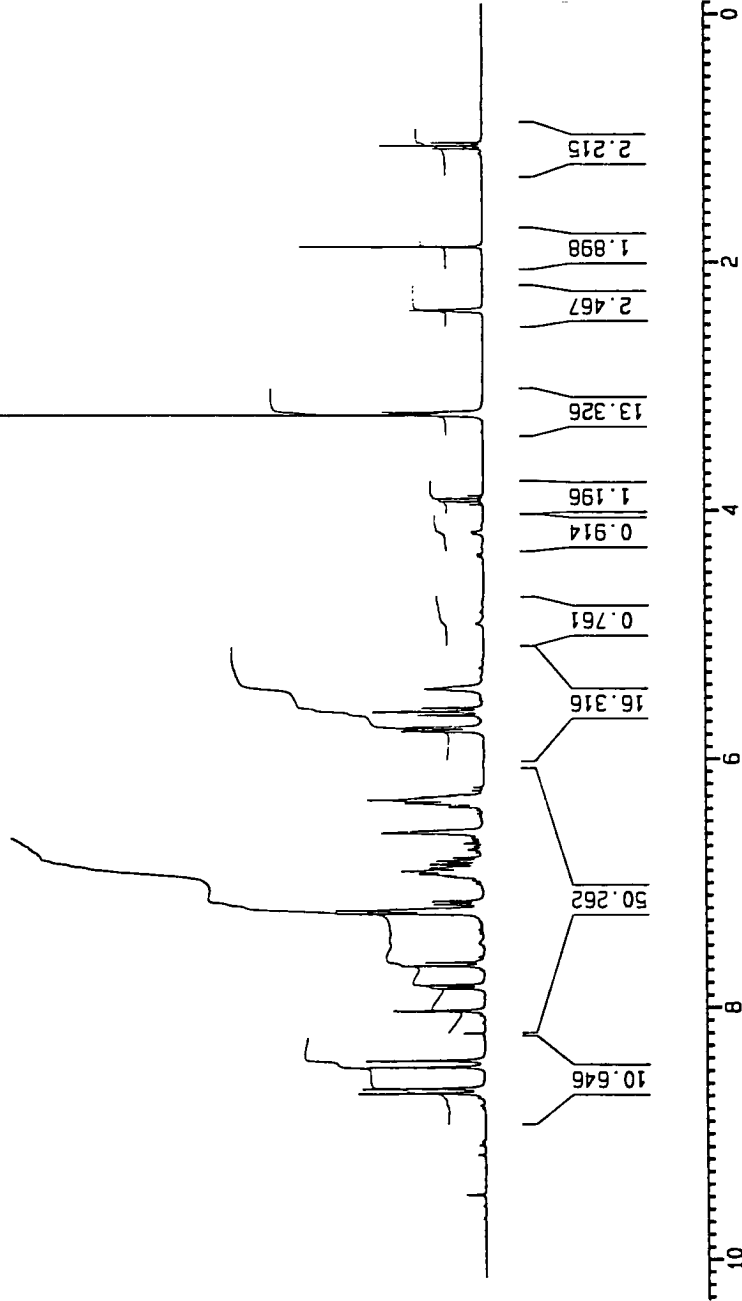
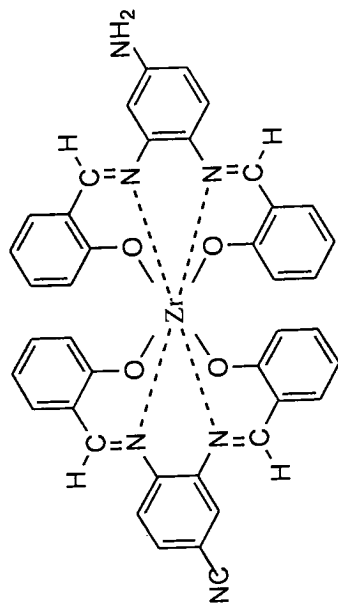


Figure 3.19 <sup>1</sup>H NMR Spectrum of Zr(adsp)(cdsp)

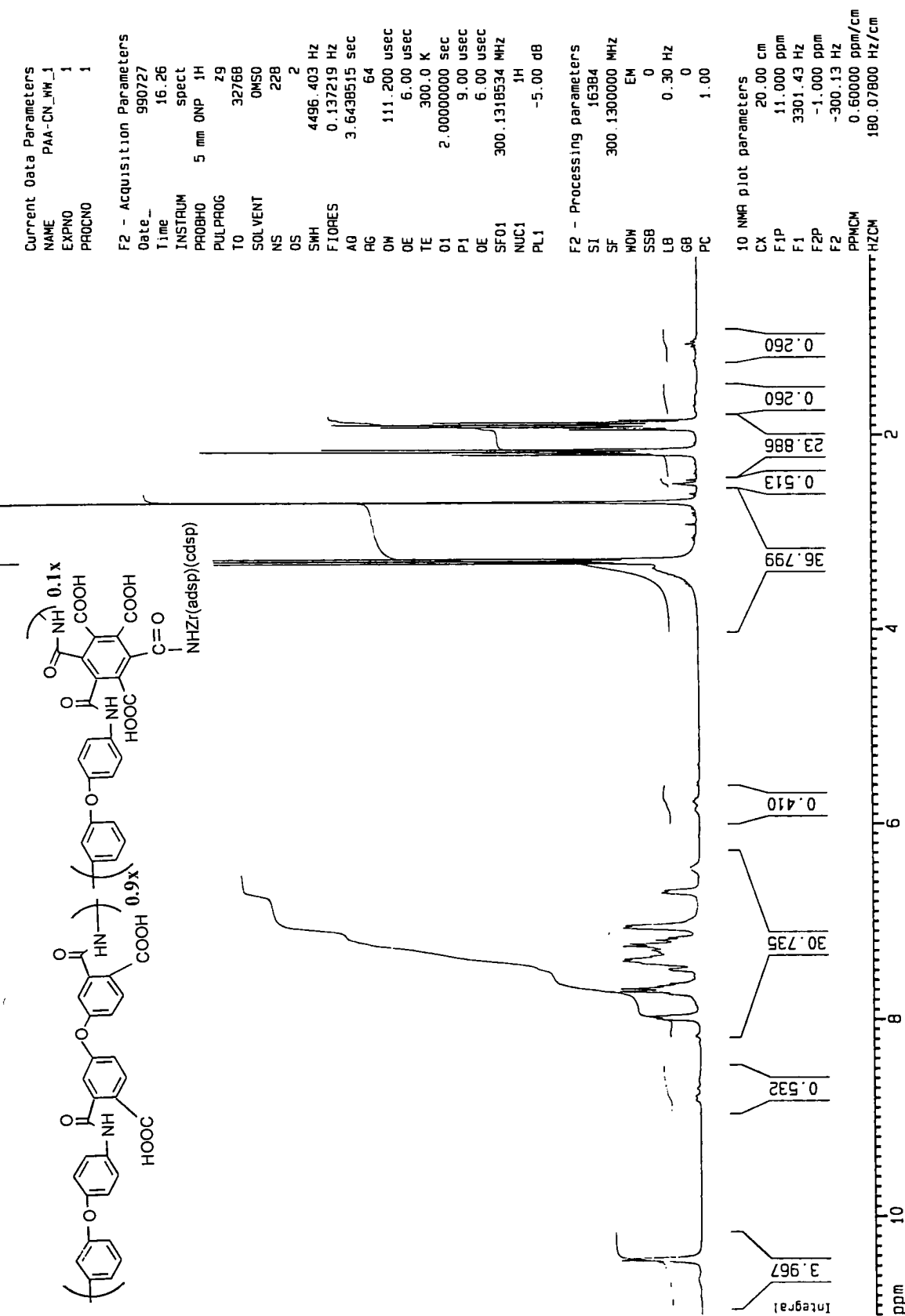


Figure 3.20  $^1\text{H}$ NMR Spectrum of Zr(adsp)(cdsp) Pendent Polyamic Acid

Current Data Parameters  
 NAME Zr-3-OME\_WW\_1  
 EXPNO 1  
 PROCNO 1

# F2 - Acquisition Parameters

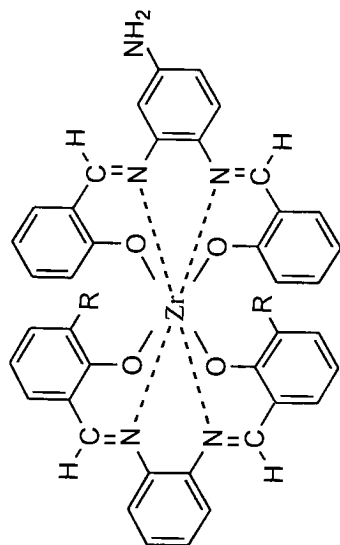
Date\_ 990728  
 Time 14.25  
 INSTRUM spect  
 PROBHD 5 mm QNP 1H  
 PULPROG zg30  
 TO 32768  
 SOLVENT DMSO  
 NS 16  
 DS 2  
 SMH 6172.839 Hz  
 FIDRES 0.188380 Hz  
 AQ 2.6542580 sec  
 RG 161.3  
 OW 81.000 usec  
 OE 6.00 usec  
 TE 300.0 K  
 D1 1.0000000 sec  
 P1 9.00 usec  
 OE 6.00 usec  
 SF01 300.1318534 MHz  
 NUC1 1H  
 PL1 -5.00 dB

# F2 - Processing parameters

SF 16384  
 SF 300.1299873 MHz  
 WDW EM  
 SSB 0  
 LB 0.30 Hz  
 GB 0  
 PC 1.00

# 1D NMR plot parameters

CX 20.00 cm  
 F1P 11.000 ppm  
 F1 3301.43 Hz  
 F2P -1.000 ppm  
 F2 -300.13 Hz  
 PPMCM 0.60000 ppm/cm  
 HZCM 180.07799 Hz/cm



R=OCH<sub>3</sub>

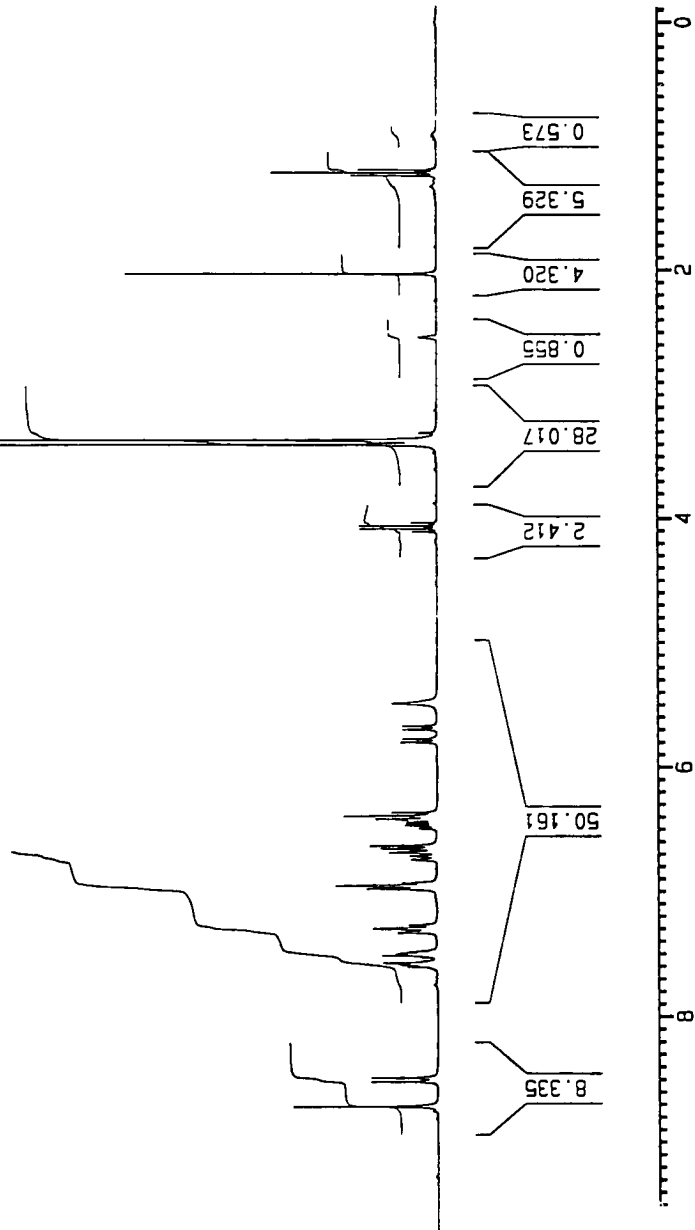


Figure 3.21 <sup>1</sup>H NMR Spectrum of Zr(adsp)(3-OCH<sub>3</sub>dsp)

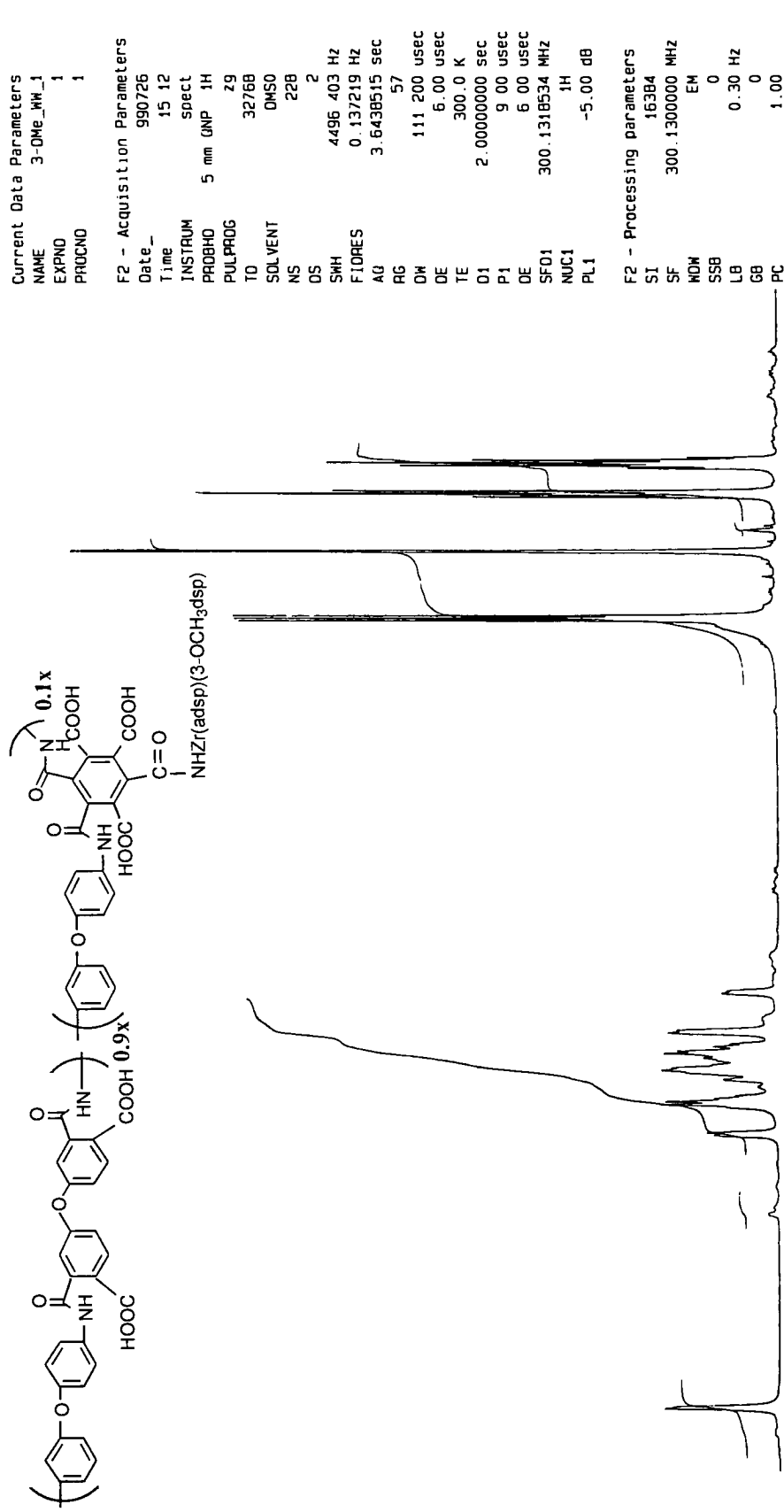


Figure 3.22 <sup>1</sup>H NMR Spectrum of Zr(adsp)(3-OCH<sub>3</sub>dsp) Pendent Polyamic Acid



Current Data Parameters  
 NAME Zr-5-OCH<sub>3</sub>\_W\_1  
 EXPNO 1  
 PROCNO 1

F2 - Acquisition Parameters

Date\_ 990728  
 Time 14.43  
 INSTRUM spect  
 PROBHD 5 mm QNP 1H  
 PULPROG zg30  
 TO 32768  
 SOLVENT DMSO  
 NS 16  
 DS 2  
 SWH 6172.839 Hz  
 FIDRES 0.188380 Hz  
 AQ 2.6542580 sec  
 RG 362  
 OW 81.000 usec  
 OE 6.00 usec  
 TE 300.0 K  
 O1 1.00000000 sec  
 P1 9.00 usec  
 DE 6.00 usec  
 SF01 300.1318534 MHz  
 NUC1 1H  
 PL1 -5.00 dB

F2 - Processing parameters

SI 16384  
 SF 300.1299621 MHz  
 WDW EM  
 SSB 0  
 LB 0.30 Hz  
 GB 0  
 PC 1.00

10 NMR plot parameters  
 CX 20.00 cm  
 F1P 11.000 ppm  
 F1 3301.43 Hz  
 F2P -1.000 ppm  
 F2 -300.13 Hz  
 PPMCM 0.60000 ppm/cm  
 HZCM 180.07799 Hz/cm

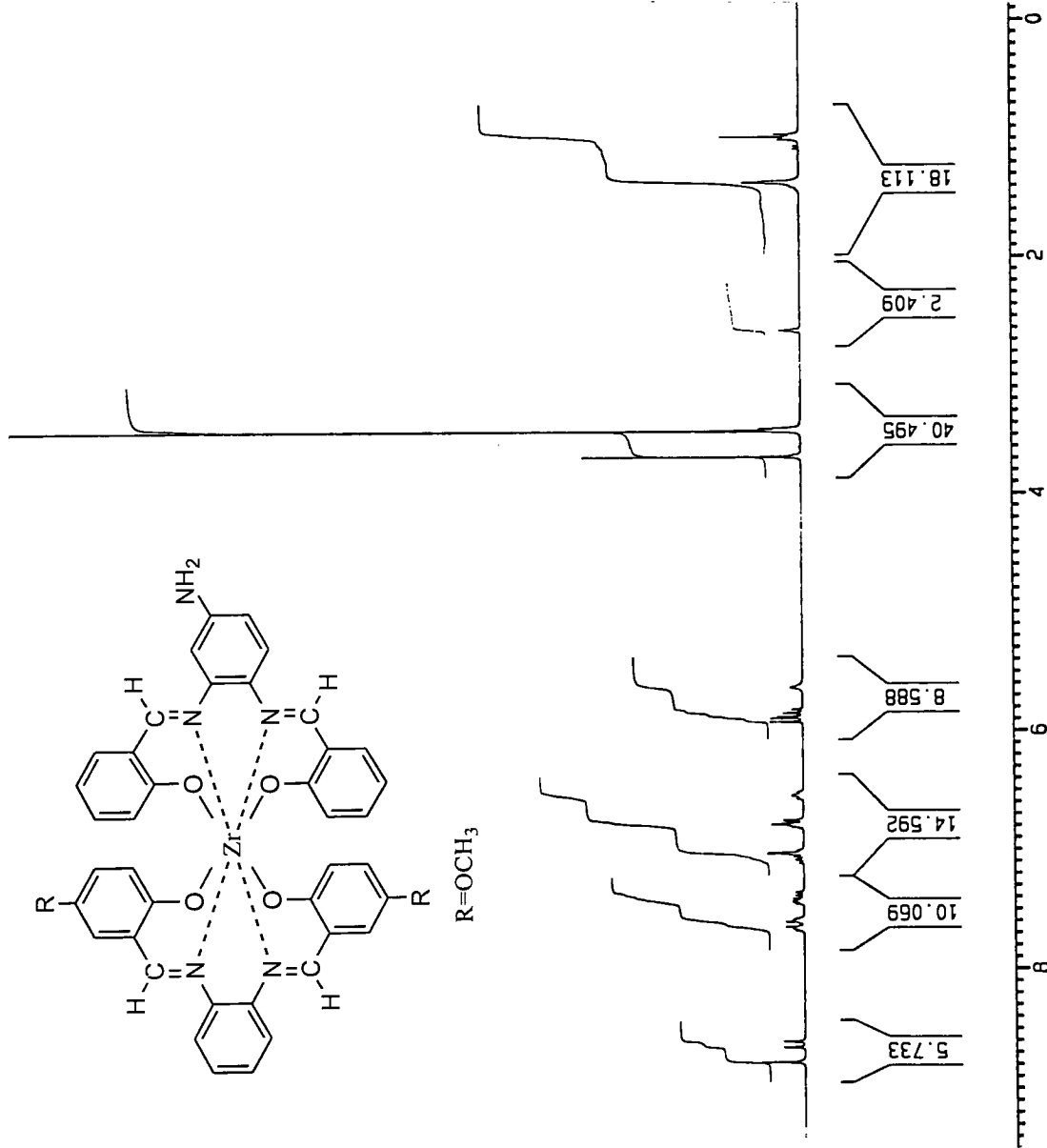
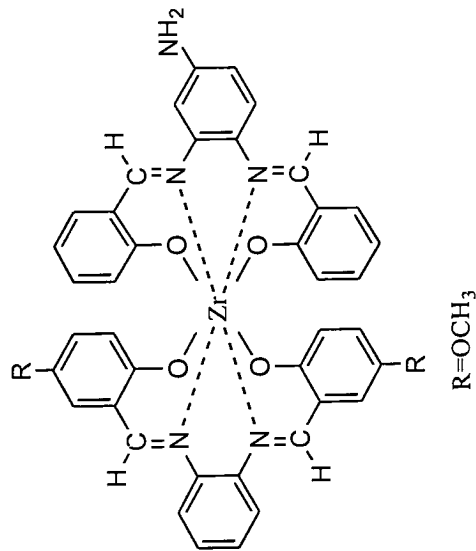


Figure 3.23 <sup>1</sup>H NMR Spectrum of Zr(adsp)(5-OCH<sub>3</sub>)<sub>3</sub>

Current Data Parameters

NAME 5-Ome\_WW\_1  
EXPNO 4  
PROCNO 1

F2 - Acquisition Parameters

Date\_ 990726  
Time 16.04  
INSTRUM spect  
PROBHD 5 mm QNP 1H  
PULPROG zg  
TD 32768  
SOLVENT DMSO  
NS 228  
DS 2  
SMH 4496.403 Hz  
FIDRES 0.137219 Hz  
AQ 3.6438515 sec  
RG 64  
DM 111.200 usec  
DE 6.00 usec  
TE 300.0 K  
D1 2.00000000 sec  
P1 9.00 usec  
DE 6.00 usec  
SFO1 300.1318534 MHz  
NUC1 1H  
PL1 -5.00 dB

F2 - Processing parameters

SI 16384  
SF 300.1300000 MHz  
WDW EM  
SSB 0  
LB 0.30 Hz  
GB 0  
PC 1.00

1D NMR plot parameters

CX 20.00 cm  
F1P 11.000 ppm  
F1 3301.43 Hz  
F2P -1.000 ppm  
F2 -300.13 Hz  
PPMCM 0.60000 ppm/cm  
HZCM 180.07800 Hz/cm

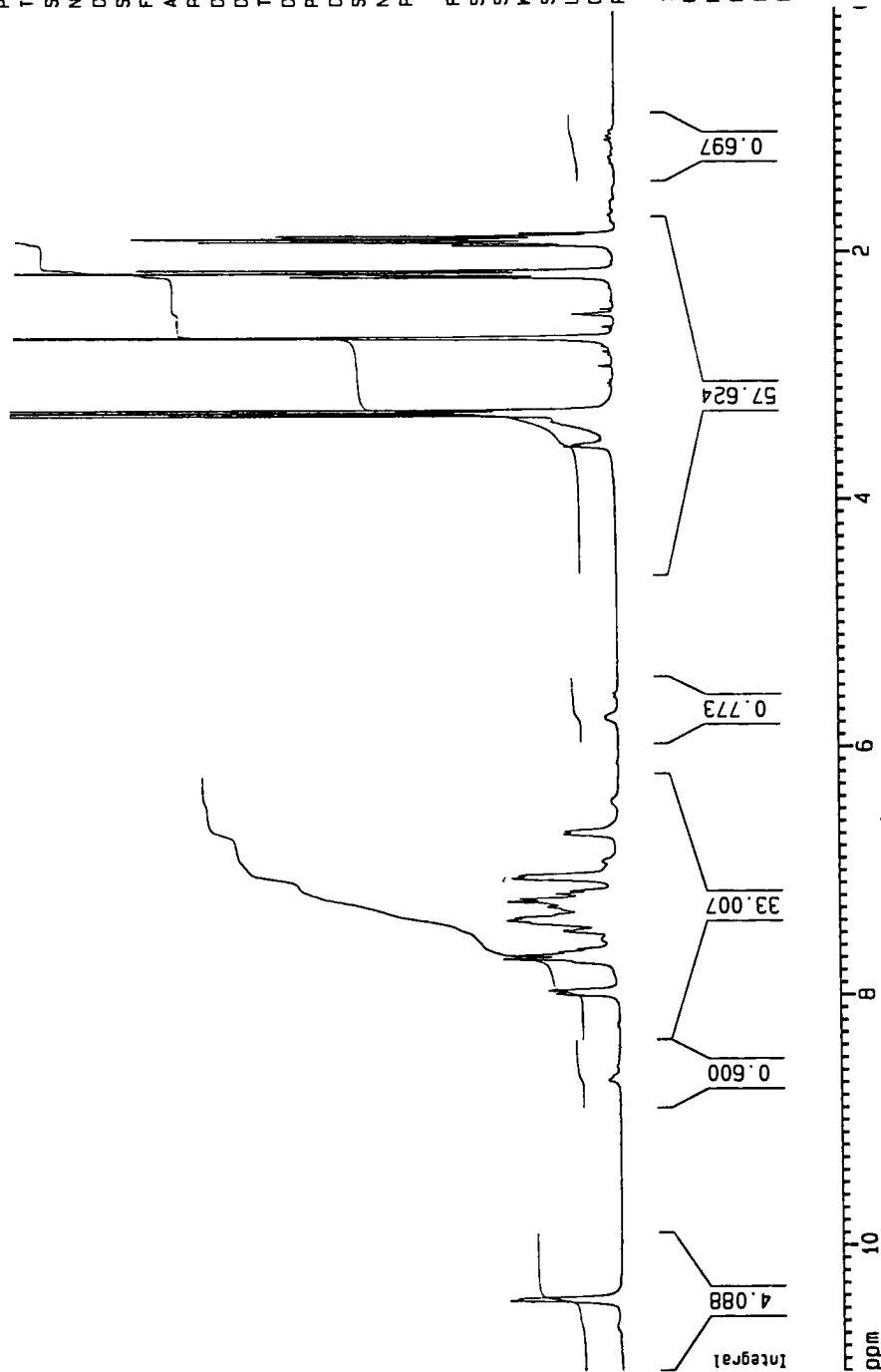
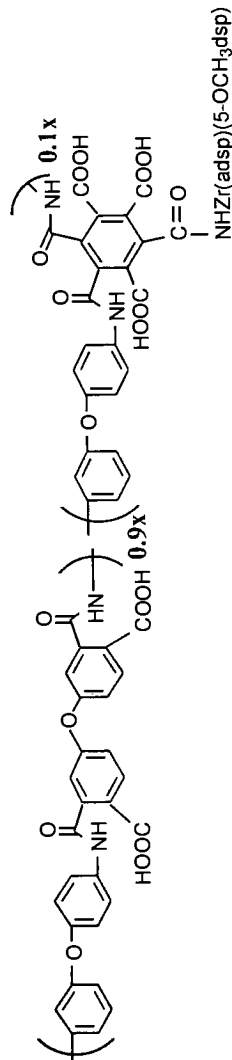


Figure 3.24 <sup>1</sup>H NMR Spectrum of Zr(adsp)(5-OCH<sub>3</sub>dsp) Pendent Polyamic Acid

### 3.4.3 Thermogravimetric Analysis (TGA)

TGA was employed to determine the thermal stability of polyamic acids and polyimides with or without zirconium pendent groups. The approximate mol% of pendent groups can be estimated via the amount of  $ZrO_2$  residue, which was produced upon the thermal decomposition in air.

Figure 3.25 shows the TGA graph of parent polyamic acid. Two stages of weight loss are seen, the first stage is the imidization step, the second stage is the decomposition step. The imidization step starts at 136.7 °C, ends at 204.6 °C, midpoint is 171.3°C. The thermal decomposition step starts at 583.4°C, ends at 642.0 °C, midpoint is 612.0 °C. Figures 3.26-3.30 show the TGA graphs of zirconium pendent polymers. Table 3.5 shows the TGA results, including the imidization and thermal decomposition steps, for the parent polyamic acid and zirconium pendent polyamic acids.

Table 3.5 TGA Results for Parent Polyamic Acid and Zirconium Pendent Polyamic Acids

Sample	Imidization (°C)			Thermal decomposition (°C)		
	onset	midpoint	offset	onset	midpoint	offset
PAA	137.6	171.3	204.6	583.4	612.0	642.0
PAA/Zr(adsp)(dsp)	138.0	174.9	210.6	551.5	582.3	613.9
PAA/ Zr(adsp)(mdsp)	136.2	167.2	199.4	521.3	554.3	592.1
PAA/ Zr(adsp)(cdsp)	136.8	170.7	204.1	535.7	568.4	607.6
PAA/Zr(adsp) (3-OCH <sub>3</sub> dsp)	133.7	169.9	205.7	547.8	576.5	604.5
PAA/Zr(adsp) (5-OCH <sub>3</sub> dsp)	133.9	166.7	199.5	529.3	560.8	594.7

From Table 3.5, we see that the parent polymer and the zirconium pendent polymers have the same imidization temperature, which is about 130-140 °C. But the zirconium pendent polymers have lower thermal stability than the parent polymer, the thermal decomposition temperature of zirconium pendent polymers is about 30-50 °C lower than the parent polymer. However, since all the thermal decomposition temperatures are above 500 °C, the thermal stability of all of the synthetic polymers is outstanding. There are no substantial differences in imidization properties or thermal stabilities among the zirconium pendent polymers.

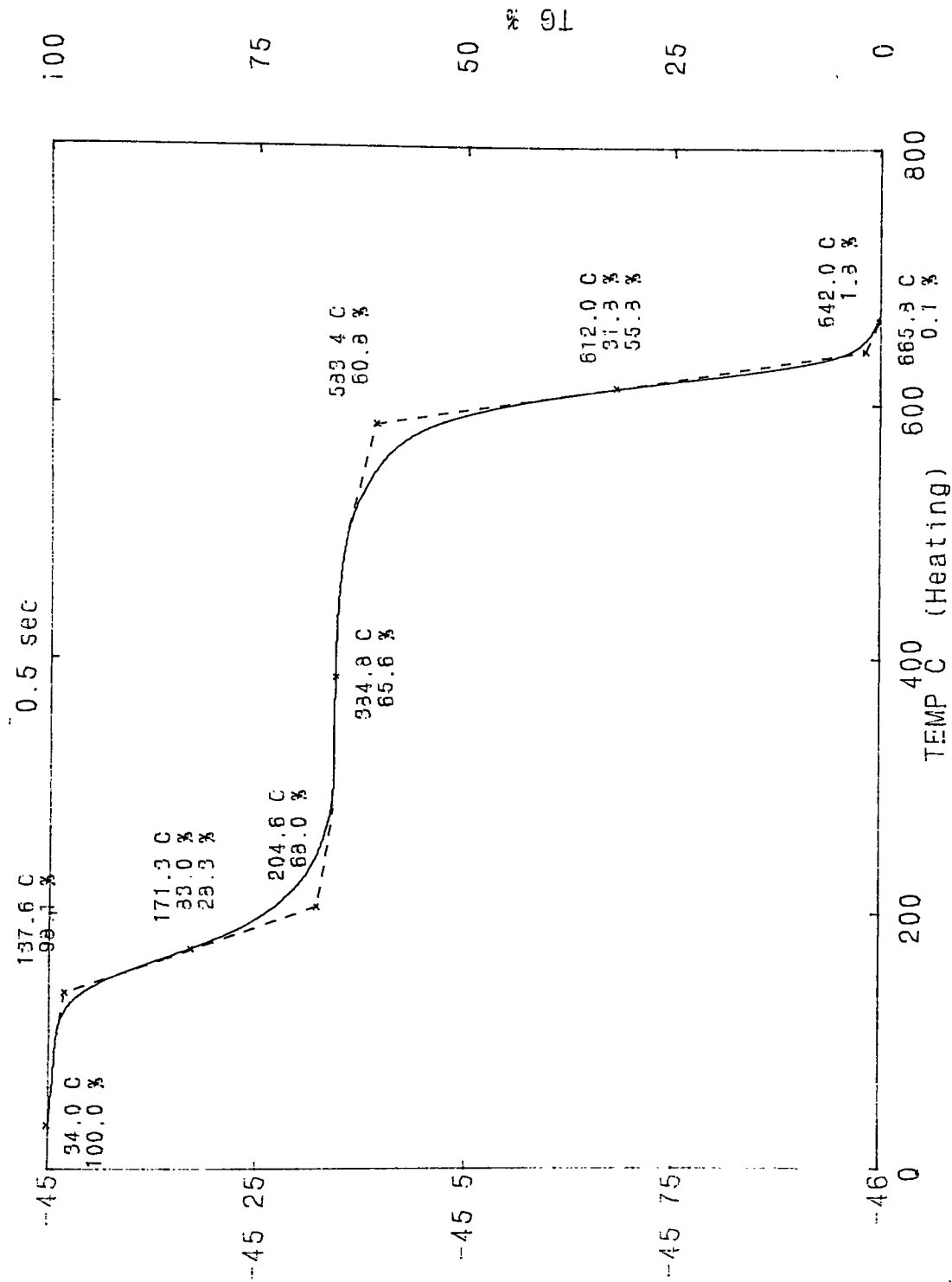


Figure 3.25 TGA Graph of Parent Polyamic Acid

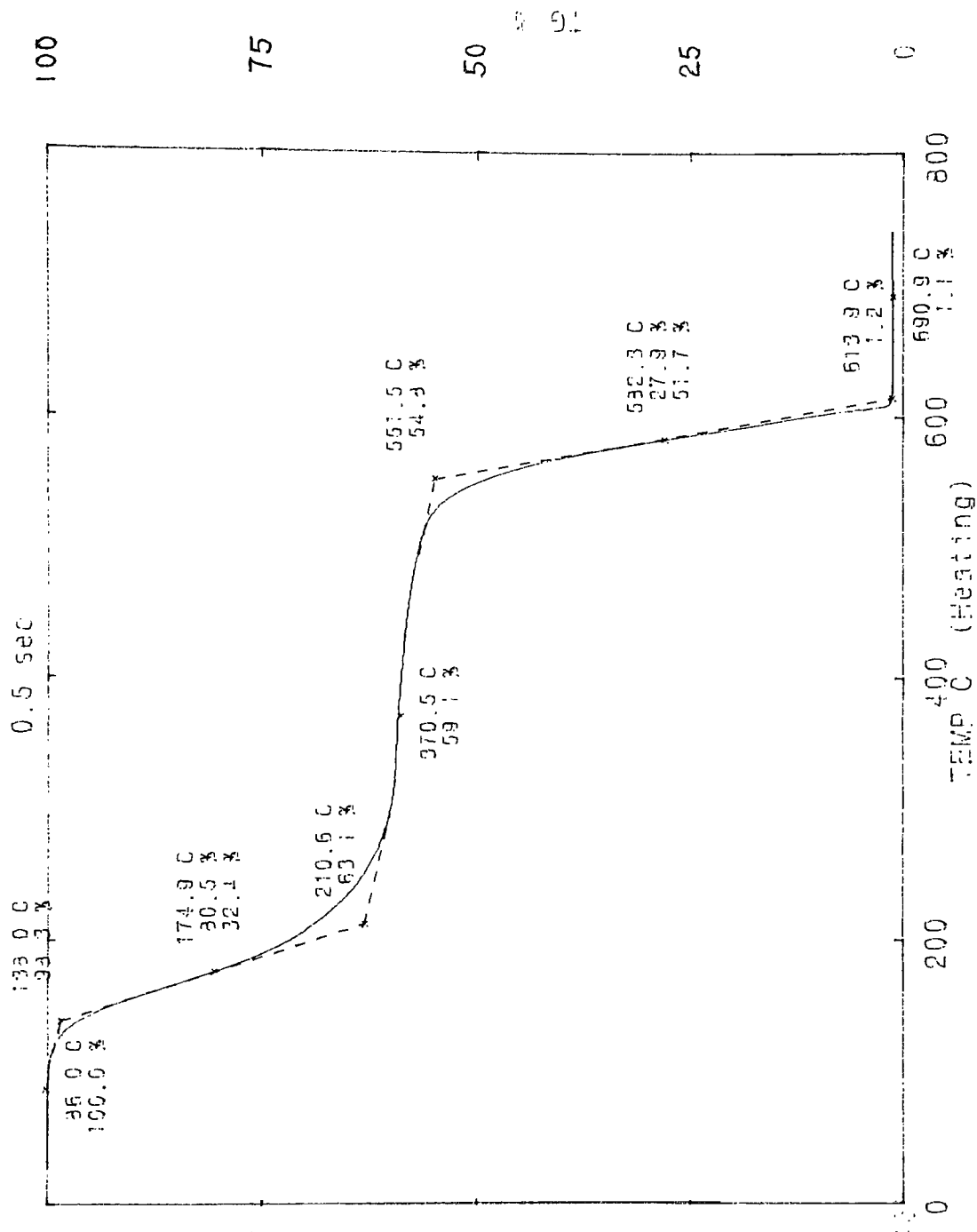


Figure 3.26 TGA Graph of Zr(adsp)(dsp) Pendent Polyamic Acid

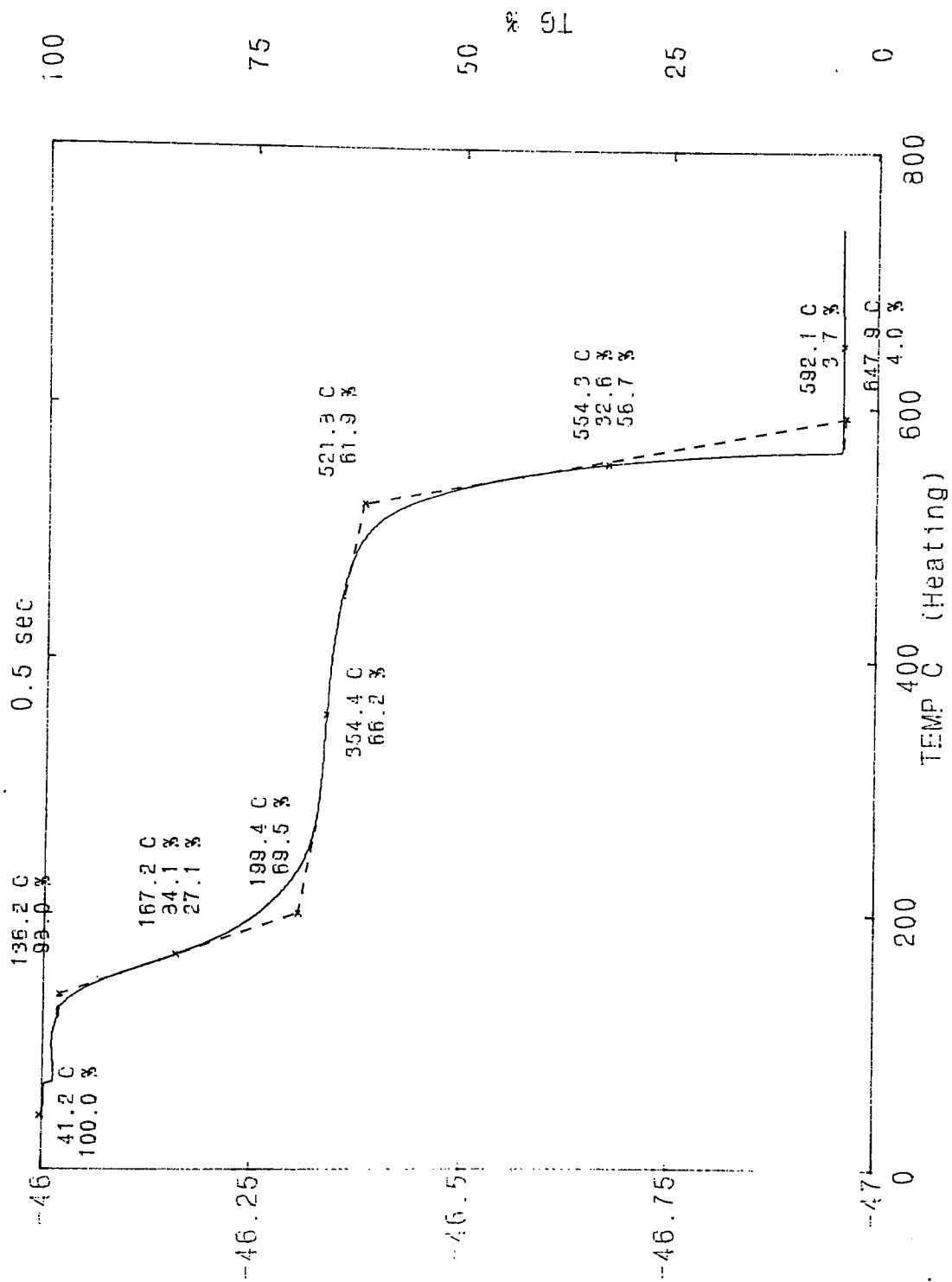


Figure 3.27 TGA Graph of Zr(adsp)(mdsp) Pendent Polyamic Acid

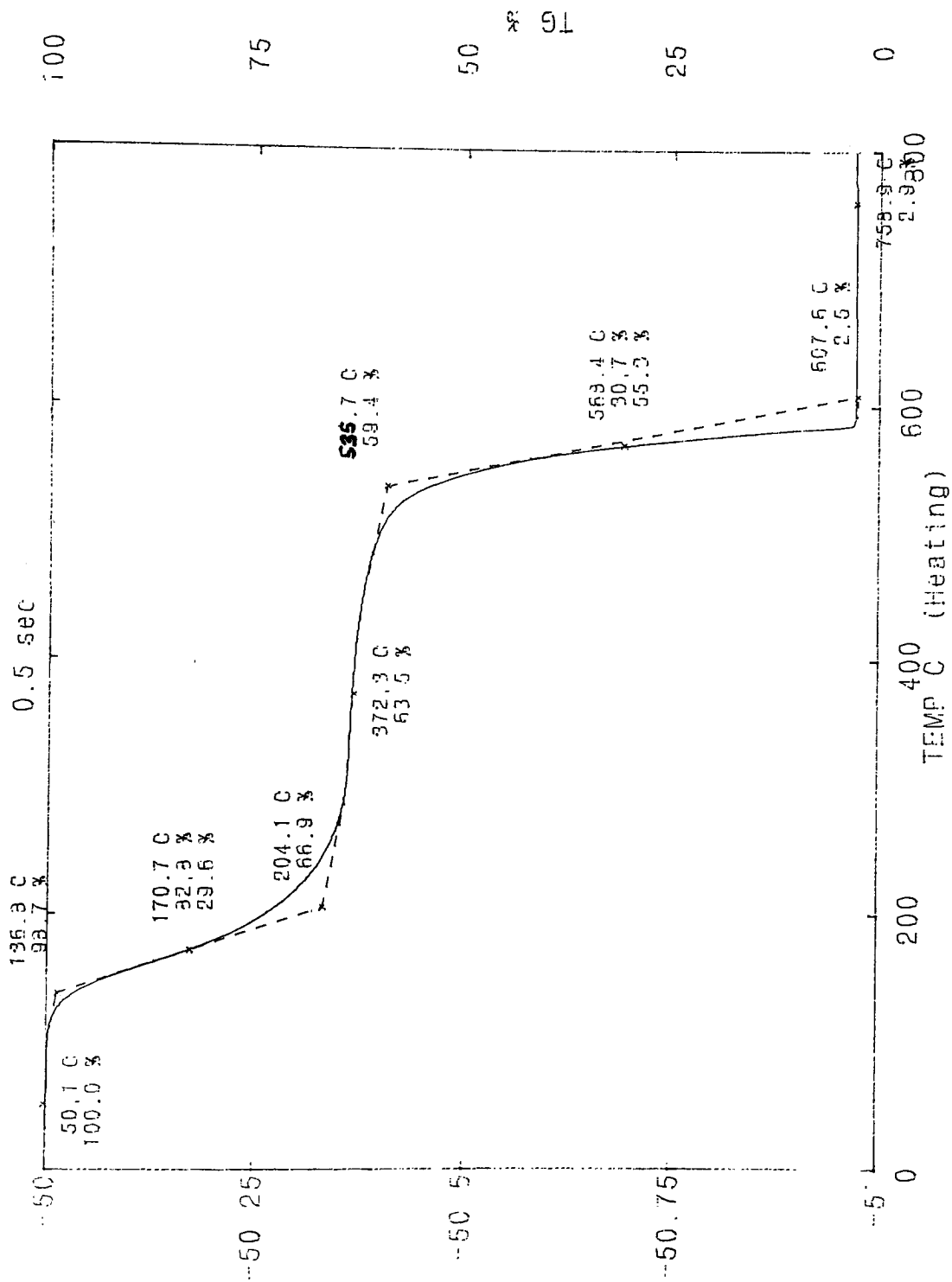


Figure 3.28 TGA Graph of of Zr(adsp)(cdsp) Pendent Polyamic Acid

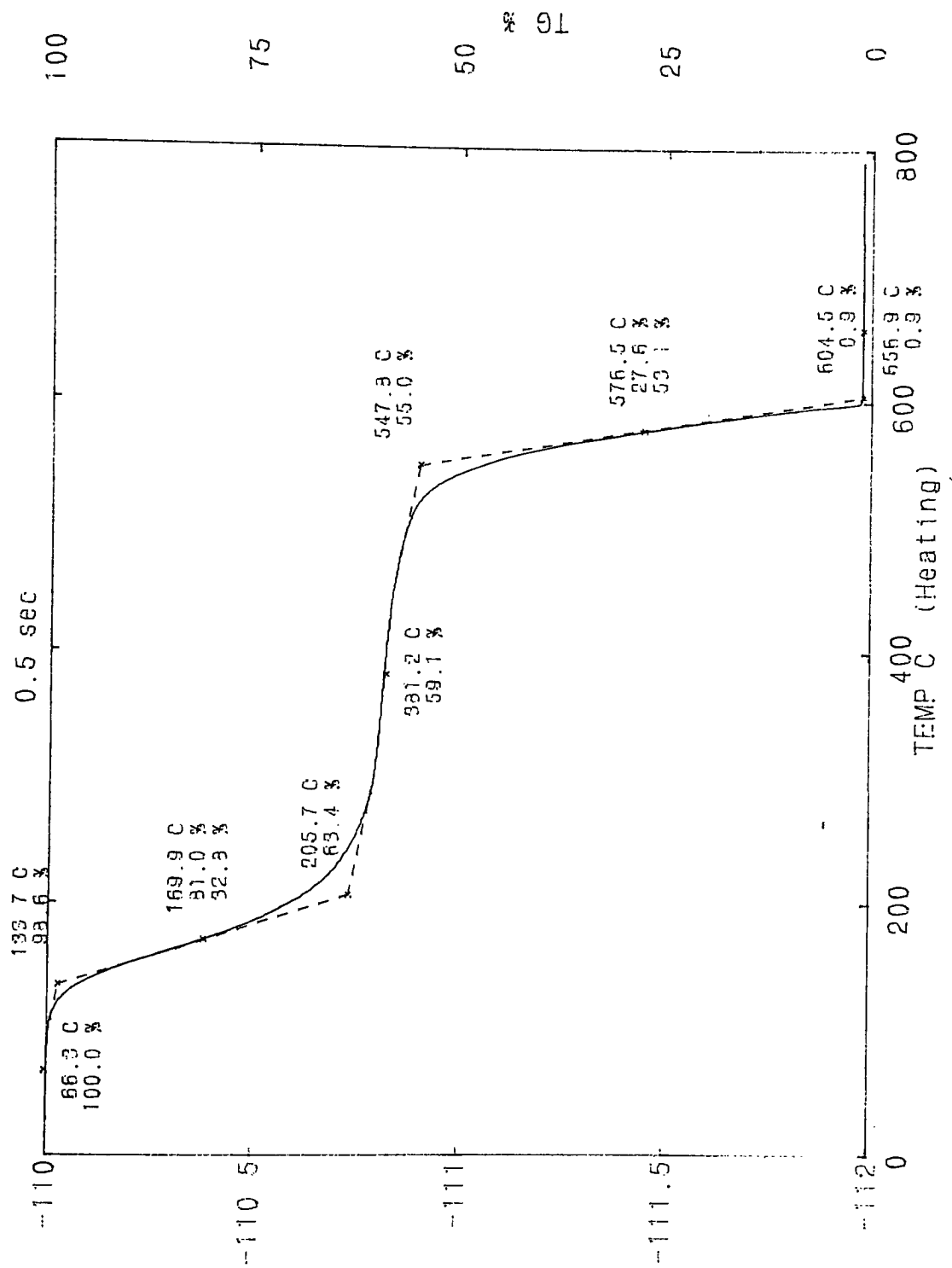


Figure 3.29 TGA Graph of Zr(adsp)(3-OCH<sub>3</sub>dsp) Pendent Polyamic Acid



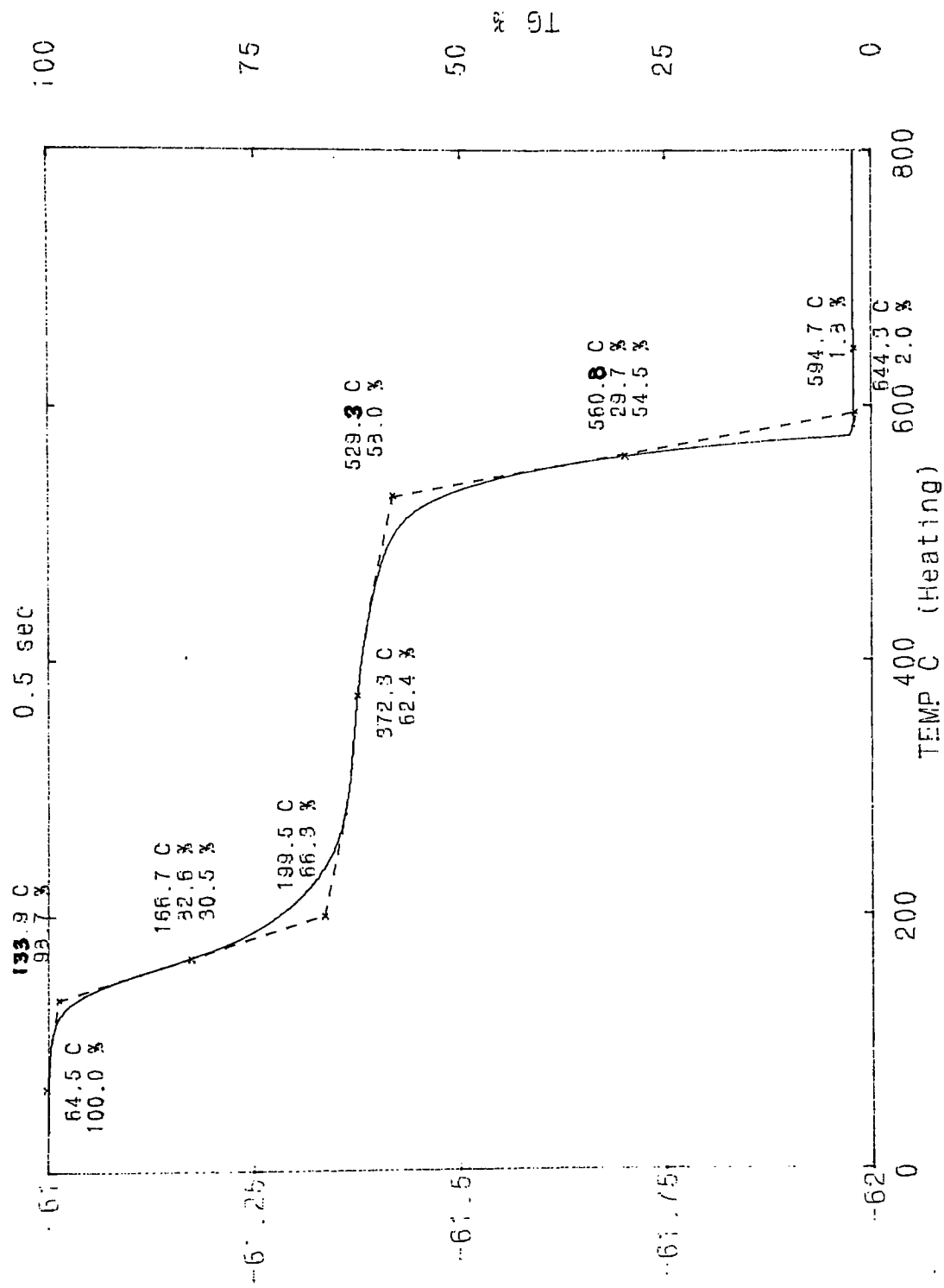


Figure 3.30 TGA Graph of Zr(adsp)(5-OCH<sub>3</sub>dsp) Pendent Polyamic Acid

Table 3.6 shows the ZrO<sub>2</sub> residue of zirconium complexes pendent polymers after thermal decomposition in TGA at 800 °C.

Table 3.6 ZrO<sub>2</sub> Residue after Thermal Decomposition Step in TGA

Sample	Theoretical	Experimental	Error(%)
PAA/Zr(adsp)(dsp)	2.3	1.1	52.2
PAA/ Zr(adsp)(mdsp)	2.2	4.0	81.8
PAA/ Zr(adsp)(cdsp)	2.2	2.5	13.6
PAA/Zr(adsp) (3-OCH <sub>3</sub> dsp)	2.2	0.9	59.1
PAA/Zr(adsp) (5-OCH <sub>3</sub> dsp)	2.2	1.8	18.2

$$\text{Theoretical residue} = \frac{\text{mass of ZrO}_2 \text{ from Zr complex for 10\% (mol) pendent polymer}}{\text{mass of zirconium pendent polymer}}$$

### 3.4.4 Differential Scanning Calorimetry (DSC)

There is generally one endothermic peak in the first scan for both parent polyimide and zirconium pendent polyimides. Typical DSC curves of heat flow versus temperature of polyimide samples are shown in Figures 3.31- 3.36, respectively.

Glass transition temperatures,  $T_g$ , determined by DSC for all of the imidized films, are listed in Table 3.7. Glass transition temperature for all of the polyamic acids films could not be determined because only solvent evaporation curves were observed when the heating circle did not exceed 100 °C. The absence of  $T_m$  in the DSC curves indicated a lack of thermoplastic behavior in the polyimides.

Table 3.7 Glass Transition Temperature from DSC Result for Polyimide Films

Sample	First heating circle (°C)			Second heating circle (°C)		
	onset	midpoint	offset	onset	midpoint	offset
PI	230.8	234.4	239.0	252.2	255.7	260.0
PI/Zr(adsp)(dsp)	229.7	236.4	242.6	296.0	319.8	328.8
PI/ Zr(adsp)(mdsp)	229.4	238.4	253.2	307.1	319.2	329.3
PI/ Zr(adsp)(cdsp)	235.0	248.2	254.4	287.4	304.8	313.4
PI/Zr(adsp) (3-OCH <sub>3</sub> dsp)	235.2	255.1	257.5	276.1	287.1	291.1
PI/Zr(adsp) (5-OCH <sub>3</sub> dsp)	239.1	255.2	260.4	292.3	312.2	315.5

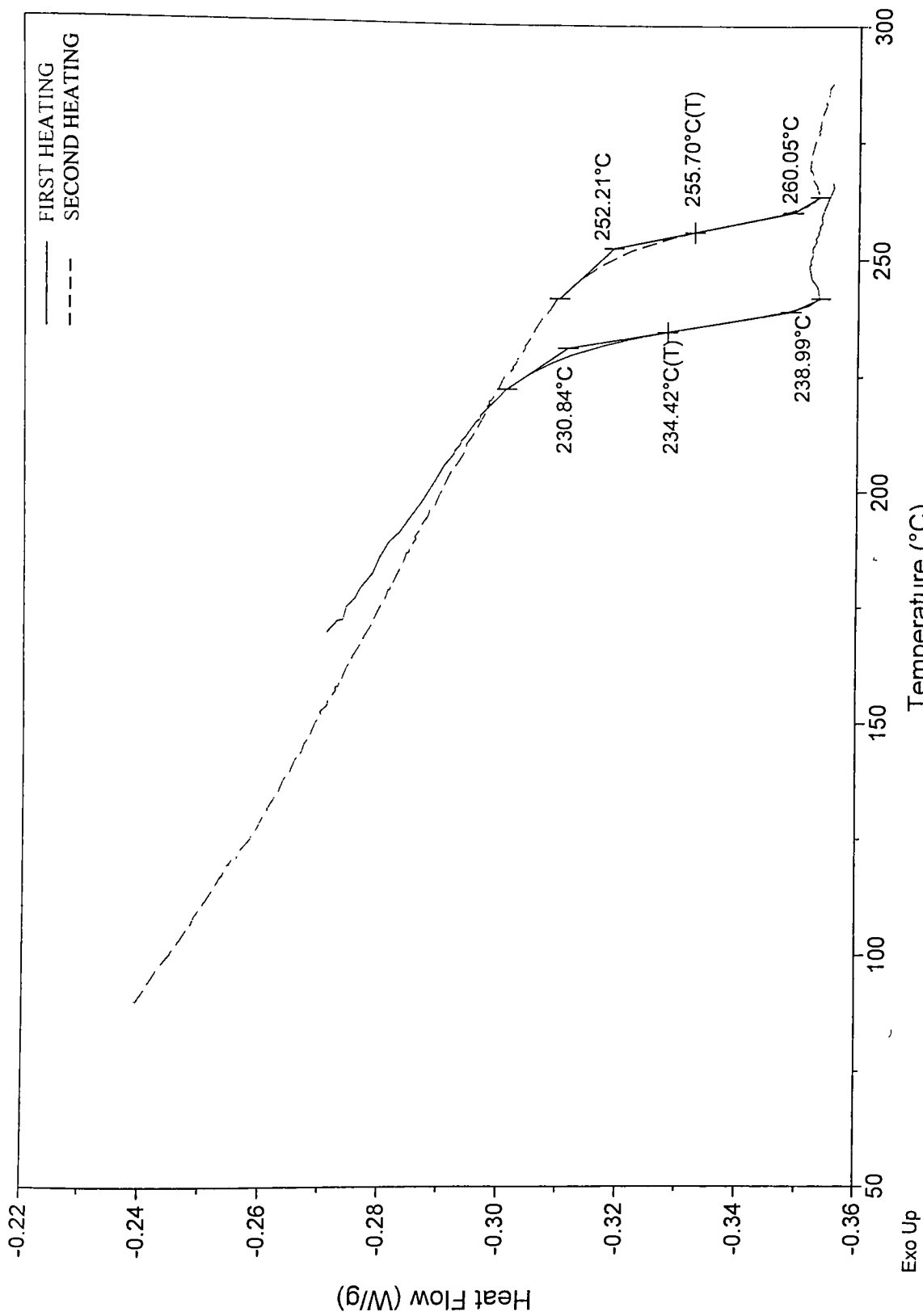


Figure 3.31 DSC Graph of Parent Polyimide

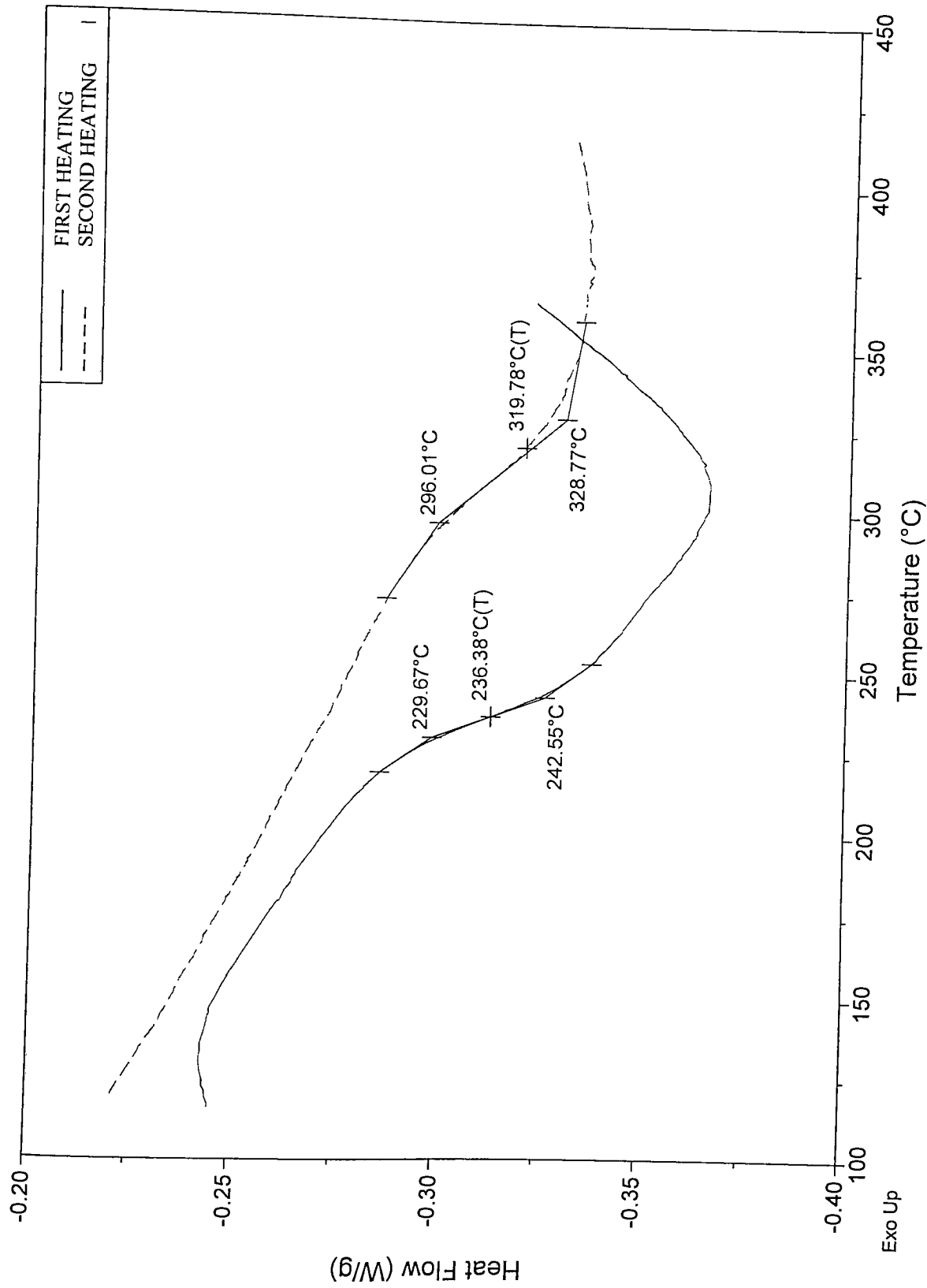


Figure 3.32 DSC Graph of Zr(adsp)(dsp) Pendent Polyimide

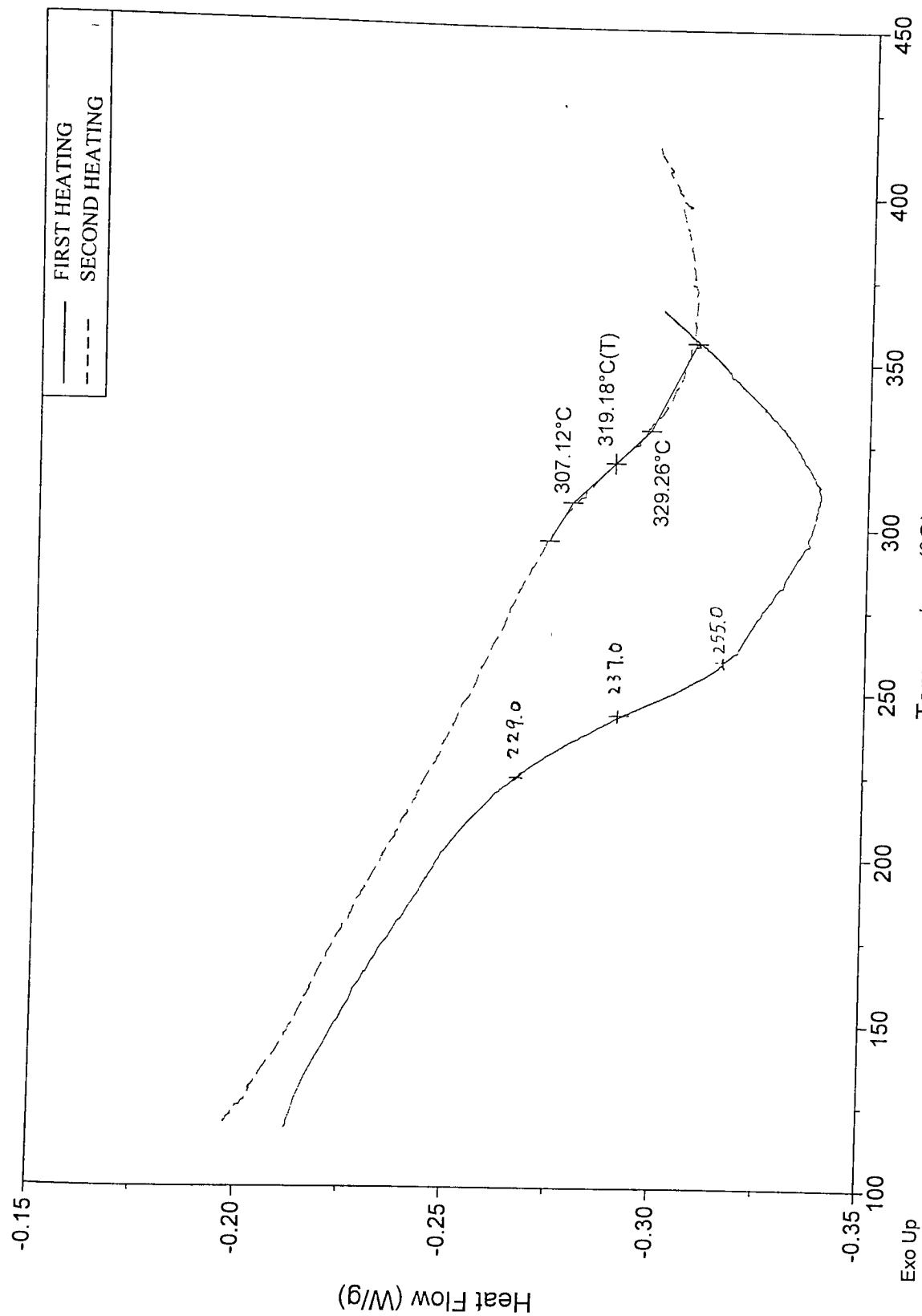


Figure 3.33 DSC Graph of Zr(adsp)(mdsp) Pendent Polyimide

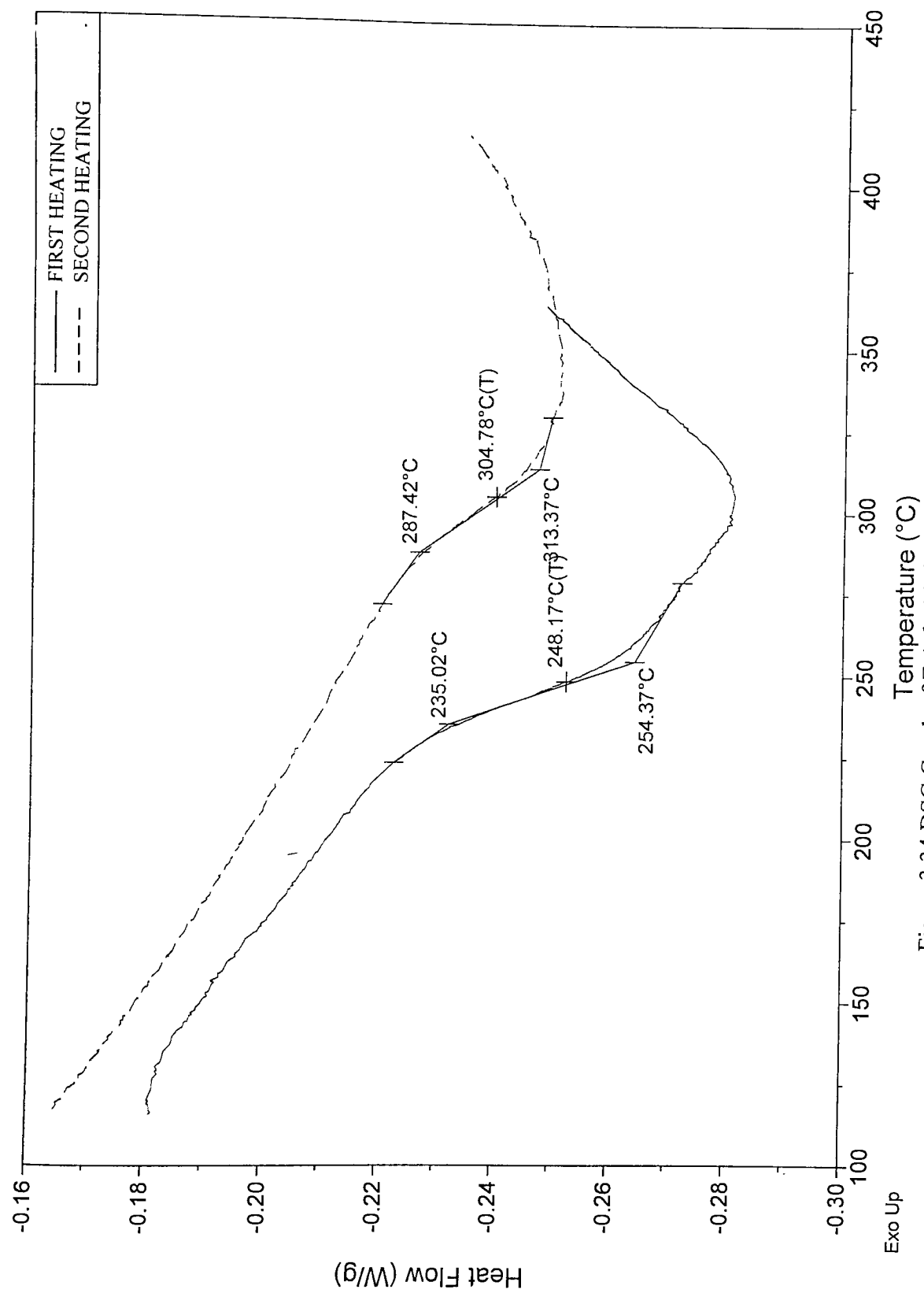


Figure 3.34 DSC Graph of Zr(adsp)(cdsp) Pendent Polyimide

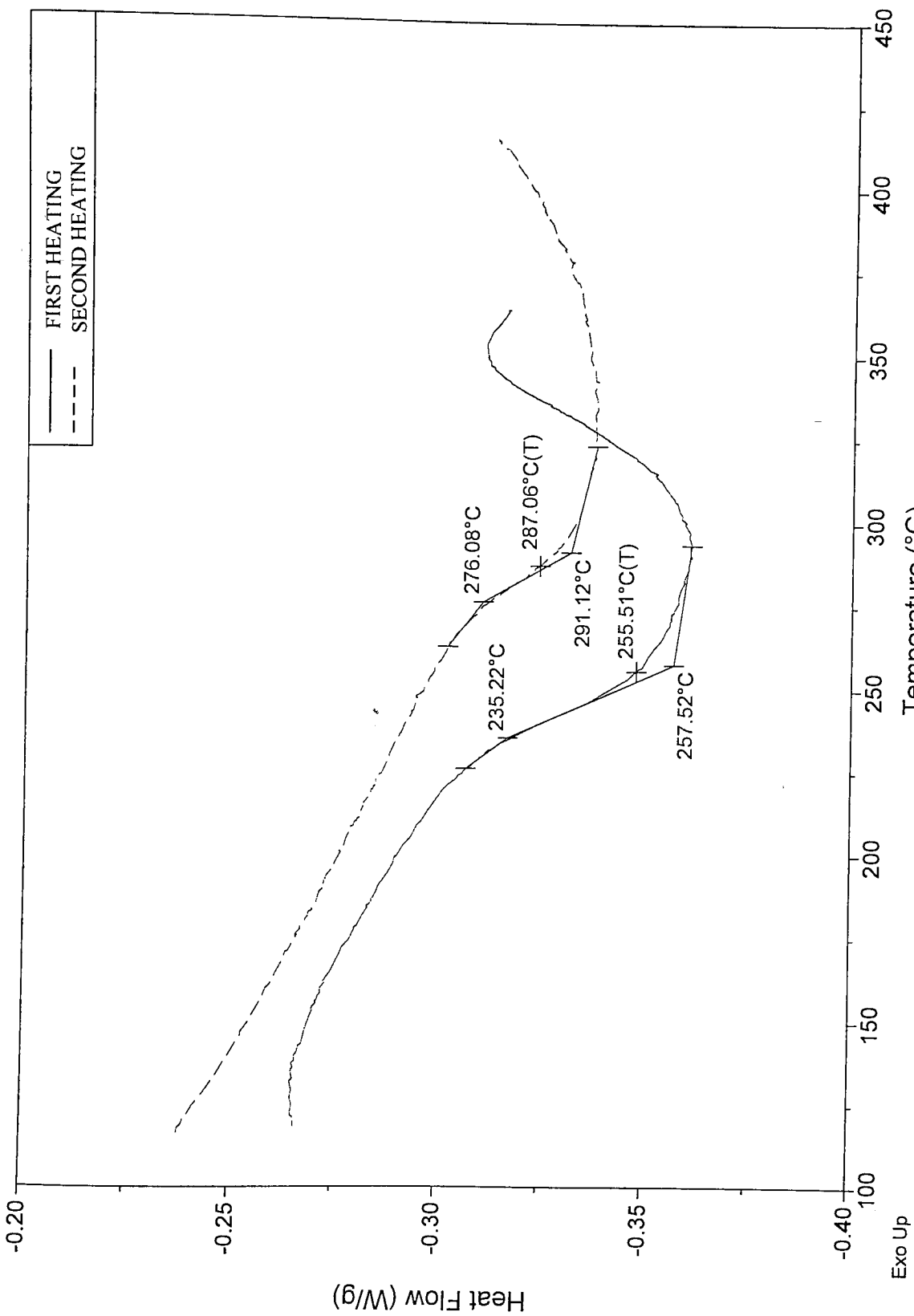


Figure 3.35 DSC Graph of Zr(adsp)(3-OCH<sub>3</sub>dsp) Pendent Polyimide

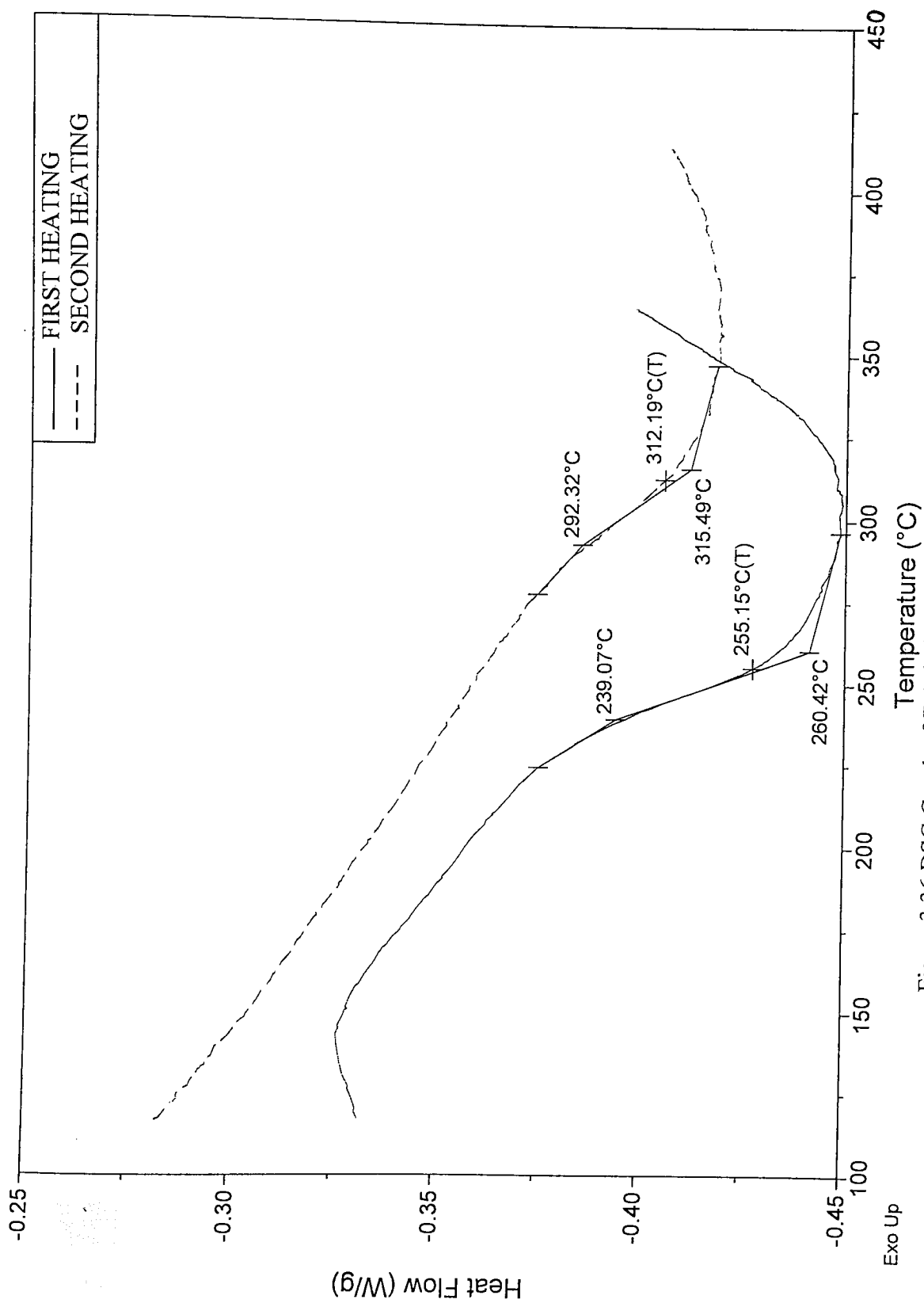


Figure 3.36 DSC Graph of Zr(adsp)(5-OCH<sub>3</sub>dsp) Pendent Polyimide



From Table 3.7, we see that the  $T_g$  of parent polyimide is 252.2 °C, which is much lower than the zirconium pendent polyimides, whose  $T_g$ s are 296.0, 307.1, 287.4, 276.1, and 292.3 °C, respectively. The highest  $T_g$  is observed for the Zr(adsp)(mdsp) pendent polyimide.

### 3.4.5 Scanning Electron Microscopy (SEM)

All of the pendent polyimide films are more pitted than the parent polyimide film, less so for the Zr(adsp(5-OCH<sub>3</sub>dsp) pendent polyimide.

The surface appearance of parent polyimide and zirconium pendent polyimide films before and after oxygen plasma etching for three hours were recorded by scanning electron microscopy. The SEM pictures show the parent polyimide and zirconium pendent polyimide surfaces before and after atomic oxygen etching in Figures 3.37- 3.39.

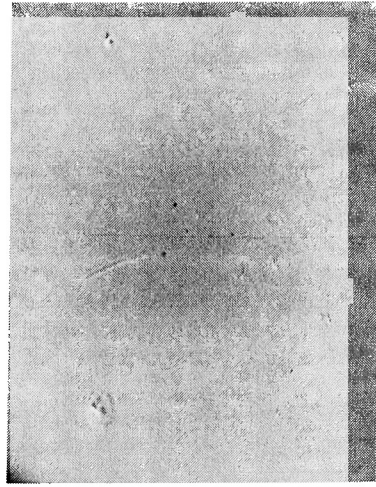
The original zirconium pendent polyimide films are transparent with a yellow- or orange-tinted color, which depends on the different zirconium complexes. Upon exposing each film to atomic oxygen via plasma etching, chalky white residue appeared on the surface.

All the polyimide film surfaces appeared uniform before etching. After three hours atomic oxygen exposure, it is apparent that the surfaces of polyimide films are much rougher.

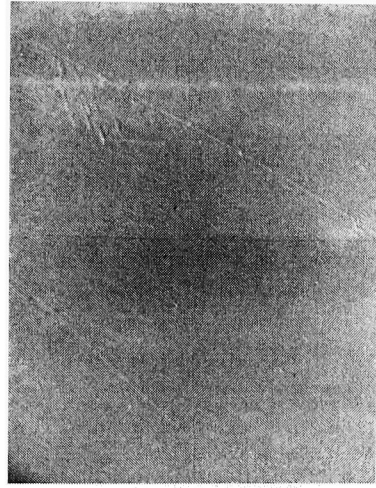
### 3.4.6 Gel Permeation Chromatography (GPC)

The GPC analysis results of parent polyamic acid and zirconium pendent polyamic acids are shown in Table 3.8 and Figures 3.40-3.45.

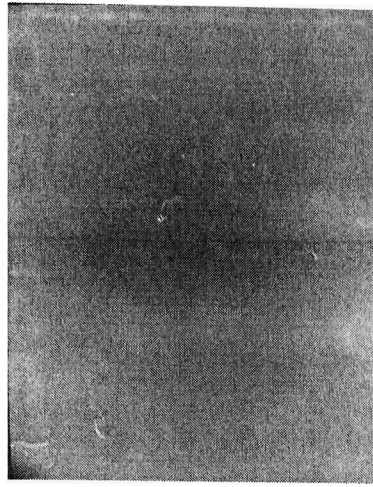
All the samples show high molecular weight. The polydispersity of the parent polyamic acid is lower than the zirconium pendent polyamic acids. However, some polymer chains having more MADA units than the others, causes the polydispersity to increase upon attaching the pendent group to the polymer backbone.



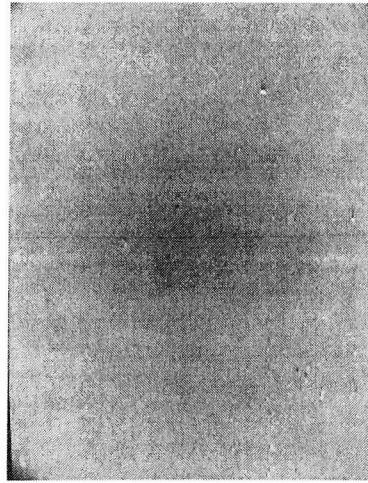
PI wo/AO  
Magnification 2,500



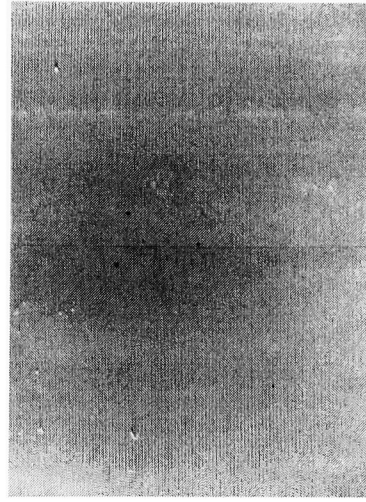
PI/Zr(H) wo/AO  
Magnification 2,500



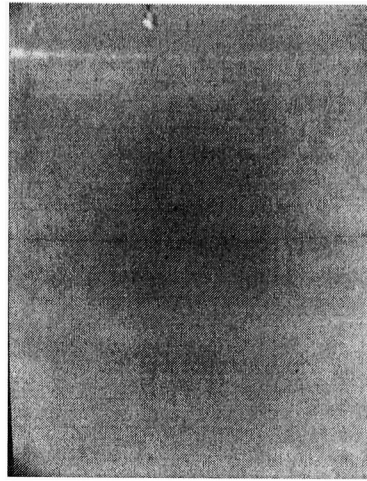
PI/Zr(m) wo/AO  
Magnification 2,500



PI/Zr(c) wo/AO  
Magnification 2,500

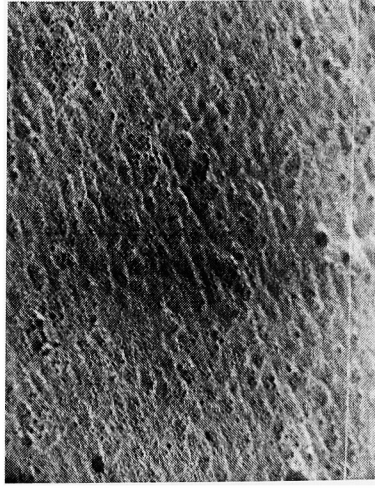


PI/Zr(3-OMe) wo/AO  
Magnification 2,500

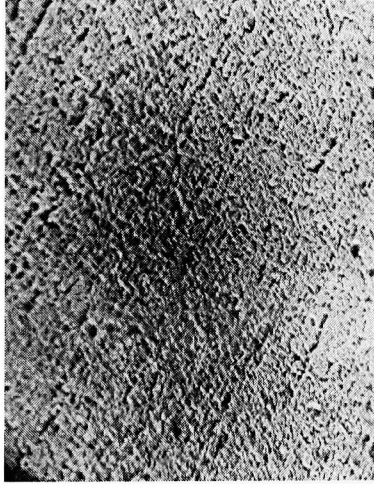


PI/Zr(5-OMe) wo/AO  
Magnification 2,500

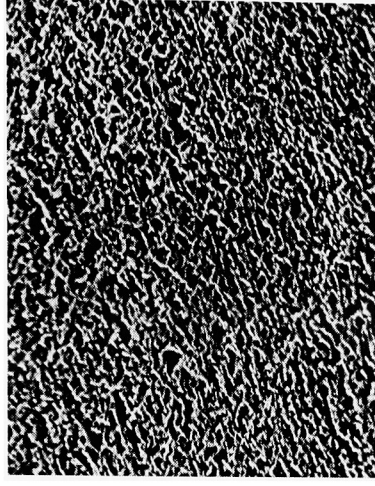
Figure 3.37 SEM Pictures before Atomic Oxygen Etching



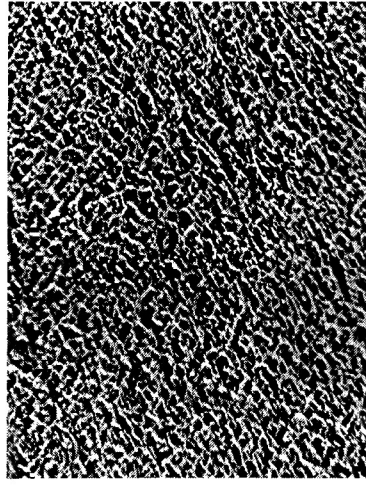
PI w/AO  
Magnification 2,500



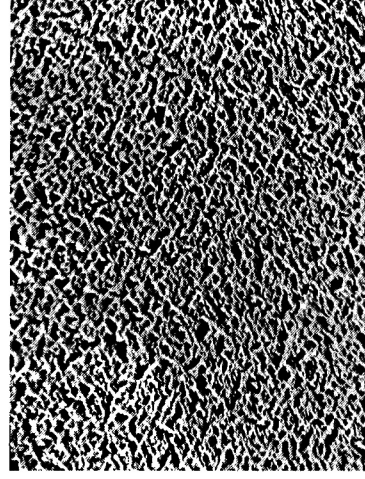
PI/Zr(H) w/AO  
Magnification 2,500



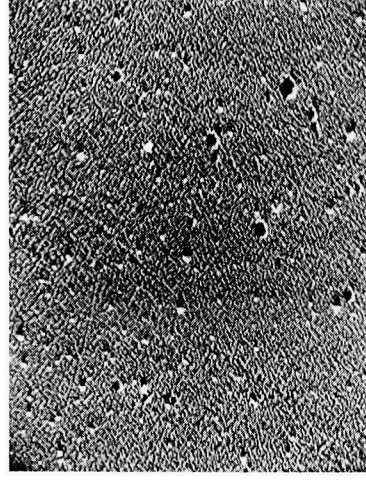
PI/Zr(m) w/AO  
Magnification 2,500



PI/Zr(c) w/AO  
Magnification 2,500

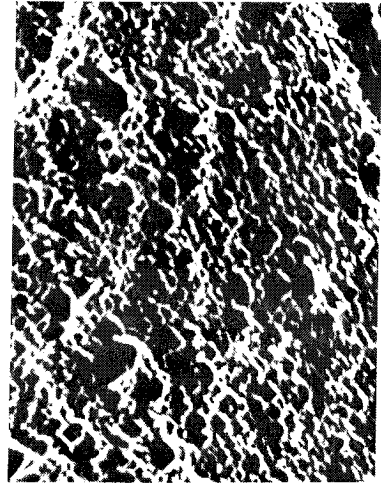


PI/Zr(3-OMe) w/AO  
Magnification 2,500

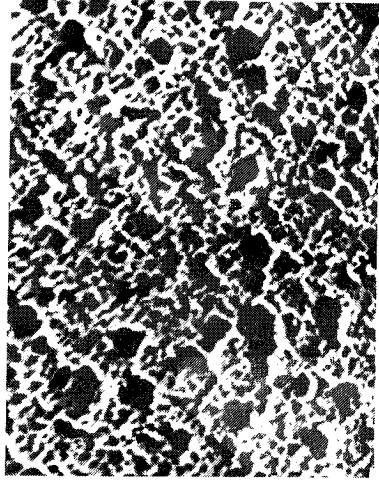


PI/Zr(5-OMe) w/AO  
Magnification 2,500

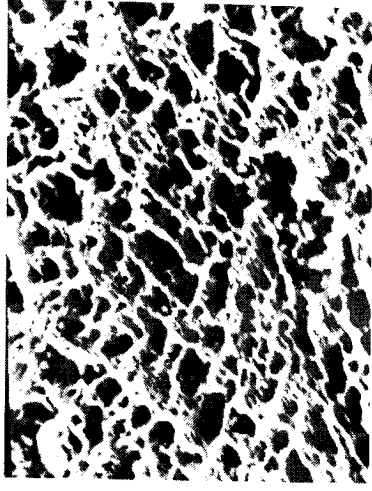
Figure 3.37 SEM Pictures before Atomic Oxygen Etching



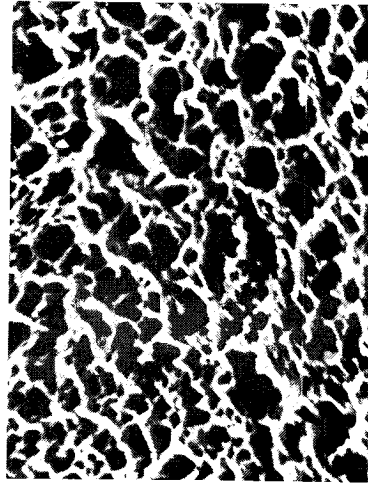
PI w/AO  
Magnification 10,000



PI/Zr(H) w/AO  
Magnification 10,000



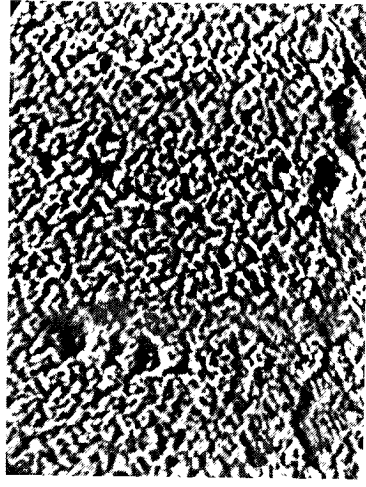
PI/Zr(m) w/AO  
Magnification 10,000



PI/Zr(c) w/AO  
Magnification 10,000



PI/Zr(3-OMe) w/AO  
Magnification 10,000



PI/Zr(5-OMe) w/AO  
Magnification 10,000

Figure 3.39 SEM Pictures before Atomic Oxygen Etching at 10,000 Magnification

# Differential Molecular Weight Distribution

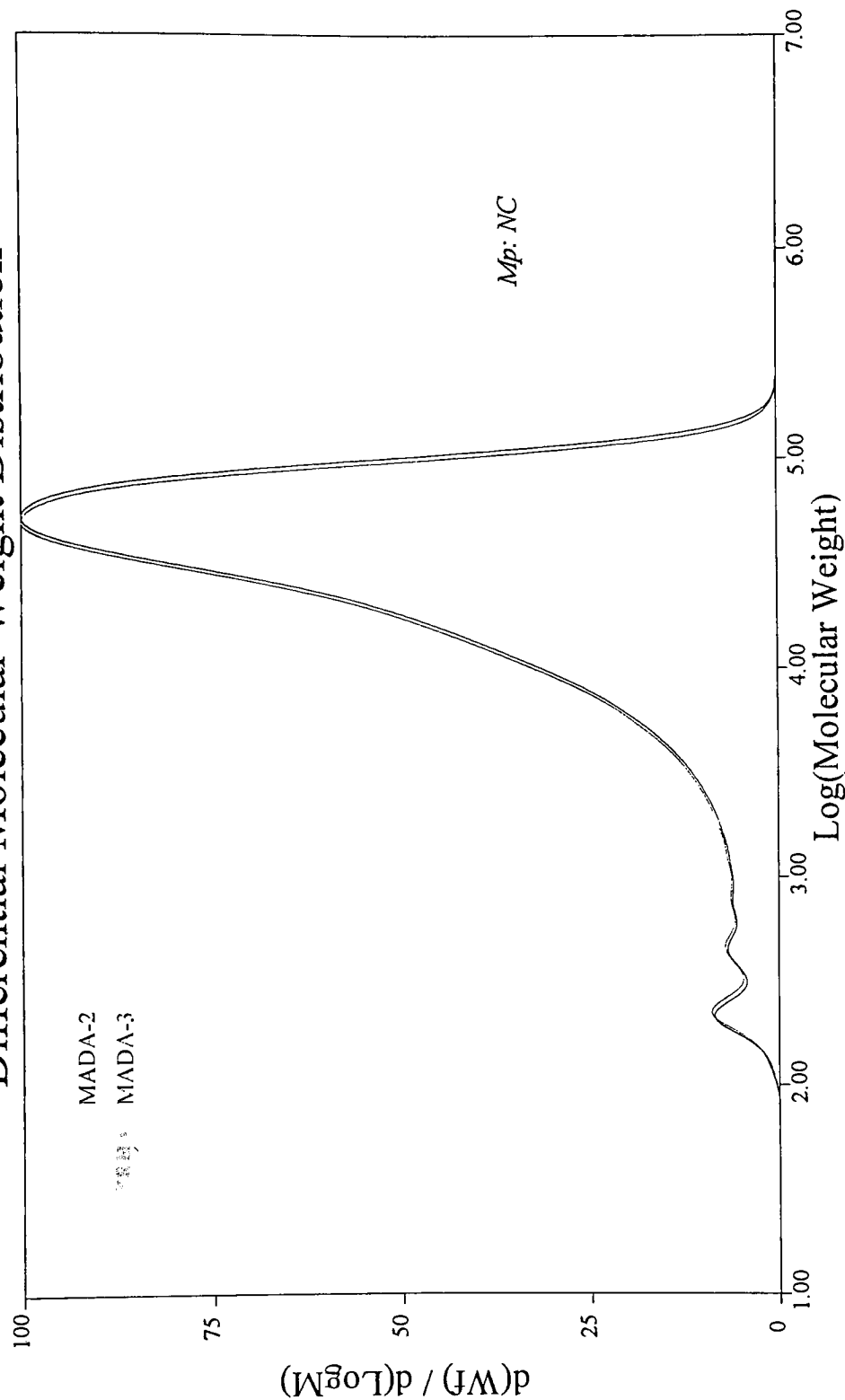


Figure 3.40 GPC Graph of Parent Polyamic Acid

# Differential Molecular Weight Distribution

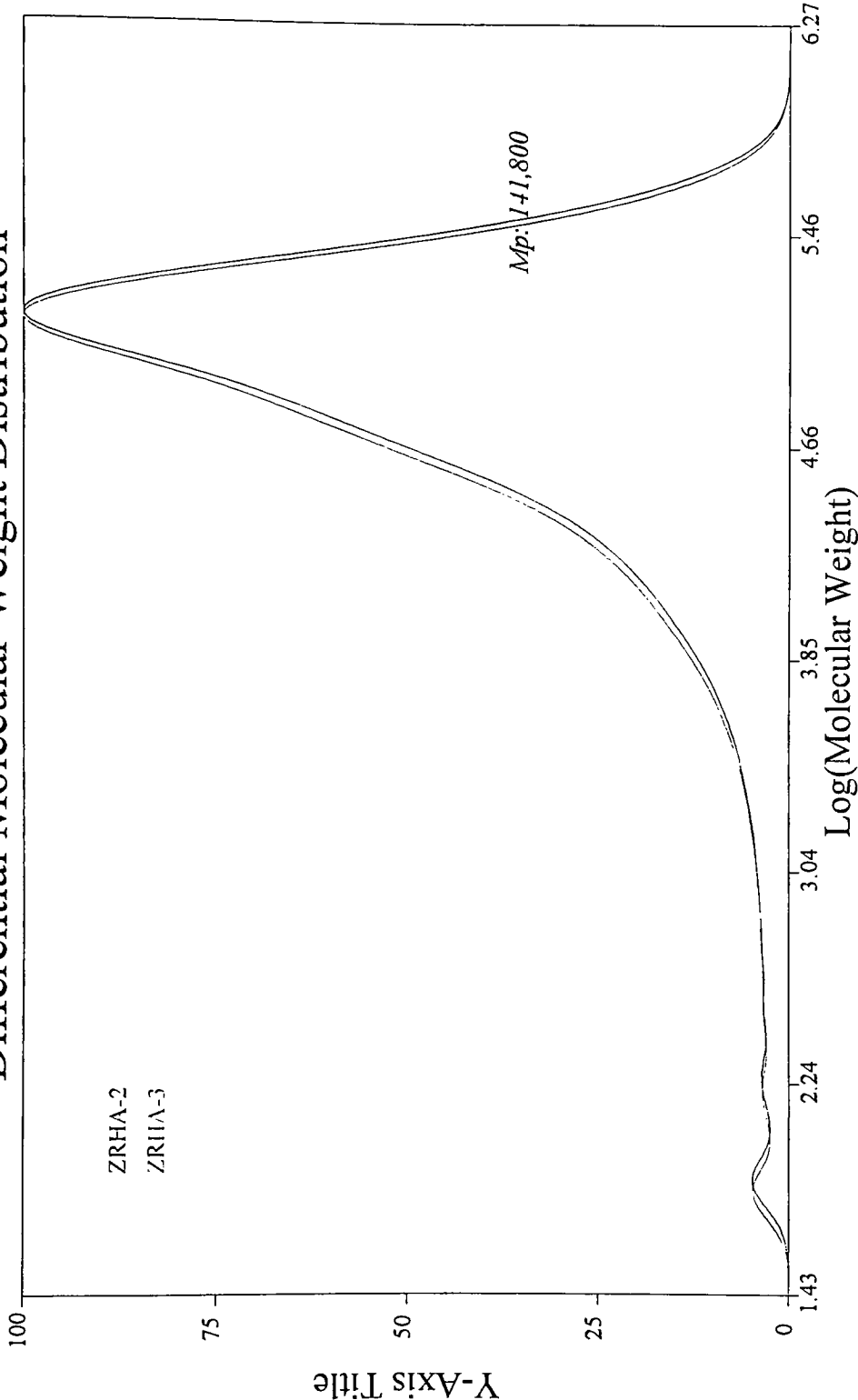


Figure 3.41 GPC Graph of Zr(adsp)(dsp) Pendent Polyamic Acid

# Differential Molecular Weight Distribution

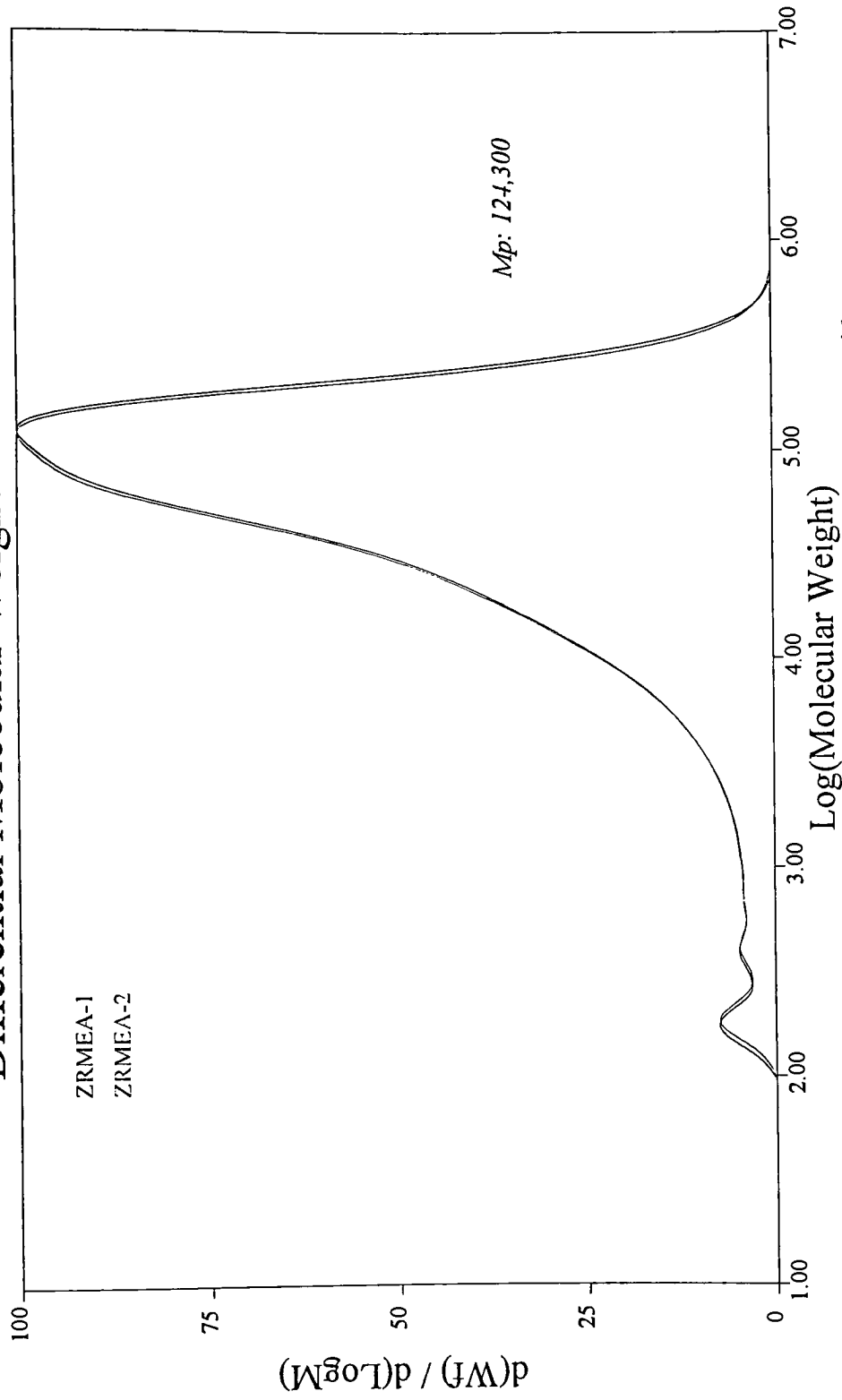


Figure 3.42 GPC Graph of Zr(adsp)(mdsp) Pendent Polyamic Acid

# Differential Molecular Weight Distribution

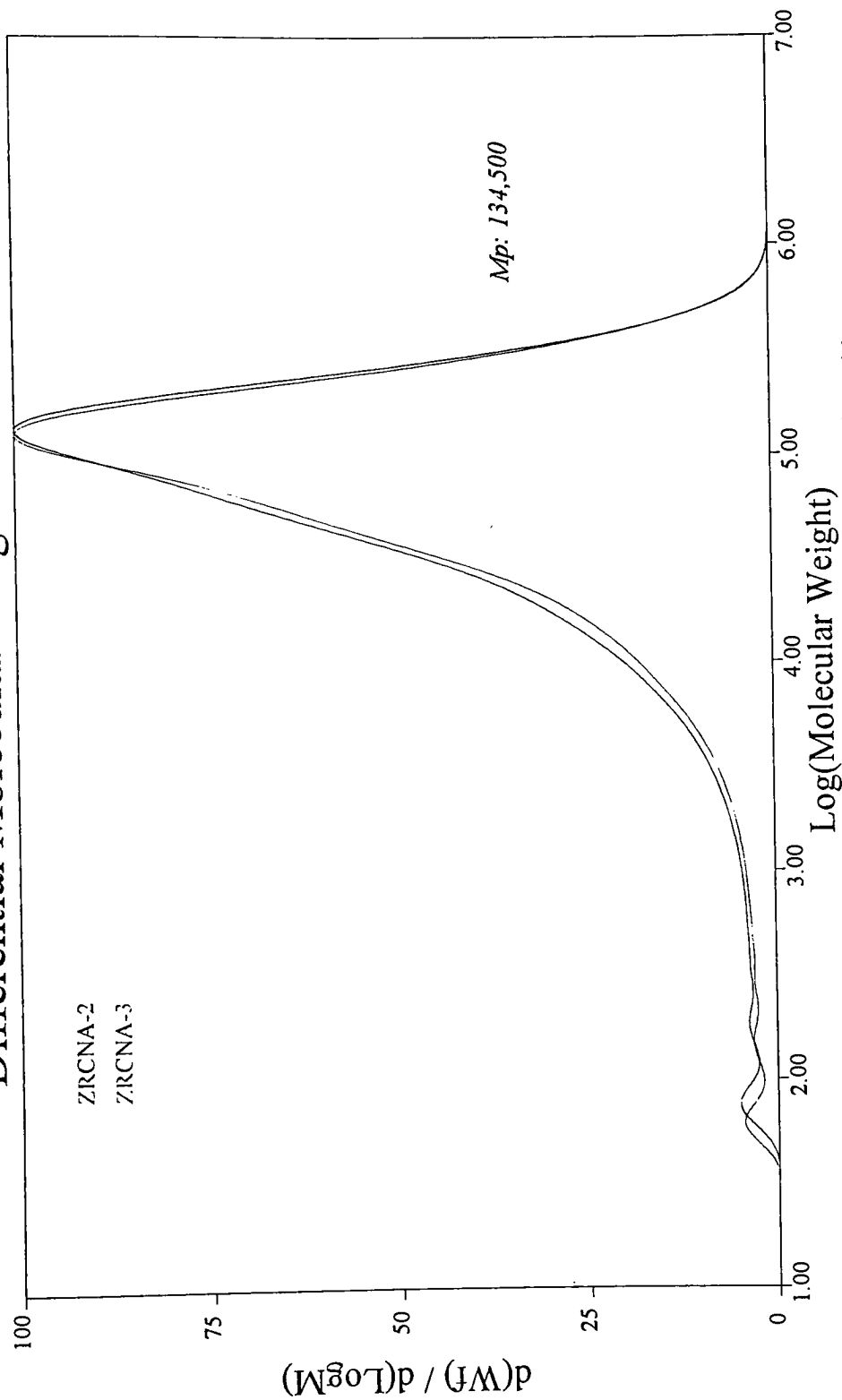
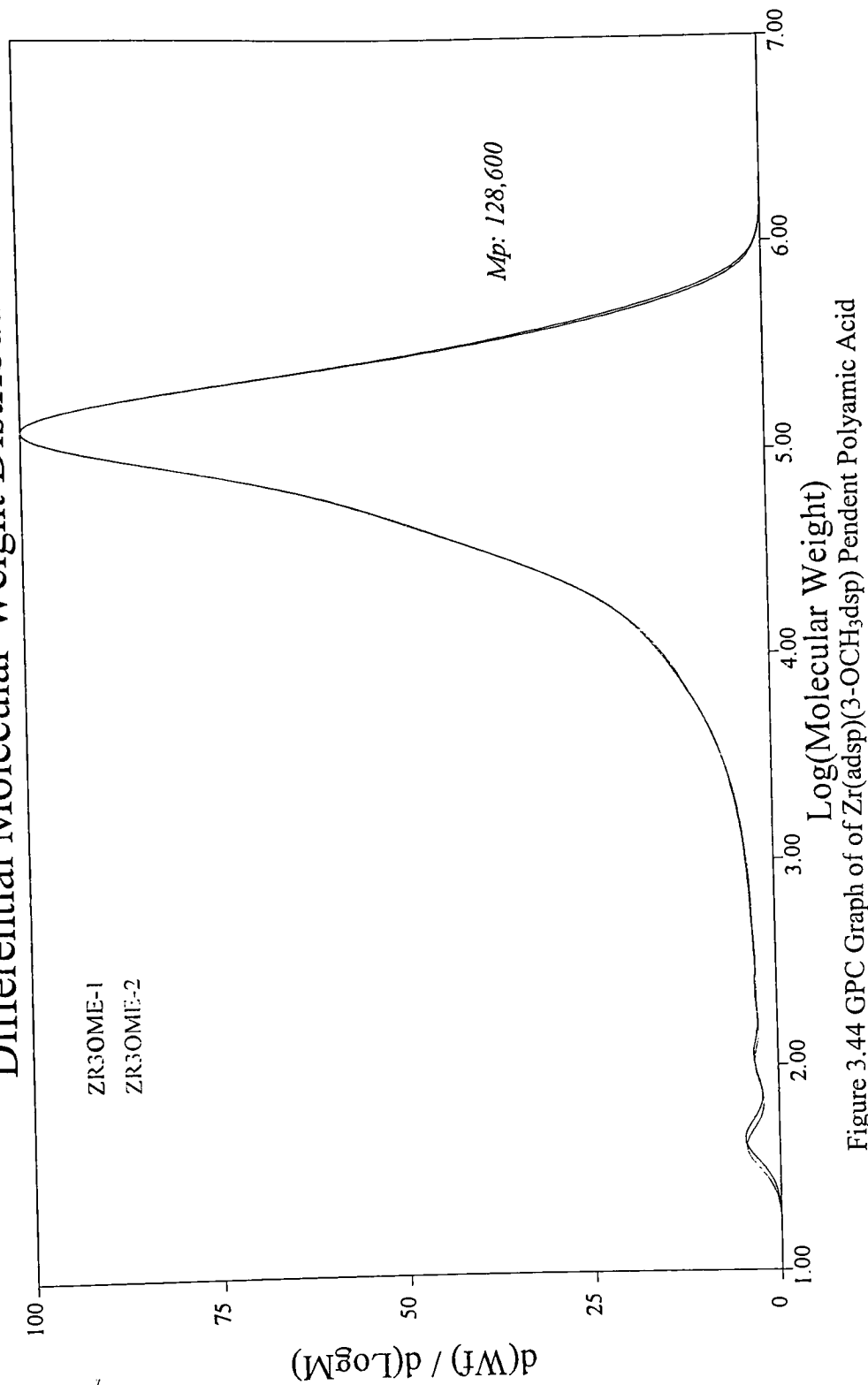


Figure 3.43 GPC Graph of of Zr(adsp)(cdsp) Pendent Polyamic Acid



# Differential Molecular Weight Distribution

Figure 3.44 GPC Graph of Zr(adsp)(3-OCH<sub>3</sub>dsp) Pendent Polyamic Acid

# Differential Molecular Weight Distribution

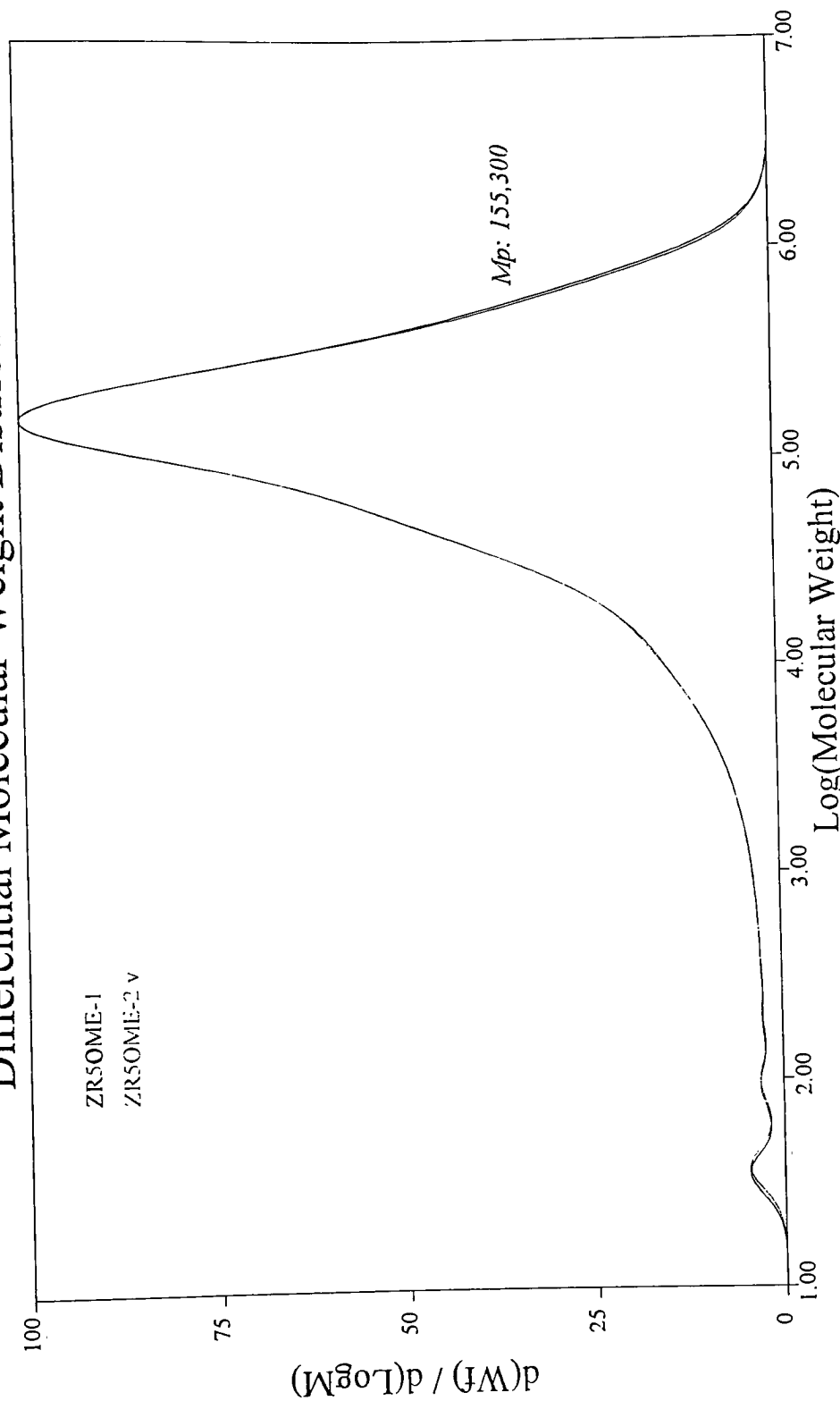


Figure 3.45 GPC Graph of Zr(adsp)(5-OCH<sub>3</sub>dsp) Pendent Polyamic Acid

Table 3.8 GPC Results for Polyamic acid and Zirconium Pendent Polyamic Acids

Sample	M <sub>n</sub> (g/mol)	M <sub>w</sub> (g/mol)	M <sub>z</sub> (g/mol)	Intrinsic Viscosity (dL/g)	Polydispersity (M <sub>w</sub> / M <sub>n</sub> )
PI	4160	39200	64300	0.375	9.40
	3990	37400	61600	0.378	
PI/Zr(H)	3100	118300	226700	0.459	38.40
	2910	112500	219200	0.465	
PI/ Zr(m)	5260	86600	159100	0.273	15.89
	5500	84400	155600	0.277	
PI/ Zr(c)	3220	104400	205800	0.410	33.38
	3090	106200	206600	0.508	
PI/Zr(3-OCH <sub>3</sub> )	1970	123400	249200	0.647	64.23
	1910	125700	254300	0.663	
PI/Zr(5-OCH <sub>3</sub> )	1870	183200	450600	0.581	94.39
	1980	180200	439500	0.566	

### 3.4.7 Light Scattering Tests

The weight average molecular weight is the only molecular weight that can be obtained from light scattering test. Table 3.9 shows the light scattering test results. Note the low second viral coefficient for the PAA/Zr(adsp)(cdsp) and the corresponding high weight average molecular weight vs. the other pendent polyamic acids tested.

Table 3.9 Light Scattering Test Results

Sample	Mw (g/mol)	Second Viral Coefficient ( $\times 10^4$ )
PAA	47000	3.36
PAA/Zr(adsp)(dsp)	59300	2.84
PAA/ Zr(adsp)(mdsp)	74200	2.56
PAA/ Zr(adsp)(cdsp)	130000	1.35
PAA/Zr(adsp) (3-OCH <sub>3</sub> dsp)	68800	3.08
PAA/Zr(adsp) (5-OCH <sub>3</sub> dsp)	73500	2.34

### 3.4.8 Contact Angle

Contact angle measurement was performed to check the surface properties of parent polyimide film, zirconium pendent polyimide films, and LARC-IA films. Table 3.10 shows the result of contact angle measurement.

Table 3.10 Result of Contact Angle Measurement

Sample	Contact Angle
PI	58.8
PI/Zr(adsp)(dsp)	60.8
PI/ Zr(adsp)(mdsp)	58.7
PI/ Zr(adsp)(cdsp)	60.5
PI/Zr(adsp)(3-OCH <sub>3</sub> dsp)	60.8
PI/Zr(adsp)(5-OCH <sub>3</sub> dsp)	60.7
LARC-IA <sup>a</sup>	62.7
LARC-IA <sup>b</sup>	62.6

a. LARC-IA film was made at 360 °C, 10T.

b. LARC-IA film was made at 340 °C, 5T.

The contact angles with water for LARC-IA film of which was made at 360 °C under the pressure of 10T and film made at 340 °C under the pressure of 5T are very close. The contact angles of the zirconium pendent polyimides are bigger than the parent polymer except for the Zr(adsp)(mdsp) pendent polymer.

### 3.4.9 Film Flexibility and Solvent Resistance Test

After the polyimides film samples were immersed in acetone, chloroform, dimethylacetamide (DMAc), methyl ethyl ketone, and toluene for 30 min, they were still flexible and past the fingernail crease (see Table 3.11).

Table 3.11 Solvent Resistance Test

Sample \ Solvent	Control <sup>a</sup>	Acetone	MEK <sup>b</sup>	DMAc <sup>c</sup>	Chloroform	Toluene
PI	X <sup>d</sup>	X	X	X	X	X
PI/Zr(H)	X	X	X	X	X	X
PI/ Zr(m)	X	X	X	X	X	X
PI/ Zr(c)	X	X	X	X	X	X
PI/Zr(3-OCH <sub>3</sub> )	X	X	X	X	X	X
PI/Zr(5-OCH <sub>3</sub> )	X	X	X	X	X	X

a. film behavior without solvent exposure

b. methyl ethyl ketone

c. N,N-dimethylacetamide

d. X = fingernail creasable at RT

## DISCUSSION

### 4.1 Synthesis

#### 4.1.1 Zirconium Complexes

All complexes containing the (ndsp)(Rdsp) ligand used in this study were prepared by 1:1:1 mole ratio reactions of  $\text{Zr}(\text{O-n-Bu})_4$  with the corresponding free Schiff base ligands. Zirconium complexes,  $\text{Zr}(\text{adsp})(\text{dsp})$ ,  $\text{Zr}(\text{adsp})(\text{mdsp})$ ,  $\text{Zr}(\text{adsp})(\text{cdsp})$ ,  $\text{Zr}(\text{adsp})(3\text{-OCH}_3\text{dsp})$ , and  $\text{Zr}(\text{adsp})(5\text{-OCH}_3\text{dsp})$ , were produced from  $\text{Zr}(\text{ndsp})(\text{dsp})$ ,  $\text{Zr}(\text{ndsp})(\text{mdsp})$ ,  $\text{Zr}(\text{ndsp})(\text{cdsp})$ ,  $\text{Zr}(\text{ndsp})(3\text{-OCH}_3\text{dsp})$ , and  $\text{Zr}(\text{ndsp})(5\text{-OCH}_3\text{dsp})$  by hydrogenation, respectively. Since different functional group of the zirconium complexes causes different polarity of the complexes, various eluting systems were used in the chromatography step. The methylene chloride/ethyl acetate system was used as the eluting system in the chromatography step by varying the ratio of the two components. But chloroform/ethyl acetate was used as eluting system in the separation of  $\text{Zr}(\text{adsp})(\text{cdsp})$  due to the solubility problem. All TLC and spectral analysis of the known products are consistent with those previously reported<sup>15</sup> or recorded in lab notebooks.

The composition of the only new zirconium complex product that was made in this research project,  $\text{Zr}(\text{adsp})(\text{mdsp})$ , was confirmed by the elemental analysis result and  $^1\text{H}$ NMR spectrum. (See Table 3.1 and Figure 3.17) The elemental analysis result shows that the experimental data well matches the theoretical data. The  $^1\text{H}$ NMR spectrum indicates that the methyl group is present by the appearance of the peak at 2.4ppm, which integrates for 3 H, and  $\text{NH}_2$  is present by the appearance of peak at 4.0ppm, which integrates for 2 H.

#### 4.1.2 Mellitic Dianhydride (MADA)

There are four possible products that could be obtained in the preparation of MADA step (see Figure 4.2).

B and C are dianhydride isomers, A is a monoanhydride which is produced when the heating time is not long enough, D is a trianhydride which is produced when the mellitic acid is over heated. The two dianhydride isomers are the desired monomers for the polymerization. The existence of the monoanhydride monomer will terminate the

polymerization resulting low molecular weight polymer, the existence of the trianhydride monomer will cause branching or cross-linking in the polymerization process resulting gelation and/or a smaller degree of polymerization.

#### 4.1.3 Parent Polyamic Acid

Since the reaction is a step polymerization, the molecular weight of the product polymer highly depends on the purity of the monomers and the solvent. It is critical to control the sublimation temperature during the process of purifying 3,4'-ODA and ODPA. If the sublimation temperature exceeds 30 °C above its melting point, decomposition of ODPA occurs and causes the formation of pink crystals instead of white crystals. When 3,4'-ODA was over heated during the sublimation process, a light brown crystal was obtained.

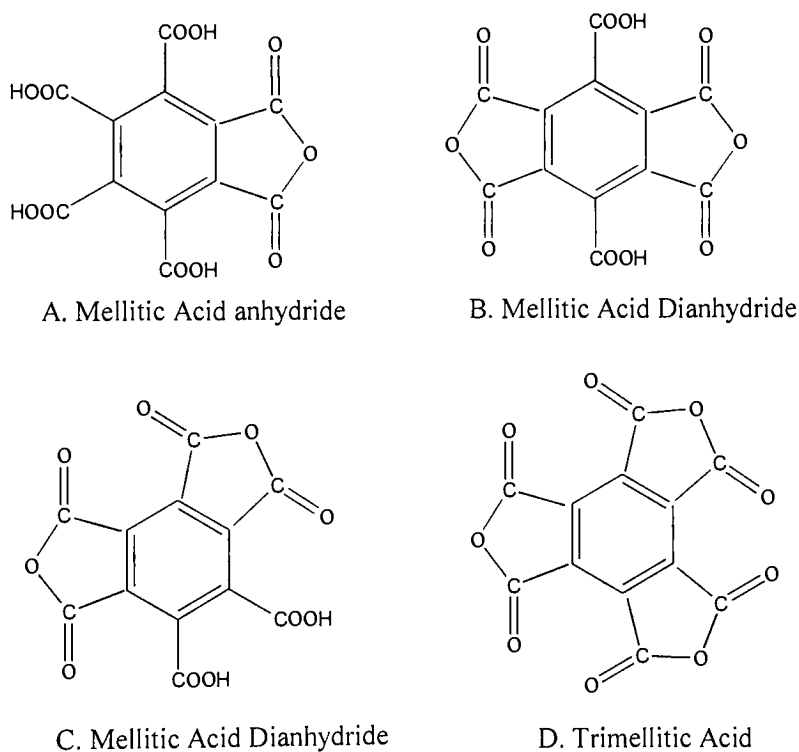


Figure 4.1 MADA and Byproducts

For producing a high molecular weight polymer, the purity of the solvent is also very important. In order to get absolute anhydrous NMP, calcium hydride was used to remove water from NMP. The presence of water molecular will open the anhydride ring during

polymerization, which lowers the reactivity of the monomer and produces low molecular weight polymer.

Another factor relevant to the production of a high molecular weight polymer is the reaction temperature. This temperature should be as low as possible so as to extend the reaction time. Because the degree of polymerization is a function of reaction time, the desired molecular weight can be obtained by quenching the reaction, e.g., by cooling.<sup>16</sup> The synthesis of polyamic acid was carried out at 0 °C with slow addition of the diamine (3,4'-ODA) to the dianhydride system (ODPA and MADA). Efficient cooling is also required to compensate for the heat of reaction and minimize the reverse reaction. Efficient stirring is required to enable the best mixing, also favoring the formation of higher molecular weight polymer.

Keeping the monomers in exact stoichiometric ratio is very important for obtaining high molecular weight polymer in step polymerization.

#### **4.1.4 Zirconium Pendent Polyamic Acids**

The addition of DCC as dehydration reagent to the polyamic acid and zirconium complex mixture was expected to form anhydride-like intermediate between the adjacent carboxylic acid groups in the MADA repeat unit to promote the attachment reaction.

During the pendent polymer synthesis, the formation of gel can be explained by the conversion of the polyamic acid to the NMP insoluble polyisoimide where the adjacent carboxylic acid group and amic acid group react to form the isoimide ring.<sup>23, 24</sup> The reaction of the amino group in the zirconium complex with the isoimide functional group in the parent polyamic acid chain produces the NMP-soluble zirconium pendent polyamic acid.<sup>25</sup>

The presence of the amino group in the mixed ligand complexes allowed further reaction with the anhydride-like intermediate formed from the dehydration of the adjacent carboxylic acids in MADA with DCC at room temperature. During the synthesis, DCC was added into the mixture of polyamic acid and zirconium complex solution very slowly, otherwise gelation would occur.

All the zirconium pendent polyamic acids are new products except Zr(adsp)(dsp) pendent polyamic acid.<sup>19</sup>



#### 4.1.5 Zirconium Pendant Polyimides

Upon preparing 2-layer zirconium pendant films, cracks were apparent after imidization. The attachment of pendant zirconium complex may reduce the flexibility of the polymer chain, which would cause weaker adhesion of polymer films. Or for material not adjacent to the glass, the greater difference in dimensional stability for the conversion from zirconium pendant polyamic acid to polyimide may be causing the crack.

All the zirconium pendant polyimides are new products except Zr(adsp)(dsp) pendant polyimide.<sup>19</sup>

### 4.2 Polymer Characterization

#### 4.2.1 Thin Layer Chromatography (TLC)

The completion of zirconium complex attachment to the polymer backbone is confirmed by TLC. Before adding DCC to the mixture of polyamic acid and zirconium complex solution, free zirconium complex spot appears on the TLC plate, but after the addition of DCC solution, the spot corresponding to free zirconium complex was no longer present.

#### 4.2.2 Infrared Spectrometry (IR)

The differences in FT-IR spectra between the zirconium pendant polyimide films and the parent polyimide film can be attributed to the attachment of the zirconium complexes.

The FT-IR spectra of zirconium complexes, parent polyimide, and zirconium pendant polyimides are consistent with the proposed structures. The attachment of zirconium complex to the polymer backbone was confirmed by the band at  $1851\text{ cm}^{-1}$ , which was only shown in the spectrum of the parent polyimide. Since the amino group from zirconium complex reacted with the MADA residues of the parent polymer, anhydride rings could no longer be formed during the imidization process. Thus, the band at  $1851\text{ cm}^{-1}$ , which indicates the existence of the anhydride group, does not appear in the pendant polyimide spectra, which also confirms that zirconium complexes attached to the polymer backbone.

#### 4.2.3 Nuclear Magnetic Resonance (NMR)

The samples used in NMR measurement were prepared from dried polyamic acids. The poor signal-noise ratio is caused by the poor solubility of the polymers in DMSO-d<sub>6</sub>.

<sup>1</sup>H NMR was performed to verify the structures of the parent polyamid acid and zirconium pendent polyamic acids. E.g., small peaks at chemical shifts matching those of the free complex are observed in addition to larger peaks that correspond to the polymer backbone. In conjunction with the TLC results, these observations confirm the attachment of the zirconium complexes to the parent polyamic acid.

#### 4.2.4 Thermogravimetric Analysis (TGA)

The weight loss under 100 °C in the TGA graph of parent polyamic acid and zirconium pendent polyamic acids is due to the loss of NMP trapped in polymers. The weight loss around 200 °C is due to water vapor escaping during in imidization step.

The decomposition temperatures of the zirconium pendent polymers are slightly lower than the parent polymer, but they are still reasonable high enough for the NASA application that drives this research.

The proximity of the mass of ZrO<sub>2</sub> residue produced in TGA measurement with the theoretical mass, not only confirms the attachment the zirconium complex to the polymer backbone, but also confirms the approximate amount of zirconium complex attaching to the polymer.

#### 4.2.5 Differential Scanning Calorimetry (DSC)

All samples were analyzed twice by DSC. The T<sub>g</sub> from first analysis is lower than from second. This is a typical the property of polymers. “Fresh” polymer is used to measure T<sub>g</sub> values, because T<sub>g</sub> is a time-related parameter.

Comparing the T<sub>g</sub> s of the parent polyimide and the zirconium pendent polyimides with the T<sub>g</sub> of LARC-IA, which is 223 °C,<sup>18</sup> those of the polyimides synthesized in this research are much higher.

The difference between the parent polyimide and the LARC-IA is the MADA in the former's polymer repeat unit. Because of MADA, the flexibility of the polymer backbone decreases and results in higher T<sub>g</sub>s. The higher T<sub>g</sub>s of the zirconium pendent polyimides

compared to the parent polyimide are due to the zirconium complexes, which also decrease the flexibility of the polymers and cause the  $T_g$ s to be higher. Because of their poor solubility,  $T_g$ s need to be lowered to improve the processibility of these polyimides.

#### **4.2.6 Scanning Electron Microscopy (SEM) and Atomic Oxygen Durability**

##### **Characterization**

SEM is a powerful technique for studying the surface characteristics of the polyimide films. We obtained information on how the zirconium pendent polyimides resist atomic oxygen using this technique.

Upon atomic oxygen plasma etching, the attached zirconium complex was decomposed to  $ZrO_2$ , which remained on the surface of the polyimide film. This phenomenon suggests means by which the zirconium complex enhances the atomic oxygen resistance. Considering the SEM pictures of the polyimide films after atomic oxygen etching, the difference between the parent polymer and the zirconium pendent polymer is not obvious. However, increasing the mole percentage of zirconium complex in the polymer chain and increasing the thickness of the polymer film will produce more  $ZrO_2$  on the surface of the film. When the  $ZrO_2$  white powder forms a uniform substantial layer, it will greatly improve the atomic oxygen resistance property. The parent polyimide film showed less atomic oxygen resistance than the zirconium pendent polymers.

#### **4.2.7 Gel Permeation Chromatography (GPC)**

GPC is used to determine the molecular weight and molecular weight distribution of parent polyamic acid and zirconium pendent polyamic acids. The parent polyamic acid and zirconium pendent polyamic acid in NMP have broad molecular weight distribution. This might be attributed to the presence of some variation in the mole percentage of MADA in the polymer chain, which would cause comparable variation in the mol percentage of zirconium complexes, and thus broaden the molecular weight distribution.

Average molecular weights from GPC are rough approximations due to the use of polystyrene as standard.

#### 4.2.8 Light Scattering Tests

The molecular weight obtained from GPC is based on polystyrene standards, whose properties are very different from polyimides. In order to get more information about the molecular weight of the parent polyamic acid and the zirconium pendent polyamic acids, light scattering test was performed.

Weight average molecular weight is the only molecular weight that can be obtained from the light scattering tests. The molecular weights from light scattering results are more consistent than those from GPC measurements with the exception of the Zr(adsp)(cdsp) pendent polymer, which is due to the aggregation of the polymer chain (see below). Therefore, under suitable condition, e.g. a good solvent, light scattering test is a more accurate method for molecular weight measurement of polyamic acids.

Also we can get some information about the interaction between polymer and solvent from the value of second virial coefficient. Second virial coefficient can be used to describe the interaction between the polymer and solvent. The smaller the second virial coefficient, the poorer the interaction between polymer and solvent. Therefore, aggregation may occur when this value is low. Since the second virial coefficient of Zr(adsp)(cdsp) pendent polyamic acid is almost half as the other's, and the molecular weight of Zr(adsp)(cdsp) pendent polyamic acid is almost double in comparison to the rest of the polyamic acids, formation of aggregates (average two polymer chains each) is likely. Since the aggregate behaves like a large polymer, it perhaps is no surprise that the Zr(adsp)(cdsp) pendent polyamic acid gave the best films.

#### 4.2.9 Solvent Resistance

The fact that treatment with different organic solvents caused no changes reflects the flexibility of these films and indicates that no dissolution of low molecular weight polymer occurred.

Compared to LARC-IA, enhanced solvent resistance was observed for parent polyimide film and zirconium pendent polyimide films, presumably due to the presence of rigid MADA residues in the polymer chain. These results have helped define a chemical approach for improving solvent resistance in polyimide materials.

#### **4.2.10 Contact Angle Measurement**

The results of contact angle measurement tell us that LARC-IA has higher surface tension than the parent polyimide and the zirconium pendent polyimides. That is to say that water is easier to spread on the surface of all the parent polyimide film and the zirconium pendent polyimide films than the LARC-IA films. This also indicates that zirconium pendent polyimides probably have better adhesion to glass than LARC-IA.

## SUGGESTION FOR FUTURE WORK

Future work may concern the following points:

1. Determine the maximum single layer film thickness before film cracking could be observed upon imidization.
2. Increase the mole percentage of zirconium complex in polyamic acid by increasing the mole percentage of MADA in polyamic acid.
3. Imidize the zirconium pendent polyamic acid films above their  $T_g$  to avoid one mechanism of crack formation upon imidization.
4. Remove the residual oligomers, and DCC byproduct from the polyamic acid solution to narrow the polydispersity.

## CONCLUSIONS

One new zirconium complex was made,  $\text{Zr(adsp)(mdsp)}$ , with a good elemental analysis result.

The 3,4'-ODA/ODPA/10% MADA polyamic acid was synthesized by using the solution polycondensation technique. Their atomic oxygen resistant zirconium-containing polyimide precursors, i.e., mixed ligand zirconium complex pendent polyamic acids, were synthesized by appending various zirconium complexes to the parent polyamic acid backbone. One of them,  $\text{Zr(adsp)(dsp)}$  pendent polyamic acid, was synthesized before. This time, the starting materials were each sublimed three times, which resulted in higher solution viscosity and higher average molecular weight. The other four pendent polyamic acids,  $\text{Zr(adsp)(mdsp)}$  pendent polyamic acid,  $\text{Zr(adsp)(cdsp)}$  pendent polyamic acid,  $\text{Zr(adsp)(3-OCH}_3\text{dsp)}$  pendent polyamic acid, and  $\text{Zr(adsp)(5-OCH}_3\text{dsp)}$  pendent polyamic acid, are new polymers.

NMR integration and TGA  $\text{ZrO}_2$  residues support 10% (mol) concentration of zirconium pendent groups.

The GPC and light scattering results show that both the parent polymer and the zirconium pendent polymers have moderately high average molecular weights. But  $\text{Zr(adsp)(cdsp)}$  pendent polyamic acid is different from the parent and the other zirconium pendent polyamic acids due to the interaction between the polymer and the solvent.

The TGA results show that both the parent polymer and the zirconium pendent polymers have high decomposition temperatures, which indicate that both polymers possess high thermal stability.

The DSC results tell us that the polyimides synthesized in this research have higher  $T_g$ s than LARC-IA, which means they may be more difficult to process than LARC-IA.

For each zirconium pendent polyimide, atomic oxygen exposure produces white surface coating of  $\text{ZrO}_2$ .  $\text{Zr(adsp)(5-OCH}_3\text{dsp)}$  pendent polyimide film shows a different atomic oxygen resistant property than the others, possibly reflecting a different porosity.

The solvent resistance result shows that all the polyimide films possess high chemical stability.

Based on the contact angle measurements the potential for use of these pendent polymers as adhesives is good.

## REFERENCES

1. Leger, L. J. "Oxygen Atom Reaction with Shuttle Materials at Orbital Altitudes", NASA TM-58246, **1982**.
2. Rutledge, S. K.; Cooper, J. M.; Olle, R. M. "The Effect of Atomic Oxygen on Polysiloxane-polyimide for Spacecraft Applications in Low Earth Orbit", Space Operations, Applications and Research Symposium, Albuquerque, MN, June 26-28, **1990**.
3. Banks, B. A.; Rutledge, S. K. "Low Earth Orbit Atomic Oxygen Simulation for Materials Durability Evaluation", Proceeding of the 4th International Symposium on Spacecraft in the Space Environment, Toulouse, France, September 6-9, **1988**.
4. Golub, M. A. "ESCA Study of Kapton Exposed to Atomic Oxygen in Low Earth Orbit of Downstream from a Radio Frequency Oxygen Plasma", *Polym. Commun.*, 29, **1988**.
5. Banks, B. A. "SiO<sub>x</sub> Coatings for Atomic Oxygen Protection of Polyimide Kapton in Low Earth Orbit", Coating Technologies for Aerospace Systems Materials Specialist Conference, Dallas, TX, April 16-17, **1992**.
6. Banks, B. A. "Ion Beam Sputter-Deposited Thin Film Coating for the Protection of Spacecraft Polymers in Low Earth Orbit", *Aerospace Science Meeting*, Reno, Nevada, January 14-17, **1985**.
7. Rutledge, S. K.; Olle, R. M. "Durability Evaluation of Photovoltaic Blanket Materials Exposed on LDEF Tray S1003", *The First LDEF Post-Retrieval Symposium*, Kissimmee, Florida, June 2-8, **1991**.
8. Banks, B. A.; Dever, J. A. "Atomic Oxygen Interactions with FEP Teflon and Silicones on LDEF", *The First LDEF Post-Retrieval Symposium*, Kissimmee, Florida, June 2-8, **1991**.
9. Banks, B. A.; Rutledge, S. K. "The Implication of the LDEF Results on Space Station Freedom Power System Materials", *5th International Symposium on Materials in a Space Environment*, Cannes-Mandelieu, France, September, 16-20, **1991**.
10. Illingsworth, M. L.; Banks, B. A.; Smith, J. W.; Jayne, D.; Garlick, R. G.; Rutledge, S. K.; de Groh, K. K. "Plasma and Beam Facility Atomic Oxygen Erosion of a Transition Metal Complex", *Plasma Chem. and Plasma Proc.* February, 209-225, **1996**.



11. Handbook of Chemistry and Physics, CRC, 74<sup>th</sup> edition, **1993-1994**.
12. John Emsley, "The Elements", 2<sup>nd</sup> edition, Oxford Univ. Press, **1992**.
13. Terschak, J. A.; Chen, Y.; Illingsworth, M. L. Private Communication.
14. He, L. "Atomic Oxygen Resistant Zirconium-Containing Polyimides", *MS Thesis, RIT*, June **1996**.
15. He, L.; Wagner, S. R.; Illingsworth, M. L.; Jensen, A. J. "Homogenous Polyimide Films with Increase Bis(N,N'-disalicylidene-1,2-phenylenediaminato)zirconium(IV) Content" *Chem. Mater.*, 9, 3005-3011, **1997**.
16. Dai, H. "Synthesis and Characterization of Zirconium Complex Pendent Polyimides", *MS Thesis, RIT*, August **1997**.
17. Hou, T. H.; Johnston, N. J.; St. Clair, T. L. "IM7/LARC<sup>TM</sup>-IA Polyimide Composites", *High Perform. Polym.*, 7, 105-124, **1995**.
18. Progar, D. J.; St Clair, T. L. *J. Adhesion*, 21, 35-57, **1987**.
19. Yang, K. "Zirconium Pendent Polyamic acid and Polyimide Based on 3,4'-ODA and ODPA", *MS Thesis, RIT*, June **1999**.
20. Archer, R. D.; Day, R. O.; Illingsworth, M. L. "Transition-Metal Eight-Coordination. 13. Synthesis, Characterization, and Crystal and Molecular Structure of the Schiff-Base Chelate Bis(N,N'-disalicylidene-1,2-phenylenediamino)zirconium(IV) Benzene Solvate", *Inorg. Chem.*, 18, 2908, **1979**.
21. Illingsworth, M. L.; Rheingold, A. L. "Synthesis an Molecular Structure of the Eight-Coordinate Complex Bis(4-amino-N,N'-disalicylidene-1,2-phenylenediaminato)zirconium(IV), a New Reagent for Preparing Coordination Polymers", *Inorg. Chem.*, 26, 4312, **1987**.
22. Cotler, R. J.; Sauers, C. K. "The Synthesis of N-Substituted Isomaleimides" *J. Org. Chem.* 26, 10, **1961**.
23. Wallace, J. S.; Arnold, F. E.; Tan, L. S. "Insitu Rigid-Rod Aromatic Polyimides" *Poly. Preprints*, 316, 28(2), **1987**.
24. Chow, D. "Atomic Oxygen Resistant Zr Pendent Polyimide Based on 1,3-Aminophenoxybenzene", *MS Thesis, RIT*, May **2000**.

## APPENDIX

$^1\text{H}$ NMR Spectrum of  $\text{Zr}(\text{adsp})(\text{mdsp})$  in deuterated methylene chloride

# Current Data Parameters

NAME Zr\_m\_MW  
EXPNO 51  
PROCNO 1

## F2 - Acquisition Parameters

Date\_ 991217

Time 11.26

INSTRUM spect

PROBHD 5 mm DNP 1H

PULPROG zg30

TD 32768

SOLVENT CDCl2

NS 16

DS 2

SMH 6172.839 Hz

FIDRES 0.188380 Hz

AD 2.6542580 sec

RG 574.7

OW 81.000 usec

DE 6.00 usec

TE 300.0 K

O1 1.00000000 sec

P1 9.00 usec

DE 6.00 usec

SFO1 300.1318534 MHz

NUC1 1H

PL1 -5.00 dB

## F2 - Processing parameters

SI 16384

SF 300.1300109 MHz

WDW EM

SSB 0

LB 0.30 Hz

GB 0

PC 1.00

## 1D NMR plot parameters

CX 20.00 cm

F1P 11.000 ppm

F1 3301.43 Hz

F2P -1.000 ppm

F2 -300.13 Hz

PPMCM 0.60000 ppm/cm

HZCM 180.07800 Hz/cm

